Early Aβ-targeting interventions in mouse models of Alzheimer pathology

Dissertation

zur Erlangung des Grades eines

Doktors der Naturwissenschaften

der Mathematisch-Naturwissenschaftlichen Fakultät

und

der Medizinischen Fakultät

der Eberhard-Karls-Universität Tübingen

vorgelegt

von

Ruth Elisabeth Uhlmann

aus Bielefeld, Deutschland

April 2020

Tag der mündlichen Prüfung: 23.04.2020

Dekan der Math.-Nat. Fakultät:	Prof. Dr. W. Rosenstiel
Dekan der Medizinischen Fakultät:	Prof. Dr. I. B. Autenrieth
1. Berichterstatter:	Prof. Dr. M. Jucker
2. Berichterstatter:	Prof. Dr. P. Heutink
Prüfungskommission:	Prof. Dr. M. Jucker
	Prof. Dr. P. Heutink
	Prof. Dr. P. Kahle
	Prof. Dr. U. Rothbauer

Declaration

I hereby declare that I have produced the work entitled

"Early Aβ-targeting interventions in mouse models of Alzheimer pathology",

submitted for the award of a doctorate, on my own (without external help), have used only the sources and aids indicated and have marked passages included from other works, whether verbatim or in content, as such. I swear upon oath that these statements are true and that I have not concealed anything. I am aware that making a false declaration under oath is punishable by a term of imprisonment of up to three years or by a fine.

Tübingen, 23.04.2020

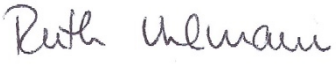

Signature

Eine Perspektive auf die Alzheimer'sche Erkrankung:

Der Panther

Sein Blick ist vom Vorübergehen der Stäbe
so müd geworden, dass er nichts mehr hält.
Ihm ist, als ob es tausend Stäbe gäbe
und hinter tausend Stäben keine Welt.

Der weiche Gang geschmeidig starker Schritte,
der sich im allerkleinsten Kreise dreht,
ist wie ein Tanz von Kraft um eine Mitte,
in der betäubt ein großer Wille steht.

Nur manchmal schiebt der Vorhang der Pupille
sich lautlos auf -. Dann geht ein Bild hinein,
geht durch der Glieder angespannte Stille -
und hört im Herzen auf zu sein.

Rainer Maria Rilke

Table of Contents

Abstract

Alzheimer's disease (AD) is the leading form of dementia affecting approximately 35 million people worldwide. So far, only symptomatic treatment is approved which does not change the course of the disease. Over the last years, prevention trials for AD started to rise new hope for effective therapies based on the knowledge that changes in amyloid-β (Aβ) levels can be detected more than two decades before symptom onset. However, the most beneficial timepoint for early intervention and the best treatment strategies remain unknown. We examined the concepts of β-site amyloid precursor protein cleaving enzyme 1 (BACE1) inhibition and anti-Aβ immunization as prevention strategies. In the first study of this thesis, the optimal timepoint for intervention during pathogenesis was determined. Amyloid precursor protein (APP) transgenic mice were treated for three months with a potent BACE1 inhibitor at an early, intermediate or late stage of pathology or chronically for either half-lifelong or lifelong duration. Effects on neurodegeneration and associated pathologies were established. In the second study, well described anti-Aβ antibodies were applied to APP transgenic mice at initial stage of β-amyloidosis. Their ability to neutralize seeding-active Aβ assemblies was investigated in order to assess preventive effects at sub-threshold Aβ levels before Aβ increase can be detected. Furthermore, antibody recognition profiles using size-fractionated brain-derived Aβ assemblies were established. In the first study, early BACE1 inhibition robustly reduced Aβ deposition and halted neurodegeneration, whereas at later stages of pathology, neurodegeneration became uncoupled of β-amyloidosis. In the second study, acute immunization with an anti-Aβ antibody led to a long-term significant reduction of Aβ deposition and downstream pathologies, demonstrating the presence of pathogenic Aβ seeds before Aβ deposition can be detected. Findings imply that preclinical therapy should shift to initial stages of Aβ dyshomeostasis before β-amyloid deposition is detectable. This primary prevention approach may forestall further seed formation and neurodegeneration, thereby preventing the onset of AD.

1 Introduction

1.1 Alzheimer's disease – the importance for cure

Alzheimer's disease (AD) is the most common form of dementia, accounting for 60 to 80 percent of all dementia cases, with increasing numbers. AD is a progressive disease characterized by symptoms as memory loss, deficits in language, depression, apathy, abnormal motor behavior and further cognitive abnormalities, which worsen over the years (Bruen et al., 2008; Selkoe, 2012). Nowadays, our population becomes older and older, and life expectancy is estimated to increase further based on medical, environmental and social advantages (Ortman et al., 2014). Age is the greatest risk factor for AD, the majority of affected individuals is 65 years or above. Therefore, AD gains massive importance in future demographical changes as well as increasing costs for appropriate care. By 2060, more than 15 million people in the United States are predicted to suffer from this devastating disease (Brookmeyer et al., 2018). So far, AD is the 6th leading cause of death in United States and 5th most frequent cause for people above 65 (Heron, 2018). Recorded deaths through AD increase every year. In parallel, care cost for people with AD will increase from $290 billion (2019) to more than $1.1 trillion in 2050 (Alzheimer Association, 2019). Over the last years, research progress in various fields was able to significantly cause improvements in general health and survival. Death after heart disease, the number one cause of death, could be decreased by nine percent. Despite, numbers for AD have more than doubled with no definite cure by now (U.S. Department of Health and Human Services, Centers for Disease Control and Prevention; Tejada-Vera, 2013).

1.2 The amyloid hypothesis – an explanation for pathology

In 1906, the psychiatrist and neuropathologist Alois Alzheimer described two neuro-pathological brain abnormalities related to AD, namely extracellular Aβ plaques and intracellular neurofibrillary tangles. Extracellular plaques consist of the aggregated Aβ peptide which is the cleavage product of APP by two different proteases. In a first step, APP is cleaved by BACE1, which has been discovered to be the β-secretase at the extracellular site as depicted in in Figure 2 (Hussain et al., 1999; Sinha et al., 1999; Vassar et al., 1999; Yan et al., 1999). The resulting membrane-bound C-99 fragment consists of 99 amino acids and serves as a substrate for the γ-secretase complex. This protein complex is composed of the catalytic subunit presenilin 1/2 (PSEN1/2), nicastrin, anterior pharynx-defective phenotype 1 and the PS enhancer 2, producing Aβ fragments of different lengths (De Strooper et al., 1998; Cai et al.,

2001). The Aβ structure consists of β-strand-turn-β-strand motifs. Dependent on the state of self-aggregation, parallel or anti-parallel β-sheet structures are formed and accumulate into larger fibrils (Cerf et al., 2009). Fibril aggregation results in the amyloid structure which is defined by a cross-β X-ray pattern, high affinity to the amyloid specific dye Congo Red and a greenish birefringence pattern under cross-polarized light (Sipe et al., 2010). In healthy individuals, Aβ is constantly produced during life and persistent clearing mechanisms prevent its toxic accumulation (Haass et al., 1992). During disease state, altered processing or overexpression of Aβ cause an imbalance between the production of Aβ and its clearance. This results in large, insoluble Aβ aggregates and aggregation intermediates which provoke neuroinflammation, neurotoxicity and neurodegeneration, indicating the Aβ peptide as the key player in the pathophysiological process of AD. (Hardy and Higgins, 1992; Rovelet-Lecrux et al., 2006; Masters and Selkoe, 2012).

Neurofibrillary tangles describe the second pathological hallmark of AD, formed by the microtubule-associated protein tau. Under normal conditions, the phosphorylation status of tau regulates axonal stability (Cleveland et al., 1977). In AD, hyperphosphorylated tau self-aggregates into large tangles and disturbs its interaction with the microtubules (Weingarten et al., 1975). Aβ pathological changes have been demonstrated to precede tau pathology in humans and mice in the presence of an APP-related mutation, pointing once more at Aβ as the trigger for AD (Lewis et al., 2001; Bateman et al., 2012). Conversely, mutation-based tau accumulation does not lead to Aβ pathology (Selkoe and Hardy, 2016). However, Aβ-initiated pathogenic misfolding of tau is able to enhance certain downstream pathology (Maruyama et al., 2013).

Over the last years, studies demonstrated that the pathological initiation of AD starts more than 20 years before first clinical symptoms are expected to develop (Jack et al., 2009; Bateman et al., 2012; Reiman et al., 2012; Villemagne et al., 2013; Gordon et al., 2018). At this preclinical stage, initial dysfunctions in the brain are counterbalanced. At later symptom onset, the brain is no longer able to compensate for pathological processes and massive neuronal damage, leading to subtle, but progressing cognitive decline (Alzheimer Association, 2019).

The evolving clinical phenotype of AD can be categorized into three different, consecutive stages. The major characteristic of the mild disease stage (mild cognitive impairment; MCI) is that affected individual show greater cognitive decline than expected for patients age. But at this stage, daily activity is not affected, yet (Roberts and Knopman, 2013). Individuals

diagnosed with MCI show a 32 percent risk to develop AD at later stage (Ward et al., 2013). Patients at the moderate and severe disease stages are strongly marked by deficits in cognition and impairment of daily life up until bedridden conditions (Albert et al., 2011; Jack et al., 2011; McKhann et al., 2011; Sperling et al., 2011a).

1.2.1 Templated misfolding of Aβ

In 1982, Prusiner first described the templated misfolding and self-propagation of proteins as the pathogenic event in the proteinaceous infectious particles (prion) paradigm (Prusiner, 1982). This paradigm revealed the process of misfolded, highly infectious prion proteins (PrP) that force naïve PrPs into the same aberrant and self-propagating shape (Jarrett and Lansbury, 1993; Prusiner, 2013). PrPs cause many devastating human diseases, e.g. Creutzfeldt-Jacob disease, Gerstmann-Sträussler-Scheinker disease and kuru. But, prion-caused abnormalities were also detected in other species, as PrPs provoked scrapie in sheep as well as bovine spongiform encephalopathy in cows (Prusiner, 1998; Collins et al., 2004).

Similar to prion disease, Aβ oligomers in AD serve as a toxic seed to cause further Aβ to aggregate during the process of amyloid formation (Jucker and Walker, 2018). Previous *in vitro* studies suggest to subdivide the formation of amyloidogenic deposits into three different stages: First, misfolded Aβ oligomers cause further Aβ species to accumulate and aggregate during the lag phase of amyloid formation. Exponential growth of these oligomers and simultaneous formation of amyloid fibrils promote amyloid growth. The latest phase forms a plateau. This period is defined by a steady-state equilibrium and no net growth due to breakage of fibrillary Aβ into new seeds (Jarrett and Lansbury, 1993; Kawarabayashi et al., 2001; Das et al., 2012).

The pathogenic nature of Aβ seeds was demonstrated by decreased memory function in rats after application of isolated small oligomers from AD brains (Jarrett and Lansbury, 1993; Shankar et al., 2008). In accordance, a selective ELISA determined oligomeric Aβ in individuals who were either clinically normal or demented. Although all brains showed similar plaque densities, larger amounts of oligomeric Aβ species were present in demented cases (Esparza et al., 2013). Furthermore, transgenic mice revealed significant learning deficits after exposure of neurons to Aβ seeds (Zhao et al., 2017b). Findings indicate that neither massive Aβ aggregates nor monomers but rather soluble oligomeric seeds might be most responsible for pathophysiological changes and memory deficits in AD.

Decades of research revealed that Aβ seeds show prion-like characteristics in the context of AD (Jucker and Walker, 2013, 2018; Walker, 2018; Aoyagi et al., 2019). In APP transgenic mice, Aβ deposition was induced *in vivo* by a prion-like mechanism after inoculation of murine or human Aβ seeds (Kane et al., 2000; Meyer-Luehmann et al., 2006). In APP transgenic mouse models and AD patients, Aβ seeding activity of self-propagating Aβ oligomers was most potent in the earliest stages of pathogenesis. The seeding activity declined with advancing age and with increased progression of disease (Ye et al., 2017; Aoyagi et al., 2019). Further evidence for a prion-like disease is based on findings which demonstrated the transmissibility of Aβ in humans. Individuals, who received growth hormones from pituitary glands in adolescence or dura mater transplantation from human cadavers, reveal massive Aβ pathology in brain based on human-to-human iatrogenic transmissibility of Aβ seeds (Jaunmuktane et al., 2015; Rudge et al., 2015; Frontzek et al., 2016; Hamaguchi et al., 2016).

1.3 Deterministic genes and risk factors – possible triggers for disease

Less than one percent of all AD cases are induced by dominantly inherited mutations in APP, PSEN1 or PSEN2. These familial forms of AD strongly support the amyloid hypothesis with Aβ being the initial trigger of disease (Hardy and Higgins, 1992; Karran et al., 2011). Affected individuals tend to develop symptom onset already at mid-life. So far, more than 200 detrimental, autosomal dominant mutations have been identified, mostly accumulating near the β- or γ-cleavage site of APP to alter Aβ production. Furthermore, the APP gene is located on chromosome 21, causing increased Aβ production in individuals with Down Syndrome who have one additional copy of chromosome 21 (Alzheimer Association, 2019).

Risk factors that elevate the chance to develop AD are diverse. Individuals carrying the e4 allele of the apolipoprotein E (APOE) are more likely to come down with AD due to impaired clearance of soluble Aβ (Corder et al., 1993; Castellano et al., 2011). Two copies of the e4 allele increase the risk by 8- to 12-fold, often accompanied by early onset of the disease (Saunders et al., 1993; Farrer et al., 1997).

One further risk factor is expressed on microglial cells. In AD, microglial immune response to deposition and increased phagocytosis of Aβ lesions is strongly mediated by triggering receptor expressed on myeloid cells 2 (TREM2) expression as part of the innate immune system (Kleinberger et al., 2014; Selkoe and Hardy, 2016; Keren-Shaul et al., 2017; Mazaheri et al., 2017). TREM2 is highly associated with an increased risk for AD shown by decreased numbers

of recruited microglia to Aβ lesions after deletion of one TREM2 allele (Jonsson et al., 2013; Ulrich et al., 2014). TREM2 is a transmembrane immune receptor mainly expressed by microglia and is proteolytically cleaved by a disintegrin and metalloprotease 10 and 17 (ADAM10 and ADAM17), two α-secretases, causing the production of soluble TREM2 (sTREM2) (Schmid et al., 2002; Feuerbach et al., 2017; Jay et al., 2017; Schlepckow et al., 2017; Thornton et al., 2017). Increased levels of sTREM2 during Aβ deposition have been detected in the cerebrospinal fluid (CSF) from individuals carrying autosomal dominant mutations for AD. sTREM2 levels correlate well with other neuronal injury markers suggesting a potential role of the shed ectodomain in the context of biomarker research (Heslegrave et al., 2016; Piccio et al., 2016; Suárez-Calvet et al., 2016a, 2016b; Zhong et al., 2017, 2019). sTREM2 promotes the microglial inflammatory response by proliferation, recruitment to Aβ lesions and increased Aβ phagocytosis, supporting TREM2 as a potential target for therapeutical approaches (Zhong et al., 2017, 2019).

Besides, individuals with a positive AD family history are on high risk (Fratiglioni et al., 1993; Lautenschlager et al., 1996; Green et al., 2002). If first-degree relatives were diagnosed with AD, individuals are more likely to develop this disease (Loy et al., 2014; Gordon et al., 2018). However, the most common risk factor for AD is age (Hebert et al., 2010, 2013). Nowadays, three percent of people at the ages of 65 to 74 have AD, whereas people at the age of 85 or above are at a 32 percent risk (Hebert et al., 2013). The major share (> 99 percent) of all AD cases is characterized by a late onset of symptoms and a sporadic origin of Aβ dyshomeostasis (Ballard et al., 2011; Selkoe and Hardy, 2016).

Surprisingly, a few years ago, Jonsson et al. found a beneficial missense mutation that protects from cognitive decline by decreasing BACE1 cleavage of APP. The mutation alleviates Aβ production by up to 40 percent and alters Aβ aggregation properties. Mutation carriers show a lifelong protection from AD which additionally supports the amyloid hypothesis (Jonsson et al., 2012; Benilova et al., 2014; Zheng et al., 2015).

1.4 Aβ – a therapeutic target for potential intervention

So far, the U.S. Food and Drug Administration (FDA) has approved six drugs for the treatment of AD — Galantamine, Donepezil, Rivastigmine, Memantine, Memantine combined with Donepezil, and Tacrine, however, Tacrine has been discontinued in the United States since 2013 (Cummings et al., 2014; Gupta, 2014; Alzheimer Association, 2019). All of these drugs, except Memantine, are acetylcholine-esterase inhibitors to temporarily decelerate symptom worsening, preferentially in patients with mild-to-moderate AD (Rogers et al., 1998; Francis et al., 1999; Hansen et al., 2008; Rodda et al., 2009). During the disease process, the neurotransmitter acetylcholine becomes depleted causing reduced signal transduction in brain (Rylett et al., 1983; Nilsson et al., 1986). Along with diagnosis of first cognitive deficits, acetylcholine-esterase inhibitors can be administered to sustain the remaining signal transduction. Memantine, an uncompetitive N-methyl-D-aspartate (NMDA)-type glutamate receptor antagonist, prevents excessive receptor stimulation in order to enhance cognition. Memantine is preferentially applied to patients at the moderate-to-severe stage (Reisberg et al., 2003; Witt et al., 2004). Unfortunately, none of the present drugs changes the course of disease progression, rising need for new therapy (Alzheimer Association, 2019). Therefore, many treatment strategies now focus on Aβ as the key trigger for disease and develop Aβ-limiting approaches (Hardy and Selkoe, 2002).

1.4.1 Modulation of Aβ production

During the pathogenesis of AD, accumulation of toxic Aβ species seems to be a critical event. Therefore, reduction of Aβ before toxic seeds have formed might prevent the formation of Aβ amyloids. The *de novo* production of soluble Aβ fragments requires the functionality of BACE1 and the γ-secretase. Thus, inhibition or modulation of secretase activity tends to be a promising disease-modifying therapy for AD. The γ-secretase complex cleaves the C-99 fragment at the carboxy-terminal site into the APP intracellular domain (AICD) and an Aβ fragment of variable length depending on the exact γ-secretase cleavage position (Wolfe, 2014). Many clinical trials have tried to target γ-secretase activity by inhibitors. Within the last years, Semagacestat (Eli Lilly) and Avagacestat (Bristol) were two of the most promising candidates. But, trials were stopped due to strong side effects caused by off-target inhibition (Coric et al., 2012; Doody et al., 2013). Since the γ-secretase has more than 50 substrates, e.g. Notch, all tested inhibitors missed enhanced substrate selectivity (Kopan and Ilagan, 2004; De Strooper, 2014).

On this basis, BACE1 as a potential target with less off-target side effects came more into focus of research for upstream interference with the amyloid cascade (Al-Tel et al., 2011; Coimbra et al., 2018). Under physiological conditions, neurons show high levels of BACE1 expression, especially at synaptic terminals compared to other cell types (Deng et al., 2013; Kandalepas et al., 2013). During disease state, BACE1 is further upregulated by ~2-fold around amyloid plaques compared to healthy individuals (Fukumoto et al., 2002; Yang et al., 2003; Li et al., 2004).

Similar to the γ-secretase, BACE1 constitutes a therapeutical target by lowering Aβ production and thereby inhibiting the formation of seeding active, toxic Aβ species (Ye et al., 2015). But, safety issues were also raised for BACE inhibitors. The secretase has two isoforms, namely BACE1, which is present in the central nervous system, and BACE2, which has 64 % similarity in amino acids and is a secretase of the peripheral body (Bennett et al., 2000; Laird et al., 2005). One major challenge of current BACE1 inhibitors is their cross-inhibition of BACE2 (Farzan et al., 2000). Additionally, BACE1 does not only cleave type 1 membrane proteins similar to APP, but also more complex forms serve as a substrate. BACE1 knockout mice and their neurological phenotypes gave hint at a wide range of different BACE1 substrates involved in normal physiology (Yan and Vassar, 2014; Barão et al., 2016). Aβ production highly relies on the activity of BACE1. Thus, inhibition of BACE1 in APP transgenic mice has been reported to reduced soluble Aβ (Roberds et al., 2001; Jacobsen et al., 2014; Ou-Yang et al., 2018).

Importantly, BACE1 is highly expressed during development (Hu et al., 2006; Willem et al., 2006). Therefore, BACE1 germline knockout mice show a detrimental phenotype. The myelination process by Schwann cells is disturbed, leading to hypomyelination and failed protein-protein interaction for axon guidance and neuronal survival in mice (Montag-Sallaz et al., 2002; Dominguez et al., 2005; Laird et al., 2005; Willem et al., 2006; Hu et al., 2010; Rajapaksha et al., 2011; Cao et al., 2012; Hitt et al., 2012; Fleck et al., 2013; Barão et al., 2015). In adult conditional knock-out mice, effects on myelination are absent but reduced length and disorganization of hippocampal mossy fiber intrapyramidal bundles by reduced cleavage of the axon guidance protein close homolog of L1 (CHL1) can be observed (Salzer, 2012; Ou-Yang et al., 2018).

BACE2 knockout mice reveal a high expression of this homolog in β cells of the pancreas. Mice show elevated insulin concentrations combined with improved glucose regulation and β-cell mass (Esterházy et al., 2011).

Despite many negative results gained from BACE knockout experiments, BACE1 inhibition studies were performed. During the course of BACE1 inhibitor development, many major challenges aroused. In the beginning, peptide based analogs of APP served as an inhibitor, with low oral bioavailability, long serum half-life and weak penetration of the blood brain barrier (BBB) (Hong et al., 2002). Improvements in research generated highly lipophilic small molecule inhibitors with advantages in BBB crossing. Unfortunately, these compounds served as a substrate for the efflux pump, preventing high inhibitor concentrations in brain. However, current third generation BACE1 inhibitors show enhanced pharmacokinetics and robustly remove Aβ in brain, allowing the application in clinical trials (Evin et al., 2011; Probst and Xu, 2012).

BACE1 inhibitor studies were conducted in different transgenic mouse models for cerebral β-amyloidosis and revealed beneficial effects after partial and transient inhibition by reducing the production of soluble Aβ in brain to baseline levels (Neumann et al., 2015; Bacioglu et al., 2016). BACE1 inhibition normalized behavioral deficits and alleviated neuroinflammatory responses (Lazic et al., 2019). Side effects have been reported in wildtype (wt) mice after long-term BACE1 inhibition. In detail, deficits in spine density and formation, long-term potentiation and cognition were demonstrated (Filser et al., 2015; Zhu et al., 2018).

Many BACE1 inhibitor studies in APP transgenic mice were performed with the well characterized BACE1 inhibitor NB-360 (Novartis). NB-360 is a very potent small molecule (third generation) inhibitor with excellent brain penetration, improved metabolism and no inhibition of cathepsin D and E (CatD/E) to avoid retinal toxicity (Fielden et al., 2015). The compound does not show a major increase in efflux rate by the p-glycoprotein but declines in parallel in brain and blood over time. NB-360 BACE inhibition completely blocks the process of Aβ increase in APP transgenic mice, rats and dogs in a dose- and time-dependent manner (Neumann et al., 2015). High levels of NB-360 (13 mg/kg) inhibited soluble brain Aβ40 in depositing mice by more than 90%. Similarly, Aβ increase in CSF was prevented by 80% after single treatment (Neumann et al., 2015). Even pre-depositing mice showed similar results (Neumann et al., 2015). Extended NB-360 treatment for six months was performed in APP transgenic mice and reduced Aβ deposition by more than 70% and brain Aβ levels by more than 90% compared to age-matched controls (Bacioglu et al., 2016).

Unfortunately, NB-360 inhibits BACE1 and BACE2 equipotently. Altered BACE2 secretase activity acts on the pigment cell specific melanocyte protein (PMEL) causing reduced PMEL

processing based on impaired melanin storage in melanocytes. This leads to irreversible hair depigmentation in NB-360-treated mice (Cichorek et al., 2013; Rochin et al., 2013; Neumann et al., 2015; Shimshek et al., 2016). Nevertheless, NB-360 seems to be able to mimic beneficial results and mechanism-based side effects of BACE1 inhibitor treatment in humans, which are described in the next chapter (Neumann et al., 2015; Shimshek et al., 2016).

In a different mouse model for β-amyloidosis, BACE1 inhibition upregulated α-secretase activity (Neumann et al., 2015). The α-secretase is responsible for the non-amyloidogenic processing of APP. This secretase cleaves APP within the Aβ sequence, thereby preventing the production of toxic Aβ. As a proof of principle, a mutation in ADAM10, which is the most prominent α-secretase in neurons, has been shown to decrease its activity and causes higher Aβ production by BACE1 (Kuhn et al., 2010; Suh et al., 2013). Some therapeutical approaches try to push the non-amyloidogenic pathway by upregulation of the α-secretase. Treatment of mice with this sort of modulators has been shown to increase cognition and reduce plaques. But, off-target effects again play a major detrimental role (Lichtenthaler, 2011).

1.4.1.1 BACE1 inhibition in symptomatic AD patients

Nowadays, BACE1 inhibition is a major therapeutic strategy and led to many advanced clinical BACE1 inhibitor trials in mild-to-moderate AD patients. However, all trials thus far failed to meet their primary endpoint, namely beneficial effects on cognition (Hawkes, 2017; Egan et al., 2018, 2019; Honig et al., 2018; Mullane and Williams, 2018). In the next paragraph, past most advanced BACE1 inhibitor trials are examined.

One promising candidate was the BACE1 inhibitor Verubecestat (Merck & Co. Inc.) exhibiting good tolerability. Unfortunately, Verubecestat inhibited BACE2 to a great extent. This went along with hair depigmentation and limited brain penetration (Cebers et al., 2016; Kennedy et al., 2016; Egan et al., 2018). Verubecestat robustly reduced CSF Aβ in mild-to-moderate AD patients. But, phase 3 clinical trials failed to cause effects on disease progression and were haltered for futility at interim analysis (Kennedy et al., 2016; Egan et al., 2018). In individuals with MCI, Verubecestat was able to cause significant reduction of brain amyloid, which was shown by Positron Emission Tomography (PET) and reduced CSF Aβ by more than 60%. But, subjects showed an unexpected increase in worsening of cognition (Egan et al., 2019).

The second promising and very advanced inhibitor was Lanabecestat (AstraZeneca/Eli Lilly & Co). This BACE1 inhibitor demonstrated a dose- and time-dependent reduction of CSF, plasma and brain Aβ40 and Aβ42 in mice, guinea pigs and dogs. Unfortunately, limited selectivity of BACE1 caused hair discoloration, weight loss and cognitive worsening in subjects of a phase 3 trial and primary outcomes were missed (Streffer et al., 2016; Janssen, 2018; Henley et al., 2019; Wessels et al., 2019). For both Verubecestat and Lanabecestat, off-targeting suggested major effects on the outcome.

Therefore, great hope was placed for the BACE1 inhibitor Elenbecestat (Biogen/Eisai Co.), which had an approximately 3-fold higher affinity for BACE1 over BACE2, thereby preventing hair depigmentation and minimizing potential adverse effects by off-target inhibition. Previous phase 2 studies revealed good safety, tolerability and robust reduction of brain amyloid (Lynch et al., 2018). In 2016, two promising phase 3 trials (MISSION AD1/AD2) started in subjects with biomarker-confirmed MCI. Primary outcomes aimed at benefits in cognition. Unfortunately, both mission trials were discontinued in September of 2019 due to unfavorable risks (Eisai and Biogen, 2019).

1.4.2 Aβ elimination by immunization

Chronic neuroinflammation is one prominent characteristic of AD caused by massive brain Aβ load (Newcombe et al., 2018). During disease progression, the increasing imbalance between Aβ production and its clearance causes microgliosis, but activated microglia fail to remove arising debris (Hardy and Higgins, 1992; Butovsky and Weiner, 2018; Alzheimer Association, 2019). Therapy that is directly aimed at increased clearance by microglia, e.g. by nonsteroidal anti-inflammatory drugs, constitutes a potential treatment target (Gupta et al., 2015). Therapeutic importance of microglia in the context of disease progression was recently shown in tau transgenic-ApoE4 mice. Depletion of microglia prevented neurodegeneration in these mice. Results suggest microglia-mediated innate immune response as the major driver for neurodegeneration rather than direct neurotoxicity from tau pathology (Kemal and Vassar, 2019; Shi et al., 2019).

With regard to potential treatment of AD, the removal of various Aβ species from the brain by immunotherapy is suggested to be a major therapeutic strategy. Many immunization studies cause an Fc receptor-mediated removal of brain Aβ by upregulation of the immune response (Bard et al., 2000; DeMattos et al., 2012; Yoon and Jo, 2012; Fuller et al., 2014). Besides active

vaccination, many present therapeutical strategies use passive immunization to promote antibody-mediated clearance of Aβ. In general, Aβ-targeting antibodies can be divided into two groups regarding their binding affinity to different Aβ species. Some antibodies target rather soluble Aβ, whereas others can interact with aggregated, insoluble forms of Aβ. Besides, antibodies which target truncated forms of Aβ, e.g. amino-terminally pyroglutamate-modified Aβ, have been generated (Nussbaum et al., 2012). Antibody binding to Aβ causes increased clearance presumably by the activation of microglia-mediated amyloid degradation (Bard et al., 2000; DeMattos et al., 2012). However, several recent clinical trials of anti-Aβ antibodies in patients with mild-to-moderate AD have been stopped due to lack of efficacy. Other reasons for discontinuation were side effects like cerebral hemorrhages of amyloid-laden vessels (Pfeifer et al., 2002). In AD patients, these Amyloid-Related Imaging Abnormalities (ARIA) can be detected during Magnetic Resonance Imaging (MRI) (Sperling et al., 2011c).

1.4.2.1 Immunization studies in symptomatic AD patients

Anti-Aβ immunization constitutes a further promising therapeutic strategy in order to modify disease progression. In the beginning, active immunization to promote anti-Aβ antibody production was intensively tested in clinical trials. Unfortunately, applied antigens led to severe side effects. One example of active immunization is the compound AN-1792 (Janssen Pharmaceutica/Pfizer Inc.), which indeed revealed a *post mortem* reduction of Aβ deposition. But, this drug additionally induced meningeal inflammation in a phase 2 study and therefore was discontinued (Gilman et al., 2005; Serrano-Pozo et al., 2010).

As a result, passive immunization moved more into the focus of research, expecting less pronounced adverse events and better tolerability (Graham et al., 2017). Selected most promising antibodies are listed below.

Solanezumab (Eli Lilly & Co.) is a humanized IgG1 monoclonal antibody and binds to the mid-domain of Aβ. It recognizes soluble, monomeric Aβ, stabilizes these Aβ species and prevents the formation of neurotoxic Aβ aggregates (Yamada et al., 2009). m266, the murine version of Solanezumab, diminished memory decline in mice, but no effect on Aβ plaque load could be detected (Dodart et al., 2002). In AD patients, Solanezumab caused a dose-dependent elevation of CSF and plasma Aβ (Farlow et al., 2012; Uenaka et al., 2012). Two phase 3 studies (EXPEDITION 1/2) in subjects with mild-to-moderate AD confirmed the increase in CSF and plasma total Aβ after immunization. Unfortunately, no beneficial effect on cognition was

reached, leading to the discontinuation of the Solanezumab study arm (Doody et al., 2014). Even earlier treatment of individuals with biomarker-confirmed mild AD in the phase 3 EXPEDITION 3 trial failed to achieve improvements in the primary cognition outcome. Additionally, Solanezumab did not reduce brain Aβ in PET (Siemers et al., 2016; Honig et al., 2018).

Crenezumab (Genentech Inc.) is a humanized monoclonal IgG4 antibody. The antibody binds multiple Aβ species but has highest affinity for oligomers, fibrils and aggregated assemblies thereby promoting disaggregation (Adolfsson et al., 2012; Ultsch et al., 2016; Zhao et al., 2017a). Unfortunately, phase 2 studies did not show beneficial results (Cummings et al., 2018; Salloway et al., 2018). In January 2019, two phase 3 trials (CREAD1/2) in subjects with mild AD were discontinued based on results from interim analysis. The analysis indicated that Crenezumab will not meet primary study outcomes (ClinicalTrials.gov Identifier: NCT02670083 and NCT03114657).

Although most antibodies have failed to achieve their primary and secondary endpoints, some trials in symptomatic subjects are still ongoing. The following antibodies stir up hope for treatment success.

Donanemab (Eli Lilly & Co.) is a humanized IgG1 monoclonal antibody and binds pyroglutatmate-modified Aβ species (Alzforum). In mice, pyroglutamate-Aβ has been shown to accumulate at late stages of disease progression (DeMattos et al., 2012). Immunization studies in individuals with mild-to-moderate AD demonstrated reduced plaque load and Aβ PET signal. Some cases showed evidence for ARIA-hemosiderin (ARIA-H). Safety, tolerability and the efficacy of this antibody in early symptomatic AD are now investigated in an ongoing phase 2 trial (TRAILBLAZER-ALZ), which will be completed in 2021 (ClinicalTrials.gov Identifier: NCT03367403).

BAN2401 (Biogen/Eisai Co., Ltd.) is a humanized monoclonal IgG1 antibody and binds large soluble Aβ protofibrils. In APP transgenic mice, the murine version of this antibody (mAb158) was able to reduce Aβ protofibrils in CSF and brain (Tucker et al., 2015). In March 2019, a phase 3 trial (CLARITY AD) started to enroll individuals with early symptomatic AD. The core study focusses on changes in cognition as a primary outcome, but the extension phase additionally gives attention to biomarker changes, e.g. CSF Neurofilament light chain (NfL) and CSF Aβ as the primary outcome. This trial is one of the few trials, that is still recruiting

subjects, raising the chance for future successful intervention (ClinicalTrials.gov Identifier: NCT03887455).

The third seminal antibody in trial is Gantenerumab (Chugai Pharmaceutical Co., Ltd., Hoffmann-La Roche), which is a fully human recombinant monoclonal IgG1 antibody. The antibody binds to the amino-terminus of Aβ thereby preferentially binding oligomers and fibrils, but monomers to a less extent (Bohrmann et al., 2012). In patients with mild-to-moderate AD, Gantenerumab reduced brain Aβ amyloid burden in a dose-dependent manner (Ostrowitzki et al., 2012). Investigations in subjects with mild AD were performed in three phase 3 trials (Marguerite RoAD, GRADUATE1/2) and revealed a high safety profile at high doses. Unfortunately, Marguerite RoAD was discontinued due to failed interim futility analysis, but the two GRADUATE trials remain ongoing (Abi-Saab et al., 2017; ClinicalTrials.gov Identifier: NCT03444870 and NCT03443973).

Latest surprise was the outcome of the antibody Aducanumab (Biogen Inc.). Aducanumab is a recombinant human IgG1 antibody obtained from healthy old individuals. The antibody binds a conformational epitope of Aβ at the amino-terminus with a >10,000-fold selectivity of soluble Aβ aggregates and insoluble fibrils over monomers based on avidity effects (Sevigny et al., 2016; Arndt et al., 2018). In APP transgenic mice, the murine version of Aducanumab (*cm*Aducanumab) reduced brain Aβ load in young, but not in aged mice (Kastanenka et al., 2016). In two identical phase 3 trials (ENGAGE and EMERGE) which enrolled individuals with prodromal AD confirmed by a positive florbetapir PET, the antibody reduced brain amyloid in a dose-and time-dependent manner and also slowed cognitive decline by a decrease in the Clinical Dementia Rating-Sum of Boxes (CDR-SB) score compared to baseline. Unfortunately, Aducanumab induced ARIA-Edema (ARIA-E) but abnormalities did not evoke symptoms (Sevigny et al., 2016). However, in May 2019, Biogen and Eisai decided to terminate the ongoing ENGAGE and EMERGE studies based on interim analysis, which revealed that these studies are unlikely to meet their primary endpoints. Surprisingly, in October 2019, Biogen announced that prior analyses of a subset of the cohort led to incorrect results of the futility analysis. According to latest outcomes including a larger data set, the EMERGE trial indeed did reduce cognitive decline at the highest dose. ENGAGE trial results were less clear, but also indicated a tendency for beneficial outcome (Biogen, 2019). On this basis, Biogen now plans to pursue the FDA regulatory approval for Aducanumab within the next months. If approved, Aducanumab would be the first approved antibody to alleviate AD cognitive decline through the removal of pre-existing Aβ burden.

1.4.3 Lessons learned from Aβ clinical failures

Although the development of BACE1 inhibitors and anti-Aβ immunization therapies resulted in highly advanced strategies trying to gain control over the progression of AD, no single new drug was approved after Memantine in 2003 (Panza et al., 2019). For more than 15 years now, clinical trials fail to find a potent drug and discussed reasons for failure are diverse. Since the cause of disease still remains poorly understood, this lack of knowledge may hamper the development of new therapy by incorrect choice of agent, inappropriate drug dosing or low target engagement and adverse effects as futility (De Strooper, 2014; Karran and Hardy, 2014; Hsu and Marshall, 2017; Egan et al., 2018; Panza et al., 2019). Outcomes from clinical trials show a high rate of failure for BACE1 inhibitor trials (Mullard, 2017; Piton et al., 2018; Cummings et al., 2019). Major problems evolved in the context of efficacy as the reduction of Aβ production after initiation of deposition showed unfavorable effects on disease progression. This again raised issues of BACE1 as a suitable therapeutical target (Egan et al., 2018). Furthermore, crossing of the BBB and inhibitor selectivity over homologous proteases, e.g. BACE2, and the inhibition of substrates that are necessary for physiological function, present challenges in BACE1 inhibitor drug development. Thus, failures of BACE1 trials reveal a need for inhibitors with increased brain penetration along with advanced substrate selectivity.

Similarly, almost two decades ago, the first anti-Aβ vaccine had failed, pronouncing a long-lasting sequence of failure in amyloid-based immunotherapies. Many of the studies were associated with side effects as increased ARIA (e.g. Sperling et al., 2011c; Sevigny et al., 2016). Especially for immunization studies, failure of trials may be explained by the late initiation of treatment during the pathogenic process, i.e., when tauopathy, inflammation, neuron loss and other neurodegenerative sequelae have become pronounced. Another explanation for failure could be the missing ability of Aβ antibodies to target the most pathogenic Aβ assemblies. Thus, the inappropriate subject selection along with inadequate outcome measures could contribute to failure (e.g. Panza et al., 2019). Therefore, younger study cohorts should be investigated.

1.5 Prevention by early intervention – the ultimate approach?

Unfortunately, none of the previous clinical trials was able to cause favorable, long-lasting changes on cognition, indicating that current therapy in symptomatic AD patients might be applied too late. The process of amyloid deposition has been shown to follow three different stages, with the lag phase being the rate limiting step (Jarrett and Lansbury, 1993; Kawarabayashi et al., 2001). For an optimal and long-lasting reduction of Aβ pathology, disruption and blockage of the initial phase of Aβ aggregation appears most promising, at a preclinical stage of disease (De Strooper and Karran, 2016; Jack et al., 2018). Nowadays, cerebral Aβ positivity can be detected at least two decades before signs and symptoms appear (McDade et al., 2018; Villemagne et al., 2018). However, to determine the time point of initial aggregation, early detection of biomarker changes is essential allowing the consideration of secondary prevention, and even earlier primary prevention approaches, as described in the following paragraphs and in Figure 1.

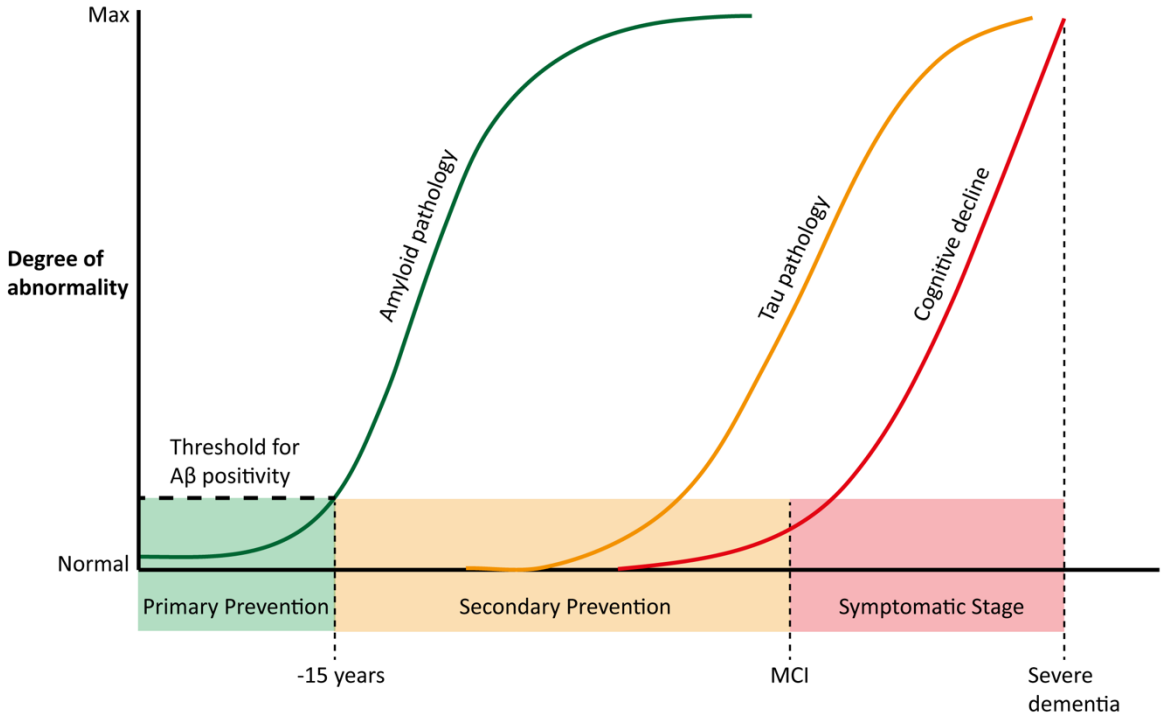

Figure 1. Different stages of preventive intervention within the continuum of AD. The stage for secondary prevention is characterized by preclinical intervention when Aβ positivity (and further biomarker changes) can be detected. More than 15 years prior to symptom onset, primary prevention is applied at sub-threshold Aβ levels to prevent disease before Aβ dyshomeostasis occurs. Current approaches focus on individuals at genetically determined high risk for AD (modified from McDade and Bateman, 2017).

1.5.1 Biomarkers as risk indicators for disease

So far, clear diagnosis of AD was only possible *post mortem* or at very late disease stage, when neuropathological lesions and neuronal loss were established (Lane et al., 2018). At this stage, clinical symptoms and activity deficits in daily living could be evaluated by different criteria (i.e. Diagnostic and Statistical Manual of Mental Disorders, 5th edition (DSM-V) or National Institute of Neurological and Communicative Disorders and Stroke – Alzheimer's Disease and Related Disorders Association (NINCDS-ADRDA)) and disease was surmised by tentative diagnosis or exclusion. However, histopathologic evidence was required for definite diagnosis.

Nowadays, diagnosis of AD is no longer based on the clinical phenotype but can be classified by pathophysiological changes irrespective of the cognitive condition according to the recent National Institute on Aging – Alzheimer's Association (NIA-AA) research framework. Thus, the pre-clinical stage was precisely re-defined enabling the diagnosis at asymptomatic stages. Individuals are classified as having preclinical AD, if asymptomatic cases show Aβ increase above a certain threshold. Above this threshold, individuals reach Aβ positivity. Additionally, new guidelines also underline the importance of Aβ before Aβ positivity is reached, i.e. at sub-threshold levels (Selkoe and Hardy, 2016; Jack et al., 2018; Bischof and Jacobs, 2019; Palmqvist et al., 2019). In detail, AD is diagnosed, if changes in Aβ and tau are detected by fluid biomarkers (Aβ42 or Aβ 42/40 ratio and phosphorylated (p-)tau), or PET imaging reveals Aβ and parenchymal neurofibrils. Neurodegeneration is claimed to be not specific for AD, but can support diagnosis by structural MRI, ^{18}F-fluorodeoxyglucose (FDG) PET or CSF total (t-)tau (Jack et al., 2018).

Reliable biomarkers are highly important to determine the time point of first Aβ aggregation thereby identifying individuals at risk. This is necessary in order to apply precise and effective treatment (Sperling et al., 2014a; Knopman, 2019). Furthermore, biomarkers can mirror disease progression and are able to predict the clinical onset of AD (Preische et al., 2019). In many diseases, biomarker measurements allow the prediction of drug target engagement and the response to therapy. Besides, they can be used to detect downstream effects as neurodegeneration (Novakova et al., 2017; Zetterberg, 2017; Olsson et al., 2019).

Knowledge about the succession of measurable biomarkers during disease progression was gained from significant changes in their trajectories (Egan et al., 2018; Honig et al., 2018; Knopman, 2019; Palmqvist et al., 2019; Selkoe, 2019). CSF Aβ42 presents the first detectable biomarker based on its decline more than two decades before first clinical symptoms appear in

both early and late onset AD, correlating with first Aβ deposition in brain (Bateman et al., 2012; Jack et al., 2013; Villemagne et al., 2013; Olsson et al., 2016; Palmqvist et al., 2019). This is in comply with the amyloid hypothesis which suggests Aβ as the initial trigger accumulating decades before the clinical stage (Hardy and Higgins, 1992). Also very early, fluid biomarkers as Aβ42/40 ratio and levels of p-tau and t-tau in CSF are altered. CSF tau has been shown to be highly linked to Aβ deposition, especially p-tau (Maia et al., 2013; Olsson et al., 2016; Schelle et al., 2017).

After Aβ deposition is detected via PET, further changes are demonstrated for CSF NfL (neurodegeneration) as well as CSF neurogranin (synaptic dysfunction) and CSF YKL-40 (glial activation and neuroinflammation) (Palmqvist et al., 2019). Since PET imaging is very expensive and CSF sampling by lumbar puncture in humans is an invasive procedure, more convenient biomarkers are needed. Based on today's ultrasensitive measurement technologies, many originally CSF-based biomarkers are now investigated in blood, which is easier accessible and allows multiple sampling. For Aβ42, Aβ40, Aβ42/40 ratio and p-tau plasma biomarkers, no difference in their timepoints of change during disease progression has been shown. But, blood markers exhibit higher variability and lower available levels, resulting in less clear results (Bacioglu et al., 2016; Zetterberg and Blennow, 2018). Hitherto, the change of one single biomarker is not enough to clearly predict and monitor disease. Most sensitive and specific detection of pathological changes can be achieved, if a combination of longitudinal data from serial PET imaging and different fluid biomarkers is obtained in order to diagnose AD or exclude other diseases (Zetterberg et al., 2003; Höglund et al., 2015; Jack et al., 2018; McDade et al., 2018; Preische et al., 2019).

Within the last years, NfL came more to the fore of biomarker research. Together with larger microtubules and smaller microfilaments, highly phosphorylated and cross-linked NfL builds up the axonal cytoskeleton. In general, neurofilaments are heteropolymers and can consist of three different subunits, a heavy, a medium and a light chain (Ishikawa et al., 1968; Petzold, 2005). The structure of all three subunits contains an α-helical rod domain, which is responsible for assembly, flanked by a non-α-helical head and tail domain. (Geisler et al., 1983; Hisanaga et al., 1990; Nakamura et al., 1990). During physiological conditions, NfL is abundantly expressed by large axons and has been proposed to constitute a compound of synapses (Yuan et al., 2015). Studies in nondemented adults and wt mice revealed a slight NfL increase during the normal aging process, similar to the age-related association of NfL and cognition (Bacioglu et al., 2016; Zetterberg et al., 2016; Osborn et al., 2019).

In neurodegenerative diseases, the expression of NfL is altered based on neuronal damage and its release into the interstitial fluid and CSF, giving insight into disease progression of various diseases, not specifically AD (Petzold, 2005; Neselius et al., 2012; Kuhle et al., 2015; Bacioglu et al., 2016; Rohrer et al., 2016; Zetterberg et al., 2016; Hansson et al., 2017; Zetterberg and Blennow, 2018). In different APP transgenic mouse lines, an early and significant increase in CSF NfL was revealed compared to wt mice. Moreover, former studies demonstrated a robust coupling of Aβ and NfL changes. After blockage of Aβ deposition in young mice, CSF NfL was highly attenuated (by more than 60%) compared to controls, suggesting NfL as a treatment response marker (Bacioglu et al., 2016).

According to the latest definition of AD, every biomarker is investigated regarding its change before and after the threshold for Aβ positivity is reached. Unlike other biomarkers, CSF NfL has two points of inflection in its trajectory evolving during the continuum of AD. NfL correlates with disease progression and other biomarkers as t-tau and p-tau, neurogranin, and chitinase-3-like protein (Zetterberg et al., 2016; Jin et al., 2019). This suggests NfL to be a very sensitive biomarker in early neurodegeneration in contrast to other markers, e.g. different imaging techniques (Osborn et al., 2019). The first increase in NfL levels is found already one decade before clinical symptom onset (Mattsson et al., 2017; Weston et al., 2017; Palmqvist et al., 2019; Preische et al., 2019). The second NfL increase, which is more pronounced, occurs after Aβ PET positivity is reached (Palmqvist et al., 2019). At this later disease stage, NfL also correlates with the Mini-Mental State Examination (MMSE) score over time, white matter changes and increased brain atrophy (Sjögren et al., 2001; Migliaccio et al., 2012; Zetterberg et al., 2016). Chronic inflammation is one factor that enhances NfL, thus leading to cognitive impairment and dementia (Jack et al., 2013; Sperling et al., 2014a). Over the last years, advantages in technology promoted NfL as the first robust blood-based biomarker for neurodegeneration (Bacioglu et al., 2016; Gisslén et al., 2016; Mattsson et al., 2017; Zetterberg and Blennow, 2018). Studies revealed that AD-positive blood NfL correlates with levels in CSF as well as glucose metabolism in many brain areas and disease stages (Weston et al., 2017; Benedet et al., 2019; Osborn et al., 2019). But, no data has been published for blood NfL in comparison to imaging biomarkers, yet (Zetterberg et al., 2016; Chatterjee et al., 2018; Mattsson et al., 2019). In future, a reliable blood test may allow the detection of very early pathological changes by blood NfL in individuals at risk for AD.

One example for intense investigations of NfL is the Dominantly Inherited Alzheimer Network (DIAN) cohort, collecting individuals with mutations in the APP, PSEN1 or PSEN2 gene

causing familial AD (Hsu and Marshall, 2017). Recent investigations revealed CSF and serum NfL changes more than six years before the calculated estimated symptom onset (EYO). Moreover, differences in the rate of change were visible in mutations carriers even 16 years earlier compared to controls (Preische et al., 2019). Therefore, detection of early pathological changes in individuals at risk for AD are highly important in order to develop potent therapy.

1.5.2 Secondary prevention to reduce the impact of risks

Failure or ambiguous outcomes of studies in mild-to-moderate AD patients suggest that intervention initiation in subjects after clinical symptom onset might be too late. Therefore, subject selections of clinical trial cohorts were modified within the last years. Nowadays, few studies were started recruiting cognitively normal subjects carrying an increased risk for AD. These initiated secondary prevention trials are characterized by an early intervention. At this stage, asymptomatic individuals already show Aβ positivity, as depicted in Figure 1. Instead of reversing cognitive decline, emerging pre-symptomatic secondary prevention trials aim at a long-lasting delay or even the total prevention of symptom onset and functional decline (Sperling et al., 2014a). Advancements in current biomarker research allow the early detection of abnormalities at preclinical AD stage, thereby identifying individuals at risk, as described in chapter 1.5.1. But, trials in non-symptomatic populations require uncommon primary outcome measures that quantify clinically highly relevant biomarker changes rather than advancements in cognition (Hsu and Marshall, 2017).

1.5.2.1 Immunization studies in asymptomatic individuals

The first discontinued secondary prevention study was Janssen's EARLY trial. Non-symptomatic subjects with high risk for AD were recruited and treated with the BACE1 inhibitor Atabecestat. Unfortunately, individuals showed side effects as depression, anxiety and sleep impairments, seriously elevated liver enzymes and no slowdown of cognitive worsening in this phase 3 trial. This led to the discontinuation of the EARLY trial in May 2018 (Streffer et al., 2016; Janssen, 2018; Henley et al., 2019).

Additionally, five further large secondary prevention trials also started to recruit cognitively normal individuals and are still ongoing, although some study arms were suspended.

The Alzheimer's Prevention Initiative (API) Autosomal-Dominant AD (ADAD) trial recruited pre-symptomatic individuals carrying an autosomal dominant mutation in PSEN1. The study uses the antibody Crenezumab for early passive immunization. Results are expected in 2020 (ClinicalTrials.gov Identifier: NCT0199884; Reiman et al., 2012; Farlow et al., 2015).

The next two phase 2/3 API trials recruit homozygous APOE4 carriers or subjects with one APOE4 allele but with evidence for amyloid deposition (GENERATION1/2; ClinicalTrials.gov Identifier: NCT02565511 and NCT03131453). These studies would like to reveal effects in a cognitively unimpaired cohort based on their age and APOE genotype. In these trials, the antibody arm uses active immunization with the compound CAD106 (Novartis) to stimulate the production of antibodies against Aβ (Winblad et al., 2012; Farlow et al., 2015). The BACE1 inhibitor arms use different concentrations of Umibecestat (CNP520; Novartis/Amgen) on a daily basis to lower the production of soluble Aβ. The small molecule BACE1 inhibitor Umibecestat is highly selective for BACE1 over BACE2 and CatD, preventing retinal degeneration. The inhibitor showed no hair discoloration, but rather had an excellent safety and tolerability profile suitable for long-term application. The efficacy study reported a high reduction by up to 95% in CSF Aβ40 after multiple dosing. If applied only once, Umibecestat was able to reduce CSF Aβ40+42 by more than 75% in beagle dogs (Neumann et al., 2018).

In July 2019, interim analyses revealed cognitive worsening after BACE1 inhibition compared to the placebo group resulting in the termination of all Umibecestat arms of the API trials. Subjects showed a faster cognitive decline along with further adverse effects as increased brain atrophy and larger body weight loss (Novartis International AG, 2019). The CAD106 group of the API program will continue.

For all API trials, the primary aim is a shift in the diagnosis of MCI/AD or to achieve a change in the composite of different cognitive tests, the API cognitive composite (APICC) (Langbaum et al., 2015). Results of this study will be expected in 2024 (Lopez Lopez et al., 2017, 2019). Secondary outcomes include changes in the CDR-SB score as well as in biomarkers, e.g. CSF Aβ and tau, brain amyloid and tau PET.

The forth preventive study is realized in the DIAN-Trials Unit (DIAN-TU), a unique cohort with focus on families carrying a mutation in APP, PSEN1 or PSEN2. Individuals at high risk to develop AD later in life allow not only longitudinal biomarker investigations but are also recruited for secondary prevention trials (Bateman et al., 2012, 2017; Morris et al., 2012; Hsu and Marshall, 2017). In the ongoing secondary prevention study, subjects receive monthly

passive anti-Aβ immunization with either Gantenerumab or Solanezumab in order to achieve changes in the DIAN-TU cognitive composite score (Bateman et al., 2017; Ostrowitzki et al., 2017). The study is expected to be completed in 2021 (ClinicalTrials.gov Identifier: NCT01760005).

Fifth, the Anti-Amyloid Treatment in Asymptomatic Alzheimer's Disease (A4) trial has been started including cognitively normal individuals at high risk for AD based on biomarker changes and Aβ amyloid burden in brain determined by PET (Sperling et al., 2011b, 2013, 2014b). Subjects receive monthly infusions of the anti-Aβ antibody Solanezumab for approximately three years. The primary outcome should show significant changes in a composite of different cognitive tests. Biomarker changes are considered in the secondary outcome measures. This study will be completed in 2022 (ClinicalTrials.gov Identifier: NCT02008357; Sperling et al., 2014b).

At present, all secondary prevention studies or -study arms using BACE inhibitors are discontinued due to cognitive worsening of the participants. The remaining ongoing secondary prevention trials exclusively use active or passive anti-Aβ immunization. An overview about the intervention targets of these immunization trials at this early stage within the process of Aβ accumulation are visualized in Figure 2.

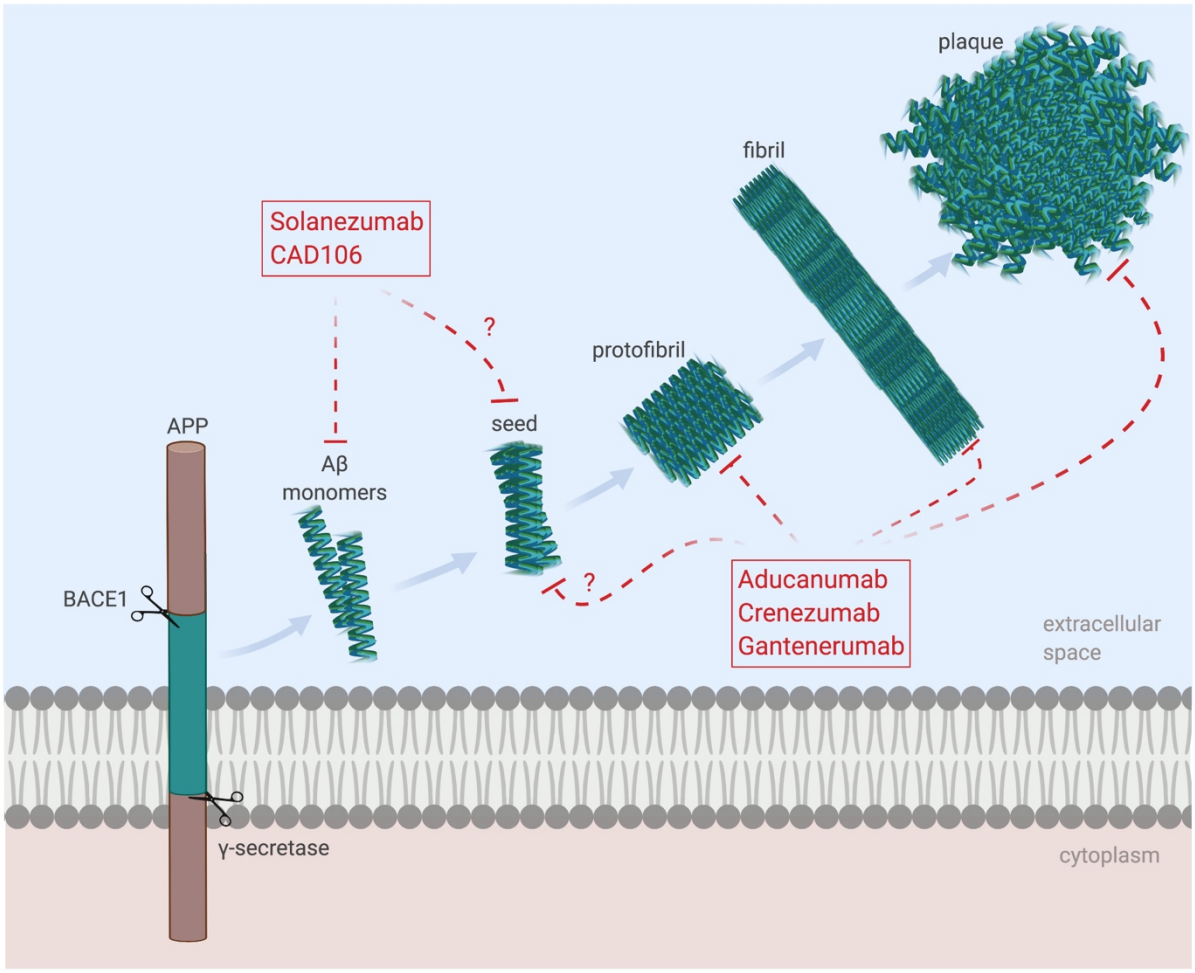

Figure 2. Potential therapeutic targets in secondary prevention trials evolve during the process of Aβ accumulation. In the amyloidogenic pathway, secreted Aβ peptides are generated by BACE1 and the γ-secretase sequential APP cleavage. Monomeric Aβ is prone to form highly seeding-active Aβ oligomers (seeds), which can further aggregate to form protofibrils. Elongation generates longer fibrils which can accumulate into large Aβ plaques. In secondary prevention trials recruiting individuals at risk for AD, active immunization and different therapeutic anti-Aβ antibodies bind various Aβ species to prevent Aβ deposition. Solanezumab and CAD106 increase the elimination of monomeric Aβ whereas Aducanumab preferentially binds soluble and insoluble aggregated forms of Aβ. Similarly, Gantenerumab and Crenezumab bind to protofibrils, fibrils and large Aβ aggregates.

1.5.3 Primary prevention to retard the risk to develop disease

Although benefits on cognition are hoped in secondary prevention trials, it is still an open question whether these interventions are able to cause long-lasting effects. PET and fluid biomarkers indicate Aβ deposition at least two decades before the appearance of signs and symptoms (McDade et al., 2018; Villemagne et al., 2018). Therefore, consistent with prior findings and the outcome of clinical trials, the best strategy to maintain non-toxic Aβ levels might be therapy acting at initial stages when Aβ is not accumulated, yet (Figure 1). Thus, the most effective therapeutic strategy is likely to be primary prevention interfering with the Aβ cascade at sub-threshold Aβ levels before Aβ deposition or biomarker changes are detectable (Hsu and Marshall, 2017; McDade and Bateman, 2017). Disadvantages of these trials would rise from long treatment duration causing high costs. Additionally, medication needs to be extremely safe because it might be applied throughout life or could be exposed to non-affected cases due to potential early misdiagnosis. However, the exact timeframe of such early intervention has not been determined yet, since both Aβ-PET and CSF Aβ readouts become positive only at a stage when Aβ deposition in brain is well underway (Palmqvist et al., 2016; Landau et al., 2018; Thal et al., 2018; La Joie et al., 2019).

The first primary prevention trial is planned in the DIAN-TU, recruiting young adults at risk for AD due to a mutation in an AD-related gene (described above). Individuals are able to participate in the study until 15 years prior to the EYO. Unfortunately, the treatment strategy is not defined yet due to recent failures of many promising drugs (McDade and Bateman, 2017).

Biogen's latest release revealed a misleading futility analysis of prior Aducanumab studies. Recent results indicate that the anti-Aβ antibody Aducanumab has great potential. Therefore, Aducanumab would be a potential candidate for a primary prevention trial (Biogen, 2019). Until first testing, the beneficial outcome in this sub-threshold treatment population remains unknown.

2 Aim of my studies

Failure of clinical trials on AD more and more urge research into younger, asymptomatic trial populations to achieve preventive and long-lasting outcomes. Biomarker research has revealed first pathological changes already decades before clinical symptom onset, indicating that current therapy is administered too late. Therefore, effective prevention therapy might be applied at initial stages of pathology or even before first biomarker changes become detectable.

In the first part of this study, the importance of early treatment initiation is assessed. We investigate the susceptibility for intervention at different stages of disease pathology. Additionally, the effect of chronic Aβ lowering in APP transgenic mice mimicking the pathological process of AD is determined. Hence, BACE1 inhibitor treatment is evaluated regarding its ability to cause significant and long-lasting treatment success by downstream alleviation of neurodegeneration.

During the crucial, initial stage of disease, highly seeding-active Aβ oligomers tend to be formed as one main contributor to the onset of AD later on. According to the amyloid hypothesis, removal of such toxic oligomeric species could be able to halter disease progression. In the second part, with greater focus on the initial phase of pathology, we test the hypothesis that biologically active Aβ seeds are present *in vivo* before Aβ aggregation and that deposition becomes detectable with current methods. Additionally, we determine whether such "pre-amyloid" seeds can be targeted therapeutically. Therefore, murine or murinized versions of well-characterized human Aβ antibodies and a new technique to determine the Aβ-assembly recognition profile of the antibodies were used. We would like to provide evidence for the presence of pathogenic Aβ seeds during the lag-phase of Aβ deposition. Thus, acute targeting of such seeds may be an effective paradigm for the prevention of AD**.**

3 Material and methods

Experimental Animals

Hemizygous Tg(Thy1-APPSw,Thy1-PSEN1*L166P)21Jckr (APPPS1), C57BL/6J-TgN (Thy1.2-hAPP751-KM670/671NL)23 (APP23) and C57BL/6JNpa-Tg(Thy1App)23/1Sdz (APP23N) mice were bred at the Hertie Institute for Clinical Brain Research (Tübingen, Germany). APPPS1 mice and non-transgenic littermates (C57BL/6; wt) were used for BACE1 inhibitor experiments. APPPS1 mice were generated on a C57BL/6J genetic background. They overexpress the human APP transgene harboring the Swedish double mutation and co-express human mutated presenilin (L166P) under the neuron-specific Thy1 promoter element (Stürchler-Pierrat et al., 1997; Radde et al., 2006). Mice exhibit a mean survival time of approximately 22 months (Ye et al., 2017). APPPS1 mice show first Aβ deposition after six weeks, starting at the neocortex and hippocampus of the forebrain. At 12 months of age, deposits have spread throughout the entire cortex (Radde et al., 2006). Mice do not show effects by gender; thus, both male and female mice were used in all BACE1 inhibitor experiments.

APP23 mice were used for the short-term and long-term immunization studies. APP23N mice were used as hosts for the *in vivo* seeding assay. APP23N mice and non-transgenic littermates (C57BL/6; wt) were used for titer experiments. No difference in phenotype of the two APP23 strains has been noted, and thus they are abbreviated in the text as APP23 mice. APP23 mice only overexpress the human APP transgene with the Swedish double mutation (Stürchler-Pierrat et al., 1997). APP23 mice develop Aβ deposition at 6-12 months of age depending on the brain region studied, and male mice exhibit deposition later than females (Stürchler-Pierrat et al., 1997; Eisele et al., 2010; Ye et al., 2017). Only male animals were used for antibody treatment to minimize variability and to expand the length of the pre-depositing phase during which nascent seeds could be analyzed.

All mice were kept under specific pathogen-free conditions. The experimental procedures were carried out in accordance with the veterinary office regulations of Baden-Wuerttemberg (Germany) and approved by the local Animal Care and Use Committee.

Human brain tissue

Tissue samples were obtained from the mid-frontal gyrus of three pathologically and clinically diagnosed AD cases (54, 62 and 77 years of age; all Braak stage VI; *post mortem* time 5.5 – 6.5 hours). The samples were obtained from the Emory University Alzheimer's Disease Research Center (ADRC). Human *post mortem* tissues were acquired under proper Institutional Review Board (IRB) protocols with consent from families.

BACE1 inhibitor treatment

Male and female APPPS1 and wt mice were fed with food pellets containing the BACE1 inhibitor NB-360 (Novartis, Basel, Switzerland) at a dose of 0.5g NB-360/kg food pellets (Neumann et al., 2015; Schelle et al., 2019). Pellets were available *ad libitum*. Animals were treated with the inhibitor for the following months of ages: young group: 1.5 – 4.5 months, adult group: 12 – 15 months, aged group: 18.5 – 21.5 months, half-lifelong group: 12 – 21.5 months and lifelong group: 1.5 – 21.5 months. Age-matched control groups received food pellets without the compound NB-360. Mice were randomly assigned to the treatment groups. During the treatment period, mice were monitored on a daily basis by animal caretakers or researchers. No significant differences in body weights between BACE1 inhibitor–treated and control mice were detected.

Aβ antibodies

The following antibodies were recombinantly generated based on publicly available sequence information: Chimeric murinized (*cm*) version of the human antibody Gantenerumab (*cm*Gantenerumab, *cm*Gant; Bohrmann et al., 2012); *cm*-version of the human antibody Aducanumab (*cm*Aducanumab, *cm*Adu; Sevigny et al., 2016; Arndt et al., 2018); m266 which is the murine parent version of Solanezumab (DeMattos et al., 2001); mC2 which is the murine parent version of Crenezumab (Adolfsson et al., 2012); and mE8, which is the murine parent version of Donanemab (DeMattos et al., 2012, www.alzforum.org/therapeutics/donanemab). For all antibodies (except *cm*Gantenerumab), the variable heavy-chain and light-chain domain were fused with the IgG2a constant heavy-chain and mouse kappa constant light-chain domains (Fuller et al., 2015; Sevigny et al., 2016). For *cm*Gantenerumab, the IgG1 constant heavy-chain

was used. In brief, synthetic genes for the variable light chain-murine kappa constant domain and variable heavy chain-mIgG constant domain were sub-cloned into expression vectors for mammalian cell expression. Transfected cells were cultured until the viability had dropped and culture media harvested by centrifugation and ultrafiltration. Antibodies were purified from clarified culture media either by protein-A or protein-G Sepharose affinity chromatography followed by buffer exchange into phosphate-buffered saline (PBS; Invitrogen, Carlsbad, CA) using standard protocols for monoclonal antibody purification. Finally, antibodies were sterile filtered using 0.2-µm filters and stored at -80°C. *cm*Gantenerumab, m266, and mC2 were provided by Lundbeck (Copenhagen, Denmark), *cm*Aducanumab was provided by Biogen (Cambridge, MA), and mE8 was provided by the Fraunhofer Institute for Cell Therapy (Dresden, Germany). Since these recombinant antibodies have been generated in different laboratories, minor differences in the expression cassettes cannot be excluded. Mouse monoclonal antibody Beta1 (IgG2a) has been described previously (Paganetti et al., 1996; Meyer-Luehmann et al., 2006). As control antibodies, monoclonal murine anti-wheat auxin IgG2a (Amsbio, Abingdon, UK) and murine IgG2a antibody P1.17 (unknown antigen; Sevigny et al., 2016) as control 1 (Ctrl 1) and control 2 (Ctrl 2), respectively, were used.

Intraperitoneal application of antibodies

Aliquoted antibodies were thawed on ice and injected intraperitoneally (0.5 mg/mouse/day) for five consecutive days. APP23 mice were sacrificed either six weeks (short term) or six months (long term) after the first injection. For the antibody titer experiments, APP23 and wt mice were sacrificed 1, 7 or 21 days after the last injection. For all experiments, mice were randomly assigned to the treatment groups except for the short-term experiment with mE8. mE8-treated APP23 mice and additional anti-wheat auxin IgG2a mice were run in a separate batch.

Collection of brain and CSF

Mice were anesthetized with a mixture of 10% ketamine (115 mg/kg body weight) and 5% xylazine (10 mg/kg body weight) in NaCl. CSF was collected as previously described (DeMattos et al., 2002; Bacioglu et al., 2016). In brief, the cisterna magna was accessed by puncture of the dura mater with a syringe (30G, 0.3mm x 8mm needle size), and CSF was collected with a 20 µl GELoader tip (Eppendorf Vertrieb, Wesseling-Berzdorf, Germany). CSF

was centrifuged at 2,000 x g for 10 minutes and frozen at -80°C. Following collection, the mouse was perfused transcardially with ice-cold PBS. The brain was removed and bisected by a mid-line sagittal cut, and the lower brainstem and cerebellum were removed by a cut through the rostral midbrain. The left forebrain was frozen on dry ice and stored at -80°C for later biochemical analyses. The right forebrain was fixed in 4% paraformaldehyde in PBS at 4°C for 48h, cryoprotected in 30% sucrose in PBS, and snap-frozen in 2-methyl-butane.

Biochemical analysis of Aβ

Brain tissue was homogenized at 10% (w/v) in sterile PBS or homogenization buffer (150 mM NaCl, 5 mM EDTA, 50 mM Tris, Pierce protease and phosphatase inhibitor (Thermo Fisher Scientific, Waltham, MA)) with the Precellys®24 high-throughput tissue homogenizer (Bertin Technologies, Montigny-le-Bretonneux, France; 7 ml lysing tubes with 2.8 mm ceramic beads) at 5,500 rpm twice for 10 seconds with a 10 second break in between. Homogenates were aliquoted and stored at -80°C until biochemical analysis. In the BACE1 inhibitor study, Aβ in brain homogenate was extracted by formic acid (FA). Thus, brain aliquots were thawed on ice, mixed 1:3.2 with cold FA (Sigma-Aldrich; minimum purity of 96% diluted in H_2O) and sonicated on ice for 35 seconds. Samples were centrifuged at 25,000 x g at 4°C for one hour. Supernatants were equilibrated (1:20) with neutralization buffer (1 M Tris base, 0.5 M Na_2HPO_4, 0.05% NaN_3 (w/v)). Aβ in the supernatant was measured as described below.

In immunized mice, Aβ was serially extracted from brain homogenate. First, 130 µl of homogenate were thawed on ice and mixed with 130 µl 2% Triton X-100 in PBS. Samples were incubated on ice for 15 minutes and vortexed every five minutes, followed by ultracentrifugation at 100,000 x g at 4°C for 15 minutes. The supernatant was collected and aliquoted for later analysis ("Triton-soluble fraction"). The pellet was mixed with cold 70% (v/v) FA (Sigma-Aldrich; minimum purity of 96% diluted in H_2O; volume according to aspirated supernatant) and sonicated on ice for 35 seconds. Samples were centrifuged at 25,000 x g at 4°C for one hour and supernatants were neutralized (1:20) with neutralization buffer (1 M Tris base, 0.5 M Na_2HPO_4, 0.05% NaN_3 (w/v)). This latter fraction was termed the "FA-soluble fraction".

In both studies, brain Aβ was measured by an electrochemiluminescence (ECL)-linked immunoassay (Meso Scale Discovery, MSD, Gaithersburg, MD) as previously described (Ye

et al., 2017). In the BACE1 inhibitor study, brain extracts were diluted in buffer (Diluent 35, Meso Scale Discovery) to enable Aβ measurement within the linear range of the assay as follows: young group: undiluted (baseline), 1:10 (BACE1 inhibitor; BI) and 1:30 (control), adult group: 1:100, aged group: 1:300, half-lifelong group: 1:300 and lifelong group: 1:10 (BI) and 1:300 (control). In the immunization study, FA-soluble brain extracts from the long-term study were diluted 1:10 in buffer (Diluent 35, Meso Scale Discovery). For the BACE1 inhibitor and immunization study, the commercially available V-PLEX Aβ Peptide Panel 1 (6E10) Kit and the V-PLEX Aβ Peptide Panel 1 (4G8) Kit (Meso Scale Discovery, MSD, Gaithersburg, MD) were used respectively, according to the manufacturer's instructions. In brief, pre-coated 96-well plates were blocked for one hour with buffer (Diluent 35, Meso Scale Discovery) and washed three times with 0.05% Tween-20 (Carl Roth, Karlsruhe, Germany) in PBS (v/v). Brain extracts were incubated with the SULFO-TAG™-labeled 6E10/4G8 detection antibody for two hours at room temperature. After washing, MSD Read Buffer T was added. The plate was immediately read on the Sector Imager 6000. Data analysis was performed using the MSD DISCOVERY WORKBENCH software 2.0. Internal reference samples were measured as controls on every plate.

Brain Aβ in homogenates from 2-8 months old untreated APP23 mice (Figure 6, panel A) was determined after FA-extraction as described above. Brain Aβ was measured by the single molecule array (Simoa) technology using the Simoa™ Human Aß40 1.0 and Simoa™ Human Aß42 1.0 Kits (Quanterix, Billerica, MA) according to manufacturer's instructions. For the Aβ measurements, the FA-extracted brain samples were diluted as follows: Aβ40: 1:16 and Aβ42: 1:4 in Simoa Aβ40 and Aβ42 sample diluent, respectively (Quanterix, Billerica, MA).

Brain sTREM2 determination

To determine sTREM2 in brain, brain homogenates were mixed 1:2 with Tris-buffered saline (TBS) and were incubated on ice for 15 minutes with regular vortexing. Extracts were centrifuged at 100,000 x g for 15 minutes. The supernatant was used to determine murine sTREM2 by an ECL-linked immunoassay (Meso Scale Discovery, MSD, Gaithersburg, MD). In detail, a 96-well plate was coated with the capture antibody AF1729 (0.2µg/ml, R&D Systems, Minneapolis, MN) at 4°C overnight. Plates were washed three times with washing buffer (0.5% Tween-20 in TBS) and blocked with 2% bovine serum albumin in washing buffer for one hour at room temperature shaking at 100 rpm. After washing, samples were added and

incubated for two hours at room temperature shaking at 100 rpm, followed by another washing step. sTREM2 was detected by the biotinylated anti-mTREM2 antibody BAF1729 (R&D Systems, Minneapolis, MN) at a concentration of 0.5µg/ml (in 0.5% bovine serum albumin in washing buffer). The plate was incubated for one hour at room temperature shaking at 100 rpm and afterwards washed again. Brain extracts were incubated with SULFO-TAG™-labeled Streptavidin (1:400 in PBS) for one hour at room temperature at 100 rpm in the dark. After washing, MSD Read Buffer T was added. The plate was immediately read on the Sector Imager 600. Data analysis was performed using the MSD DISCOVERY WORKBENCH software 2.0. Internal reference samples were measured as controls on every plate. Recombinant mouse TREM2 (Novoprotein Wuijang, Suzhou, China) from 39 pg/ml to 2500 pg/ml was used as standard.

CSF NfL concentration

NfL concentrations in CSF were determined using the highly sensitive Simoa™ NF-Light Advantage assay Kit (Quanterix, Billerica, MA). In the BACE1 inhibitor study, CSF NfL in the young, adult and aged group was pre-diluted and measured in two independent measurements to confirm results. Murine CSF samples were pre-diluted in sample diluent as follows: young group: 1:75 and 1:75, adult group: 1:75 and 1:300, aged group: 1:500 and 1:1000, half-lifelong group: 1:1000, wt half-lifelong group: 1:75 and lifelong group: 1:1000 (control); 1:500 (BI). If data from two NfL measurements was available, the mean of both measurements is shown. Mice were excluded, if < 10µl CSF could be taken. For the immunization study, murine CSF samples were pre-diluted 1:100 in sample diluent. All samples were measured in duplicate on a Simoa HD-1 Analyzer (Quanterix, Billerica, MA) according to the manufacturer's instructions, and as previously reported (Bacioglu et al., 2016; Preische et al., 2019).

Intracerebral injections of brain extract

Bilateral stereotaxic injections of 2.5 µl brain homogenate (10% (w/v) in sterile PBS (see *Biochemical analysis of Aβ*) from mice treated with Ctrl2- or *cm*Adu-antibody were performed. Homogenate from all Ctrl2 or *cm*Adu mice were pooled and mixed before injection, respectively. Brain homogenates were injected into the hippocampus using a Hamilton syringe (anteroposterior, −2.5 mm; left/right, ±2.0 mm; dorsoventral, −1.8 mm) at a rate of 1.25

µl/minute. The needle was held in the injection site for additional two minutes before being slowly withdrawn. The surgical site was cleaned with sterile PBS, the incision was closed and the mice were constantly monitored until recovery from anesthesia.

Histology and immunohistochemistry

Fixed hemibrains were sectioned coronally into 25 µm-thick slices using a freezing-sliding microtome (SM2000 R, Leica Biosystems, Wetzlar, Germany) and sections were collected in 12-well plates containing cryoprotectant solution (35% ethylene glycol and 25% glycerol in PBS). Tissue sections were stained immunohistochemically with a polyclonal antibody directed against Aβ (CN6; a successor to antibody CN3; Eisele et al., 2010). Microglial staining was undertaken by staining with a rabbit polyclonal anti-Pu.1 antibody (1:1,000, Cell Signaling, Danvers, MA) or a rabbit polyclonal anti-Iba1 antibody (1:500; Wako Chemicals, Neuss, Germany). Mouse monoclonal antibody AT8 (Thermo Fisher Scientific, Waltham, MA) recognizing tau phosphorylated at Ser-202 and Thr-205 was used to stain p-tau-positive neuritic changes (Stürchler-Pierrat et al., 1997). For all immunostainings, the Vectastain Elite ABC kit (Vector Laboratories, Burlingame, CA) was used as previously described (Eisele et al., 2010). Sections were co-stained with Congo Red according to standard protocols. To study bleedings, we used both Perls' Prussian Blue to visualize ferric iron in hemosiderin and hematoxylin and eosin (H&E), as previously described (Winkler et al., 2001).

Representative bright-field images were obtained with the Zeiss Axioplan 2 microscope (Carl Zeiss MicroImaging, Jena, Germany) with a Zeiss AxioCam HR digital color camera. Overview images were taken with the 4x/0.1 objective (Zeiss) and processed with the AxioVision 4.7 MosaiX software. Detailed plaque images were collected with the 63x oil/1.4 objective (Zeiss). For all other images, the 10x/0.3 objective (Zeiss) was used.

Quantitative morphology

Aβ load was quantified on serial, systematically sampled and CN6/Congo Red-stained coronal sections. In every 36th section, Aβ was quantified in the neocortex, whereas for seeding experiments in the hippocampus, every 12th section was analyzed. This typically resulted in 4-5 sections for the neocortex and 5-7 sections for the hippocampus. Stereological analysis was

performed blinded using a microscope with a motorized *x-y-z* stage coupled to a video-microscopy system (Stereo Investigator; MicroBrightField) as previously described (Meyer-Luehmann et al., 2006). Aβ load was determined by calculation of area (%) covered by Aβ-positive staining in two-dimensional sectors at a single focal plane (20x/0.45 Zeiss Achroplan).

To quantify the number and size of individual Aβ plaques, CN6/Congo Red double-stained sections were scanned on a Zeiss AxioScan.Z1 slide scanner (10x/0.45 Plan-Apochromat, Carl Zeiss Microscopy GmbH, Göttingen, Germany) at a digital resolution of 0.442 µm/pixel. Within each image field, z-stacks were acquired, flattened to a single plane using a wavelet-based extended depth of field algorithm. A custom-written plugin for ImageJ automatically scaled down images to a resolution of 1.326 µm/pixel for Aβ plaque visualization and segmentation. The neocortex was manually outlined, and for this analysis, every 12th section throughout the neocortex was used. Images were transformed to grayscale using the luminance function of ImageJ. Objects with an area of less than 50 µm^2 were excluded in order to avoid over-segmentation.

Cerebral β-amyloid angiopathy (CAA) frequency and severity in the neocortex were manually assessed using every 12th CN6/Congo Red-stained section. The CAA score was calculated by multiplying CAA frequency by CAA severity, as previously described (Winkler et al., 2001; Schelle et al., 2019).

For the quantification of Aβ plaque-associated microglia after immunization, Pu.1-immunopositive cells around Congo Red-positive plaques were counted on every 12th section through the neocortex. On each section, ten plaques (if less than ten plaques were found, the maximal number present was taken) were randomly determined and the microglia (nuclei) in the immediate vicinity (i.e. two-fold the plaque diameter) of each plaque were counted. The diameter and area of each Congo Red-positive plaque were determined with the Stereo Investigator software. Then, the number of microglia per µm^2 plaque was assessed. The number of total plaque-associated microglia was calculated by the average number of microglia associated with plaques multiplied by the total plaque number, as described above.

In order to assess microglial reaction to BACE1 inhibitor treatment, 25 µm-thick, Iba1/Congo Red double-stained brain sections were scanned on the slide scanner as described above. Microglia size and area coverage was automatically analyzed using a custom-written ImageJ plugin. Briefly, whole brain area was identified by the program. Grey-scale intensities were standardized by setting the maximum number of saturated pixels to 0.2% and subtracting the

background using a rolling ball radius of 100. The area covered by microglia was determined by considering all particles of intensities higher than 205 in an 8-bit scale. In each treatment group, the total area covered by microglia was normalized to the respective control group.

Antibody Recognition Profiling of Aβ assemblies (ARPA)

Aβ assemblies in 10% PBS brain homogenates were semi-natively separated by size using agarose electrophoresis (Bagriantsev et al., 2006). To this end, 2% low-melting agarose (w/v) (Thermo Fisher Scientific) in semi-denaturing buffer (200 mM glycine and 25 mM Tris base) was heated until dissolved. Sodium dodecyl sulfate (SDS) was added (final concentration of 0.1% (v/v)). The liquid agarose was poured into a gel cassette (Thermo Fisher Scientific) and a 10-well comb was placed in the gel. The polymerized gel was placed in a Bolt Mini Gel Tank (Thermo Fisher Scientific) and the chamber was filled with semi-denaturing buffer containing 0.1% SDS (v/v). Total protein concentration was determined by a bicinchoninic acid (BCA) assay (Thermo Fisher Scientific). 65 µg of brain homogenate was mixed with sample buffer (20 mM Tris-acetate (w/v), 0.5 mM EDTA (v/v), 2% SDS (v/v), 0.025% bromophenol blue (v/v), 5% glycerol (v/v)) and incubated for seven minutes at room temperature. Sample and SeeBlue Plus2 pre-stained protein standard (Thermo Fisher Scientific) were loaded. Gel electrophoresis proceeded until the phosphorylase marker band migrated 4 cm within the gel.

After protein separation, the agarose protein lane was fractionated into pieces of 0.7 cm x 0.5 cm for the comb fraction (F1), and 0.7 cm x 1 cm for all other fractions (F2 to F7) as illustrated in Figure 7 and supplementary Figure 1. Each agarose piece was placed in a 1.5 ml tube (Protein LoBind, Eppendorf AG) and used either for enzymatic liquefaction or for melting. For enzymatic digestion, elution buffer (50 mM Bis-Tris, 1 mM EDTA, pH 6.8) was added to gel fragments to a final concentration of 0.5% agarose (w/v). Samples were heated to 65°C for 10 minutes while shaking at 1,200 rpm. Liquefied samples were cooled to 43°C for 15 minutes. 0.5 U Agarase from *Pseudomonas atlantica* (Sigma-Aldrich) per 100 µl sample was added and incubated at 43°C for one hour while shaking at 1,200 rpm. Samples were snap-frozen on dry ice and stored at -80°C until further use for immunoprecipitation (as described below). Agarose pieces for melting were mixed with sample buffer (62.5 mM Tris-HCl pH 6.8; 8.3% glycerol (v/v), 2% SDS (v/v), 100 mM dithiothreitol (DTT), 0.025% bromophenol blue (w/v)) and heated to 90°C for 10 minutes. Melted fractions were analyzed by denaturing immunoblot analysis as described below.

Immunoprecipitation (IP) using Protein G Dynabeads™ (Thermo Fisher Scientific) was performed directly on PBS brain homogenates and on enzymatically digested agarose pieces (see above). Antibody bead conjugation was carried out according to the manufacturer's protocol. Aβ fractions (F1 to F7) were subjected to anti-Aβ antibody-conjugated Protein G Dynabeads™ (Thermo Fisher Scientific) and incubated overnight at 4°C while mixing. As the input for IP, 75-fold more fractionated brain homogenate was used for the young, predepositing brain homogenates compared to the β-amyloid-laden brain homogenates. Sample:bead ratios of 1:1 (amyloid-laden transgenic brain) to 5.25:1 (predepositing transgenic mice and AD brain tissue) were used. Beads were washed twice with PBS-T (0.05% Tween20 (v/v)) before elution with 1x NuPAGE LDS Sample Buffer (Thermo Fisher Scientific) containing 50 mM DTT at 70°C for 10 minutes. The supernatant was transferred to a new 1.5 ml tube (Protein LoBind, Eppendorf AG), snap-frozen on dry ice and stored at -80°C until denaturing immunoblot analysis on NuPAGE 4-12% Bis-Tris Protein Gels (Thermo Fisher Scientific) using 1x MES SDS Running Buffer (Thermo Fisher Scientific). Samples were blotted onto a nitrocellulose membrane (semi-dry; Bio-Rad Laboratories, Hercules, CA) that was equilibrated in glycine transfer buffer (192 mM glycine, 25 mM Tris base, 20% methanol (v/v)). The membrane was boiled in PBS for five minutes at 90°C and blocked in 5% milk in PBS-T (w/v) for one hour at room temperature. The membrane was probed with the anti-Aβ 6E10 antibody (1:2500; BioLegend, San Diego, CA) overnight at 4°C. The secondary horseradish peroxidase-coupled goat anti-mouse antibody (1:30,000; Jackson ImmunoResearch, Cambridgeshire, UK) was subsequently applied for one hour at room temperature. Between the antibody incubation steps, the membrane was washed five times for five minutes with PBS-T. Densitometric values from the Western Blot were obtained from highly sensitive X-ray films (Amersham Hyperfilm ECL, GE Healthcare, Chicago, IL) or a chemiluminescence imager (XSTELLA1.00; Raytest Isotopenmessgeräte GmbH, Straubenhardt, Germany) using SuperSignal West Dura Extended Duration Substrate (Thermo Fisher Scientific). Images from XSTELLA were further processed with the AIDA image analyzer v.4.27 (Raytest Isotopenmessgeräte GmbH). The amount of Aβ from a fraction was normalized to the total amount of Aβ detected in the sample. The contrast of immunoblots was adjusted for illustration purposes only.

Pharmacokinetics of antibodies in blood

Plasma antibody concentration was determined by ELISA. Lyophilized synthetic Aβ1-40 and Aβ1-42 peptides in trifluoroacetate salt (Bachem, Bubendorf, Switzerland) were dissolved in dimethyl sulfoxide (DMSO) at a concentration of 4.33 and 4.51 µg/µL, respectively. Peptides were aliquoted, stored at -80°C and later diluted to the target concentration in coating buffer (50mM Sodium Carbonate; pH 9.6 with $NaHCO_3$). Aβ1-40 was used for m266 while Aβ1-42 was used for Beta1. For *cm*Aducanumab, Aβ1-42 was pre-aggregated before adding it to the coating buffer. For pre-aggregation, 100 µM Aβ1-42 was incubated with 10 mM HCl (Merck, Darmstadt, Germany) and 150 mM NaCl (VWR Chemicals, Radnor, PA) in a final volume of 100 µL at 37°C for three days, and subsequently stored at 4°C. 96-well plates (Thermo Fisher Scientific) were washed with PBS (Gibco, Thermo Fisher Scientific) and coated with 10 ng of synthetic Aβ species in coating buffer at 4°C on a shaker at 40 rpm overnight. After coating, plates were washed four times with 0.05% PBS-T (0.05% v/v Tween-20) and blocked with 1% BSA (Sigma-Aldrich) in PBS-T at room temperature on a shaker at 40 rpm for two hours. Plates were washed with PBS-T and incubated with samples or standards diluted in 0.1% BSA in PBS-T at 4°C on a shaker at 40 rpm overnight. Every plate contained triplicates of a standard curve and plasma samples (diluted 1:200 and 1:2000), along with pooled controls from untreated male wt and six month old APP23 mice. Plates were washed with PBS-T and incubated with secondary antibody at room temperature on a shaker for two hours. For detection of m266 and Beta1, the alkaline phosphatase-conjugated AffiniPure rabbit anti-mouse IgG (H+L) antibody (1:5000; Jackson ImmunoResearch, Cambridgeshire, UK) was used. Afterwards, plates were washed with PBS-T. Plates were subsequently washed with detection buffer (10 mM diethanolamine (Sigma-Aldrich), 0.5 mM $MgCl_2$ (Merck, Darmstadt, Germany; pH 9.6)) and incubated with color reaction solution (16.89 mM 4-nitrophenyl phosphate (pNPP) (Sigma-Aldrich) in detection buffer) in the dark at room temperature for 15 minutes. Absorption was measured at 405 nm in a Mithras LB940 system (Berthold Technologies, Bad Wildbad, Germany). For *cm*Aducanumab, the peroxidase-conjugated AffiniPure goat anti-mouse IgG (H+L) antibody (1:2500; Jackson ImmunoResearch, Cambridgeshire, UK) was used for detection. Afterwards, plates were washed with PBS-T and incubated with TMB Substrate Solution (Thermo Fisher Scientific) for two minutes at room temperature followed by addition of stop solution (1M H_2SO_4; Merck). The absorbance was measured at 450 nm in a Mithras LB940 system. Absorbance values of standard curves were plotted versus the logarithmic concentration of the antibodies using the PRISM software (GraphPad; version 6). For Beta1, the curve was fitted to a 4PL symmetric model. For m266 and *cm*Aducanumab, the curve was

fitted to a 5PL asymmetric model. The standard curve was interpolated for the sample absorbance and the resulting concentrations were transformed back from the logarithmic concentration with a 10x function, to be subsequently corrected by dilution. The corrected concentrations were plotted versus time. The area under the curve was obtained through integration with the area under curve function at less than 10% distance from minimum and maximum y. The k_{el} was obtained from the natural logarithm of concentration-versus-time graph through linear regression.

Statistical analysis

All statistics were performed using the PRISM software (GraphPad; version 6) or Excel (Microsoft®; version 16). Data was tested for normality using the Shapiro Wilk Test. If the groups passed the normality test, one-way ANOVA was performed. If ANOVA revealed significant effects, *post hoc* Dunnett's multiple comparison test was applied. If the groups did not pass the normality test, the non-parametric Kruskal-Wallis test was used for comparison. Further analyses were performed using the *post hoc* Dunn's test. If only two groups were compared and data was normally distributed, the unpaired two-tailed *t*-test was used to compare population means. If the two groups did not pass the normality test, the Mann-Whitney U test was used for comparison. In the BACE1 inhibitor study, each treatment group was tested independently. The mean and standard error of the mean (SEM) are reported for each experimental group.

4 Aβ restriction by BACE1 inhibition is most effective at initial disease stages

4.1 Increase in brain Aβ, Aβ seeding activity and CSF NfL is age-dependent

Based on failure of former clinical trials using BACE1 inhibition to affect the progression of AD, we studied the effectiveness of BACE1 inhibitor treatment at different disease stages. To understand the effect of BACE1 inhibition as a potent therapeutic strategy to treat AD, we collected data from previous studies showing age-dependent increase of brain Aβ as the initial cause for Aβ pathology in a mouse model of β-amyloidosis (Figure 3A; blue). Additionally, previous data of seeding activity as one potential target of BACE1 inhibitor treatment and CSF NfL as a read-out for disease progression and treatment response were collected. All data was reassembled from previous studies performed in male and female APPPS1 mice (Bacioglu et al., 2016; Schelle et al., 2017; Ye et al., 2017 and in-house mouse biobank). Data revealed that the initial linear increase in brain Aβ starts at 1.5 months, concomitantly with first plaque deposition in APPPS1 mice at this early, prodromal disease stage. Aβ levels continue to accelerate constantly until mice are aged (approximately 18.5 months of age). During this late stage, brain Aβ reaches a plateau.

If brain material of APPPS1 donor mice is used in transmission experiments to seed Aβ in a host, the seeding activity (Figure 3A; yellow; half-maximal seeding dose; SD_{50}) of the extract is very potent at early donor age and reaches its plateau even before brain Aβ has come to the maximum increase (Ye et al., 2017). Compared to the trajectories of brain Aβ and Aβ seeding activity, CSF NfL, as a general marker for neurodegeneration, shows a much slower increase within the first months of life (Figure 3A; green). NfL levels have the steepest rise at later stage of Aβ deposition when Aβ is already in the plateau phase.

Based on the differential trajectories for brain Aβ and CSF NfL, male and female APPPS1 mice were treated with the potent BACE1 inhibitor NB-360 (Novartis) at different stages of disease progression and for different durations (Figure 3B). NB-360 intervention was performed continuously for three months in young (1.5-4.5 months), adult (12-15 months) and aged (18.5-21.5 months) mice to determine the most effective timepoint for BACE1 inhibition. Additionally, APPPS1 mice were treated chronically with NB-360 to investigate long-term advancements and potential side effects. Chronic interventions started either at 12 months (half-lifelong group) or the inhibitor was applied for the whole life starting at 1.5 months (lifelong

group). Both long-term studies were terminated at 21.5 months of age, shortly before APPPS1 mice reached their mean life span (Ye et al., 2017). In the half-lifelong group, additional wt mice were included to verify general tolerability of the inhibitor.

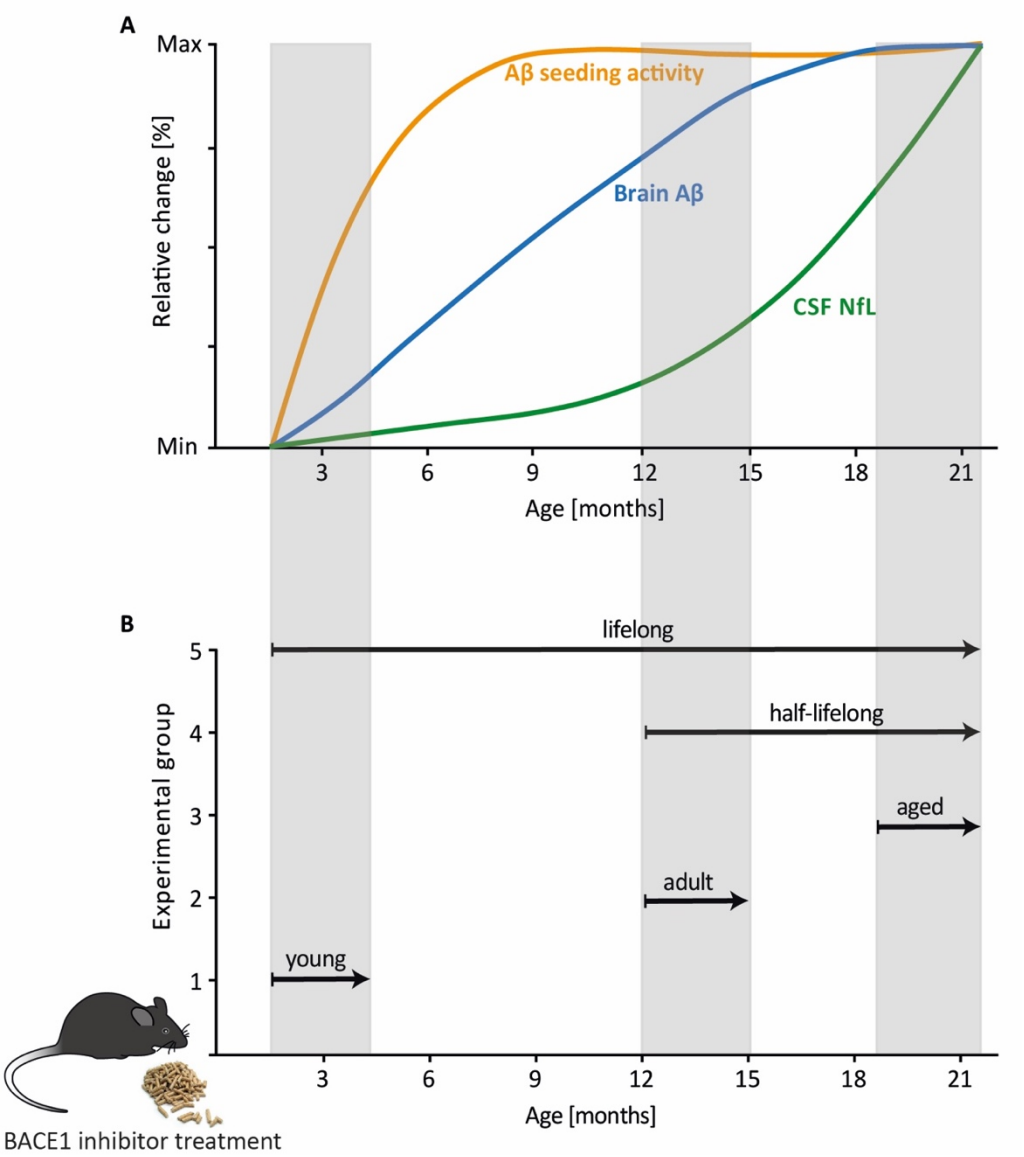

Figure 3. Age-dependent increase of brain Aβ, Aβ seeding activity and CSF NfL in APPPS1 mice computed from previous studies* result in various experimental groups. (A) Brain Aβ levels start to increase constantly from 1.5 months of age in accordance with first deposition in APPPS1 mice (blue). In aged mice (>18.5 months), brain Aβ levels reach a plateau with no net growth. Even before the detection of elevated brain Aβ levels, Aβ seeding activity of APPPS1 brain extract from donor mice (yellow) increases robustly within the first eight months and reaches a plateau very early in the process of amyloidosis (Ye et al., 2017). In contrast to brain Aβ and Aβ seeding activity, the CSF NfL profile reveals a relatively slow increase within the first 12 months of life (green). However, NfL increases rapidly in mice that are older than 12 months (late stage of Aβ pathology). *Data is collected from Bacioglu et al., 2016; Schelle et al., 2017; Ye et al., 2017 and in-house mouse biobank. **(B)** APPPS1 transgenic mice (in the half-lifelong group also wt mice) were treated with the potent BACE1 inhibitor NB-360 (Novartis) for a period of three months at an early, intermediate or late stage of Aβ deposition (at 1.5, 12, and 18.5 months, respectively) or chronically half-lifelong or lifelong (12 - 21.5 and 1.5 - 21.5 months, respectively) based on the different Aβ and NfL trajectories in these mice.

4.2 Early BACE1 inhibition halts pathology and even reduces brain Aβ

To evaluate the effect of upstream BACE1 inhibition on Aβ pathology, we determined FA-extracted brain Aβ40+42 levels in NB-360 treated APPPS1 mice. Chronic BACE1 inhibition experiments were performed and measured independently from the three months treatment groups leading to slightly higher absolute brain Aβ levels in the 21.5 months old lifelong control group compared to age-matched untreated controls from the aged and half-lifelong group (Figure 4A). NB-360 caused reliable blockage of Aβ increase in mice at different stages of Aβ pathology and after different treatment durations (Figure 4A). A general effect of BACE1 inhibition on Aβ levels remained throughout all age groups, but alleviated with increasing age. Adult mice showed a reduction by 40%, whereas Aβ levels were lowered by only 22% in aged APPPS1 mice compared to age-matched controls. Half-lifelong duration of intervention, which was initiated at 12 months of age, only decreased Aβ by 65%. However, treatment resulted in a most prominent reduction of brain Aβ in young animals by 96% compared to age-matched untreated controls. Similar to the results from the young group, a 96% reduction was achieved after lifelong treatment. Surprisingly, NB-360 treatment was even able to reduce brain Aβ below baseline levels in the plateau phase (adult and aged group; 30% and 22% below baseline, respectively).

Reduction of soluble Aβ after BACE1 inhibition might be able to affect the equilibrium between monomeric and aggregated Aβ forms, thereby disassembling deposited Aβ. To investigate this, deposited brain Aβ load was determined by stereological quantification of CN6/Congo red double-stained sections of mouse brains from all treatment groups. Similar to previous brain Aβ measurements, the increase of Aβ-positive area in BACE1 inhibitor-treated mice of all treatment groups was halted compared to age-matched controls (adult: 20%; aged: 9% and half-lifelong: 39% lower Aβ-positive area than control; Figure 4B). Again, most robust effects were obtained when BACE1 inhibitor treatment was initiated at the early stage of Aβ pathology (young and lifelong group; 85% and 69% reduction to controls, respectively). Noticeably, chronic NB-360 treatment was able to maintain low cortical Aβ load throughout life (Figure 4B/C). However, the reduction of brain Aβ below baseline level measured by ELISA (Figure 4A) was not mirrored by the decrease of Aβ deposits in the treatment groups quantified by stereology, except for the adult group (Figure 4B). Results indicate a less pronounced effect of BACE1 inhibition on deposited Aβ. Overall, massive effects of NB-360 on brain Aβ were induced by the timepoint of early intervention rather than by the duration of therapy.

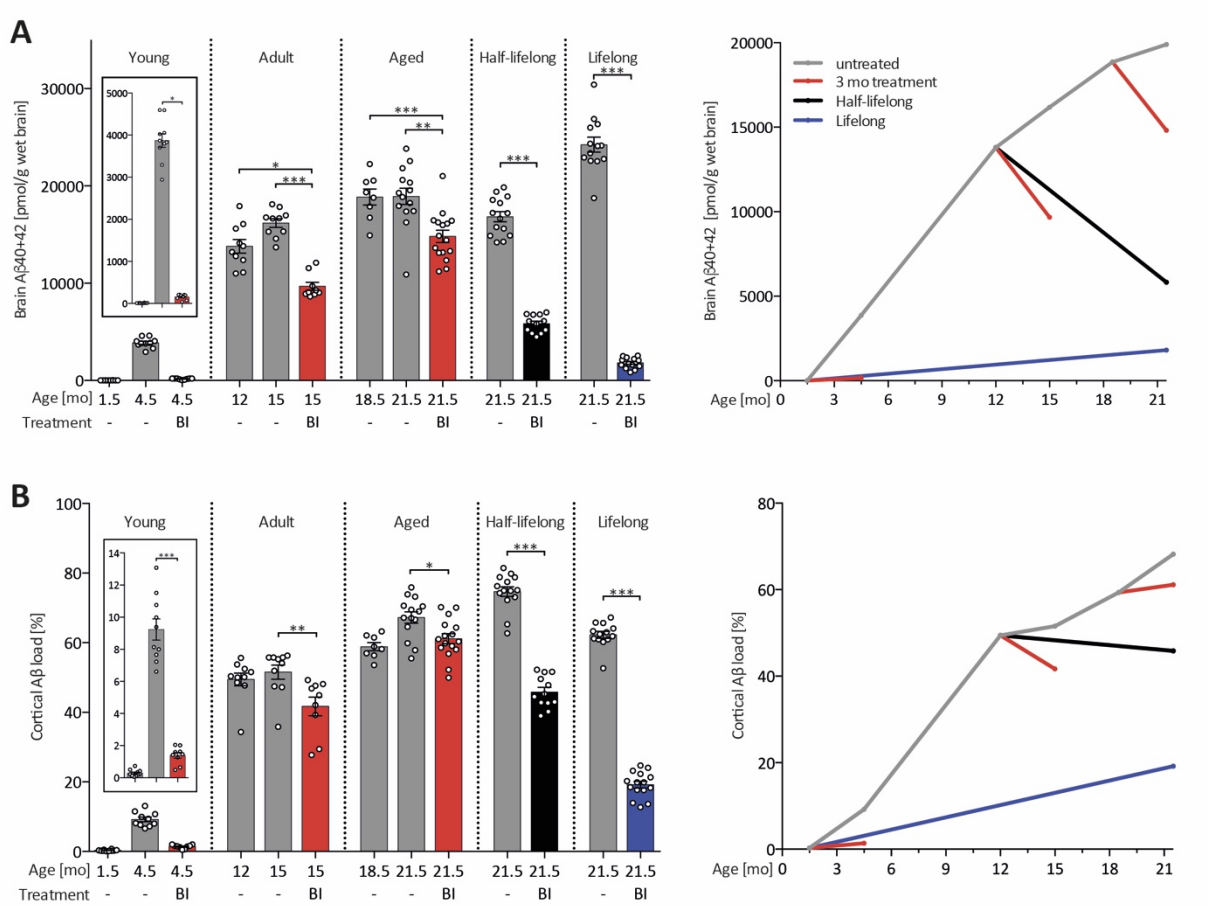
A
Young
Adult
Aged
Half-lifelong
Lifelong
Brain Aβ40+42 [pmol/g wet brain]
Age [mo] 1.5 4.5 4.5 12 15 15 18.5 21.5 21.5 21.5 21.5 21.5 21.5
Treatment - - BI - - BI - - BI - BI - BI
untreated
3 mo treatment
Half-lifelong
Lifelong
Age [mo] 0 3 6 9 12 15 18 21
B
Cortical Aβ load [%]
C
untreated
BI

Figure 4. BACE1 inhibition prevents brain Aβ increase and even reduces below baseline in APPPS1 mice. **(A)** FA-extracted brain Aβ40+42 was determined by ELISA in male and female APPPS1 mice treated with the BACE1 inhibitor (BI) NB-360 (8–10 mice per group for all 1.5-18.5 months old mice; 12–16 mice per group for 21.5 months old mice; mouse age at the end of experiment). The Kruskal-Wallis-test demonstrates significant differences after three months treatment at different stages of pathology (young: H(2)=24.90 and P<0.0001; adult: H(2)=19.44 and P<0.0001; aged: H(2)=15.23 and P=0.0005). Three months BI treatment robustly blocked the age-dependent Aβ increase in the young (treatment from 1.5–4.5 months), adult (treatment from 12–15 months) and aged group (treatment from 18.5–21.5 months) compared to age-matched controls (*post hoc* Dunn's multiple comparison test: young: P=0.0303; adult: P<0,0001; aged: P=0.0067) as well as after chronic half-lifelong (from 12–21.5 months; Mann–Whitney U test; p < 0.0001) and lifelong treatment (from 1.5–21.5 months; Mann-Whitney U test; p <0.0001) compared to age-matched controls. Moreover, Aβ was even significantly reduced below baseline levels, when three months treatment was initiated at an intermediate or late stage of Aβ pathology (*post hoc* Dunn's multiple comparison test: adult: P=0,0139; aged: P=0.0009). For illustration of Aβ increase in the Aβ curves, the mean for 21.5 months old controls (grey) was calculated based on pooled absolute values from the aged, half-lifelong and lifelong group. **(B)** Stereological quantification of Aβ plaque load after immunohistochemistry (CN6 antibody and Congo red). BI treatment significantly alleviated plaque formation compared to age-matched controls (Mann–Whitney U test for the young (p<0.0001), adult (p=0,0076), aged (p=0,0152), half-lifelong (p<0.0001) and lifelong (p<0.0001) treatment group). No gender effect was detected in any measurements. **(C)** Immunostaining with the Aβ-specific antibody CN6 and Congo Red. One representative section is shown for each treatment group. Scale bar: 500 μm. All data are represented as group means ± SEM; *P < 0.05; **P<0.01; ***P < 0.001.

4.3 BACE1 inhibition prevents neurodegeneration and downstream neuro-inflammatory pathology

To study the impact of BACE1 inhibitor treatment on the prevention of neurodegeneration as a readout for intervention success, NfL was measured in CSF collected from APPPS1 mice treated with NB-360 at different pathological stages as described previously. BACE1 inhibition alleviated the increase of CSF NfL in all treatment groups (Figure 5A). Similar to determined Aβ levels, most striking effects of BACE1 inhibition on NfL were observed in the young (69% reduction to control) and the lifelong treated group (93 % reduction to control) in accordance with previous results (Bacioglu et al., 2016). For these two groups, treatment was initiated within the prodromal phase of Aβ deposition. At more advanced stages of deposition, effects on NfL alleviated from 44% (adult group) to 22% (aged group) compared to age-matched untreated controls. Chronic BACE1 inhibition in APPPS1 mice in the half-lifelong (12 – 21.5 months) and lifelong (1.5 – 21.5 months) treatment group maintained low NfL levels throughout life. In untreated APPPS1 mice, NfL increases exponentially (shown in Figure 3A), whereas our study shifted NfL towards a more moderate increase upon BACE1 inhibition.

Furthermore, wt mice were chronically treated with the BACE1 inhibitor for a half-lifelong duration (treatment from 12-21.5 months of age). In these mice, low levels of NfL have been detected at the age of 21.5 months due to the normal aging process, which was previously reported (Bacioglu et al., 2016). Lifelong treated APPPS1 and half-lifelong treated wt mice showed similar levels of NfL. These results demonstrate that NfL pathology can be completely abolished by chronic BACE1 inhibition.

BACE1 inhibitor-treated and untreated wt mice did not show differences in NfL levels (Figure 5A). Therefore, the BACE1 inhibitor is not directly responsible for changes in NfL, but rather indirectly affects neurodegeneration through limiting Aβ increase. In treated APPPS1 mice, Aβ-driven NfL pathology has been shown to increase at advanced disease stages, although Aβ pathology is still halted by NB-360 at theses timepoints. Thus, the close relationship between brain Aβ and CSF NfL levels declines during aging.

To reveal potential side effects by NB-360 off-target inhibition, half-lifelong (treatment from 12-21.5 months) BACE1 inhibitor-treated wt mice were further investigated. Long-term treatment of wt mice did not demonstrate detrimental effects by off-target engagement compared to untreated wt controls. Merely hair depigmentation occurred in all treatment groups due to unspecific BACE2 inhibition by NB-360. As already published by others, treated

APPPS1 and wt mice developed patches of grey hair starting ventrally (Neumann et al., 2015; Shimshek et al., 2016). During chronic intervention in the half-lifelong and lifelong treatment groups, patches turned into an overall grey coat (data not shown).

Increased sTREM2, a proteolytic cleavage product of the microglial TREM2 transmembrane receptor, has been detected in CSF during Aβ deposition in patients with inherited AD. In these individuals, sTREM2 highly correlated with other biomarkers for neurodegeneration (Suárez-Calvet et al., 2016a; Zhong et al., 2019). To investigate the effect and timepoint of BACE1 inhibition on downstream neuroinflammation, we determined sTREM2 levels in brain after BACE1 inhibition. BACE1 inhibition significantly alleviated the production of sTREM2 by 30 - 40% in the adult, aged and half-lifelong group. An even stronger reduction was revealed in the young (64%) and lifelong group (81%) compared to age-matched untreated controls (Figure 5B). sTREM2 has been reported to increase microglial proliferation and clustering around Aβ-positive plaques (Zhong et al., 2019). Quantification of the microglia-covered area after immunohistochemical staining with the Iba1 antibody revealed reduced microgliosis in BACE1 inhibitor-treated mice compared to controls (Figure 5C; approximately 25% reduction in the adult, aged and half-lifelong group, young: 49%; lifelong: 65%).

In conclusion, NB-360 is able to prevent Aβ-driven neurodegeneration, if applied early during the process of β-amyloidosis before NfL becomes uncoupled from Aβ. Furthermore, it restrains neuroinflammation during treatment condition by less activation of microglia due to reduced sTREM2 and Aβ levels.

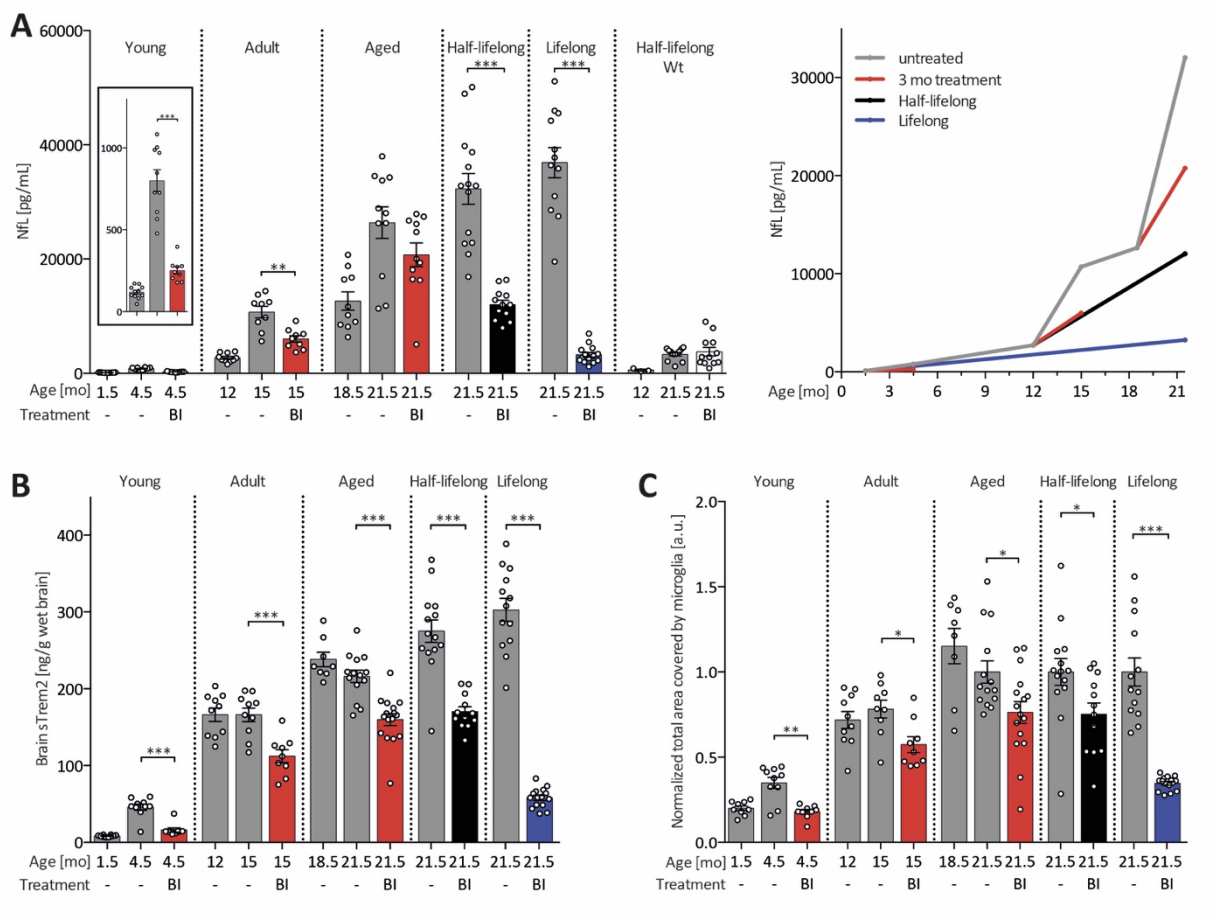

Figure 5. BACE1 inhibitor treatment reveals uncoupling of NfL and Aβ in aged mice and affects downstream neuroinflammation. (A) CSF NfL concentration in BACE1 inhibitor (BI)-treated mice is shown for a subset of mice from Figure 4 (8–10 mice per group for 1.5-18.5 months old mice; 11–14 mice per group for 21.5 months old mice; mouse age at the end of experiment). Mice were excluded, if <10 µl CSF was obtained. Results indicated robust blockage of NfL increase after three months BACE1 inhibition in the young, adult and both chronic treatment groups in APPPS1 mice compared to untreated controls (two-tailed unpaired t-test; young: $t(17)=7.501$, $P<0.001$; adult: $t(16)=4.014$, $P=0.0010$; half-lifelong: $t(24)=6.754$, $P<0.001$; lifelong: $t(24)=13.64$, $P<0.001$). This strong effect was attenuated in aged APPPS1 mice. Wt mice treated with BI from 12-21.5 months of age (half-lifelong; n=3 for the 12 months baseline group and n=12 for 21.5 months old BI and untreated wt mice) revealed a slight, age-related NfL increase, but no reduction after BI treatment. **(B)** Brain sTREM2 concentration of BI-treated mice is shown for mice from Figure 4 (8–10 mice per group for all 1.5-18.5 months old mice; 12–16 mice per group for 21.5 months old mice; mouse age at the end of experiment). BI treatment decreased the production of sTREM2 in brain at all treatment stages and durations. After three months treatment, brain sTREM2 was even reduced below baseline levels, when treatment was initiated at an intermediate or late stage of Aβ pathology. **(C)** Normalized total area covered by microglia was determined for a subset of mice from Figure 4 (8–10 mice per group for 1.5-18.5 months old mice; 12–16 mice per group for 21.5 months old mice; mouse age at the end of experiment). BI and baseline groups were normalized to the respective control group. BI was able to maintain low microglia activation states in brain (Mann–Whitney U test in the young ($p=0.0041$); adult ($p=0,0142$) and aged ($p=0,0194$) treatment group and also after chronic half-lifelong ($p=0.0202$) and lifelong treatment ($p<0.0001$). No gender effect was detected in any measurements. All data are represented as group means ± SEM; *P < 0.05; **P<0.01; ***P < 0.001.

4.4 Discussion

Inhibition of the rate-limiting enzyme BACE1 that generates new Aβ peptides after cleavage of APP during the amyloidogenic pathway constitutes one major therapeutical approach in the context of the cure of AD. So far, different BACE1 inhibitors have been investigated in clinical trials for a limited period of intervention. Unfortunately, none of the tested inhibitors reached its primary or secondary outcome measures. Some compounds even caused adverse effects leading to the discontinuation of all BACE1 inhibitor trials (e.g. Egan, 2018; Eisai and Biogen Press Release, 2019; Wessels et al., 2019). Based on the mode of action, long-term therapy with a BACE1 inhibitor seems to be necessary to maintain positive aspects of this approach. Therefore, the present study for the first time investigated the effects of a half-lifelong and even lifelong, chronic BACE1 inhibition including analyses of pathological sequelae during the process of Aβ deposition in a mouse model of β-amyloidosis. With this approach, we effectively stopped Aβ pathology and neurodegeneration by interference with the amyloid cascade at levels of Aβ production.

Results are most beneficial after chronic, lifelong treatment, when the initiation of this intervention takes place before large Aβ aggregates are deposited. At this early pathological stage, permanent and lifelong BACE1 inhibition maintains initial, low Aβ pathology in brain (Figure 4). Our results after chronic BACE1 inhibitor treatment indicate that early and permanent Aβ reduction throughout life might be necessary to cause long-lasting effects.

However, most clinical trials using BACE1 inhibition were applied in symptomatic patients with mild-to-moderate AD. Two BACE1 inhibitors, Umibecestat (Novartis) and Atabecestat (Janssen), were tested at an earlier timepoint during pathogenesis, namely in asymptomatic individuals at risk for AD (Henley et al., 2019; Novartis International AG, 2019). But, treatment did not cause advancements in cognitive decline leading to the discontinuation of BACE1 inhibitor trials. To restore confidence in BACE1 as a potential therapeutic target, we investigated the impact of BACE1 inhibition at early vs. late pathological disease stages. Thus, we treated additional APP transgenic mice for three months at an early, intermediate and late stage during the process of Aβ pathogenesis. We found out that, even more important than the duration of therapy, is the timepoint of treatment initiation for later intervention success. We demonstrated that prevention of APP cleavage by three months BACE1 inhibition robustly halters the production of soluble Aβ in brain at all disease stages. But similar to the chronic inhibition, most convincing results were obtained when treatment was started at initial disease

stages. This may explain the failure of recent clinical trials due to an inappropriate, too old subject selection.

Surprisingly, three months treatment with NB-360 was even able to remove preexisting brain Aβ, as seen in ELISA measurements by the reduction below baseline (Figure 4A). One hypothesis is that blockage of Aβ production causes disaggregation of deposited Aβ in order to maintain the equilibrium between monomeric and aggregated Aβ. If beneficial, the reduction of Aβ below baseline may indicate not only the elimination of soluble Aβ, but might also include the removal of Aβ seeds that may otherwise promote disease progression. If detrimental, reduction of brain Aβ by BACE1 inhibition could disassemble larger Aβ aggregates into smaller, highly seeding-active species. This might highly promote deposition after termination of the intervention. Unfortunately, reduced brain Aβ (below baseline) is not seen for deposited Aβ detected by immunohistochemistry (Figure 4B). One explanation is based on our brain Aβ measurement technique, which only captures Aβ40 and Aβ42 isoforms, whereas our immunohistochemical procedure is not limited to specific Aβ length suggesting that an increase of further (toxic) Aβ species during disease progression, e.g. Aβ34, conceals the reduction of Aβ40 and 42 (Liebsch et al., 2019).

In our study, brain Aβ changes over time, as illustrated in the curve, could indicate that long-term BACE1 inhibition is able to reduce Aβ to zero, but the lifespan of a mouse seems not long enough (Figure 4A). This is not the case, since NB-360 does not exhibit a 100% blockage of Aβ production allowing small amounts of Aβ still being produced. Furthermore, remaining Aβ levels in mice after lifelong BACE1 inhibition also suggest a low, but continuous Aβ accumulation during life.

Unlike latest human trial outcomes, the results of this study suggest BACE1 inhibition to be an excellent target to interfere with the amyloid cascade and decelerate disease progression, at least in mice. Chronic, long-term therapy seems to be optimal to achieve permanent lowering of Aβ. For this approach, the BACE1 inhibitor requires great safety and tolerability profiles. Especially after BACE1 inhibition, detrimental deficits in myelination and further mechanism-based side effects during development by affecting various BACE1 substrates have been reported (Dominguez et al., 2005; Laird et al., 2005; Ohno et al., 2006; Barão et al., 2016) To avoid this, we initiated NB-360 treatment in mice earliest at 1.5 months of age, immediately after development was completed. Thus, APPPS1 and wt mice were spared from any adverse effects on their physical condition, except hair depigmentation (data not shown) caused by

partial cross-inhibition of BACE2, as published before (Neumann et al., 2015; Shimshek et al., 2016). Results imply NB-360 to be highly safe and suitable for long-term application.

After BACE1 inhibitor treatment in APP transgenic mice, we achieved a more than 90% reduction of brain Aβ (Figure 4). In 2012, Jonsson et al. have found a preventive APP mutation demonstrating an Aβ reduction by 20% to be enough to protect against AD (Jonsson et al., 2012). Since a non-linear relationship between BACE1 activity and subsequent Aβ production has been reported previously, a 20% Aβ reduction is achieved in mice with 50% decreased BACE1 activity (Laird et al., 2005; McConlogue et al., 2007; Rabe et al., 2011). Based on this information, BACE1 inhibition could be further decreased without forfeiting long-lasting effects on Aβ. This might cause a positive impact on the safety profile of the drug. Further advancements in safety are expected by exclusion of side effects caused by cross-inhibition of BACE2. But, recent failure of Umibecestat, which showed enhanced specificity of BACE1 over BACE2, reveals that safety concerns rising from additional BACE2 inhibition can be hardly estimated and remain obscure (Neumann et al., 2018).

Hitherto, many different intervention strategies, not only BACE1 inhibitors, try to mitigate or prevent disease progression of AD. For all prevention trials, it is equally important to monitor disease progression and response to treatment already at pre-clinical stages of disease. Therefore, easily accessible biomarkers are essential (Bacioglu et al., 2016; Osborn et al., 2019). Thus, we determined NfL in CSF after BACE1 inhibition as an indicator for neurodegeneration. Changes in NfL should define the extent of treatment success.

BACE1 inhibitor treatment of wt mice did not reveal any effect on NfL levels (Figure 5A). Hence, results suggest that Aβ removal, rather than the inhibitor itself, prevents downstream neurodegeneration in APPPS1 mice. By lowering Aβ pathology in brain, neurodegeneration and progression of disease might be prevented. In APP transgenic mice, BACE1 inhibition reduced the Aβ-driven increase in CSF NfL throughout all treatment groups indicating a tight connection between β-amyloidosis and NfL. But, although the BACE1 inhibitor robustly halted Aβ increase, NfL changes corresponded less to Aβ at advanced disease stage. This implies an uncoupling of Aβ and NfL during the course of amyloid pathology.

In accordance with previous results showing that minor NfL accumulation is part of the normal aging process, BACE1 inhibitor-treated and untreated wt mice revealed low amounts of this protein in CSF (Bacioglu et al., 2016). These findings strengthen the hypothesis that Aβ is the initial trigger for massive NfL increase in APPPS1 mice rather than a parallel, but independent

mechanism that drives neurodegeneration and later converges with Aβ pathology (Hardy and Higgins, 1992; Masters and Selkoe, 2012; Jack et al., 2013; Wirth et al., 2013).

If transferred to human clinical trials, our findings raise issues of reliability regarding NfL as a marker for the reflection of intervention response during all stages within the continuum of AD. Additionally, since NfL is not a specific marker for AD, confirmation of findings by a second measure would be helpful (e.g. PET or CSF Aβ) in order to define AD-related neurodegeneration according to the latest NIA-AA framework (Jack et al., 2018). In humans, one major challenge is the accessibility of meaningful biomarkers. Since CSF sampling is an invasive procedure in humans, measurement of blood-based biomarkers, e.g. plasma NfL, in our study would enhance clinical relevance.

Over the last years, the role of microglia in AD pathogenesis proved to be highly influential. Genome-wide association studies have shown that many AD risk loci are located near or in genes that are expressed by microglia (Hansen et al., 2018; Verheijen and Sleegers, 2018). In our study, we could show that BACE1 inhibition robustly suppressed inflammation (Figure 5B/C). Compared to NfL, inflammation (microglia and sTREM2 measurements) correlated well with Aβ. Thus, the clear coupling of Aβ and microgliosis hints at Aβ as the exclusive trigger for the microglia activation in APPPS1 mice.

The failure of previous BACE1 inhibitor clinical trials in mild-to-moderate AD patients indicate BACE1 to be a difficult target. Nonetheless, our study maintains the idea of BACE1 as a promising target in the struggle of AD therapy. The major finding of our study reveals that BACE1 inhibition needs to be applied latest at initial stages of Aβ deposition to cause solid effects on deposition and downstream pathology similar to the idea of current secondary prevention trials (Sperling et al., 2014a). With this knowledge and the fact that Aβ accumulation already starts two decades before the onset of clinical symptoms (Villemagne et al., 2013), one explanation for insufficient trial outcomes is the late treatment timepoint of past BACE1 inhibitor clinical trials.

In this study, we used the aggressive APPPS1 mouse model, exhibiting the Swedish mutation as well as a mutation in the PS1 gene (Stürchler-Pierrat et al., 1997; Radde et al., 2006). Both mutations cause massive Aβ production, enabling investigations even in the plateau phase of Aβ, though mice do not exert a long pre-depositing phase without sub-threshold Aβ levels required for very early (e.g. primary) prevention. To further investigate primary prevention of β-amyloidosis, a less intrusive model, e.g. the APP23 model, would be useful.

Based on our results, treatment of individuals at the asymptomatic stage even below Aβ threshold, before neurodegeneration becomes uncoupled, seems to be the conclusive possibility to obtain satisfying prevention of AD. Unfortunately, these primary prevention trials imply many challenges, such as enormous costs, large group sizes and a very long treatment duration.

Furthermore, accuracy of identifying individuals at risk for AD needs to be improved by pre-symptomatic biomarkers, since patients at this stage do not show memory decline, yet. Even a positive PET as readout might already be too late for beneficial therapy. In order to promote the precision of prediction, the importance of familial AD cohorts (e.g. DIAN TU) carrying high risk to develop AD comes more and more into the focus of research. In these cases, insignificant but profound factors at sub-threshold levels which are crucial for later disease can be scrutinized. This might make early and precise intervention accessible.

5 Targetable pathogenic Aβ seeds prior to amyloid deposition

5.1 Pre-amyloid Aβ seeds can be targeted by antibodies

To study early Aβ seed formation, we assessed Aβ levels in pre-depositing male APP23 transgenic mice using ultrasensitive immunoassays (Figure 6A). All samples were FA-extracted under the assumption that Aβ seeds adopt a β-sheet-rich conformation even at pre-amyloid stages. Results revealed an initial increase in insoluble Aβ at 7-8 months of age, roughly 1-2 months before Aβ deposits become detectable by histology and 8-10 months before they are detectable by PET imaging in these animals (Figure 6A).

To determine whether this increase in FA-soluble Aβ at 7-8 months of age indicates an even earlier presence of biologically active Aβ seeds, we probed the mice at six months of age with a variety of antibodies. Since no information was available about the nature or structure of putative pre-amyloid seeds, we selected antibodies against various Aβ species and assemblies, including murine or murinized versions of antibodies that have been used in clinical trials (Figure 6B). For comparative reasons, all antibodies (except one) were available on an IgG2a background to maintain their presumed effector function in mice (Fuller et al., 2014). To achieve high antibody levels in the brain, the antibodies were applied at 0.5 mg/mouse/day for five consecutive days. The mice were analyzed six weeks later, at 7.5 months of age, a time when they show FA-extractable Aβ but still have no histologically detectable Aβ deposition in the brain (Figure 6B).

None of the tested antibodies altered Aβ levels in the Triton-soluble fraction. However, in the mice that received *cm*Aducanumab, Aβ was markedly reduced in the FA-soluble fraction (Figure 6C). For Aβ42 (the Aβ species ending with amino acid 42) the reduction reached 50%. To probe whether *cm*Aducanumab indeed removed early Aβ seeds, a well-established *in vivo* seeding assay was performed (Ye et al., 2017), i.e., minute amounts of brain homogenates from the *cm*Aducanumab- and control antibody-treated mice were infused into young, 3-month-old APP23 mice (Figure 6D). While brain extract from the control antibody-treated mice strongly seeded Aβ deposition in the host mice eight months later, seeding activity was reduced by more than 80% in the brain extract from the *cm*Aducanumab-treated mice (Figure 6D).

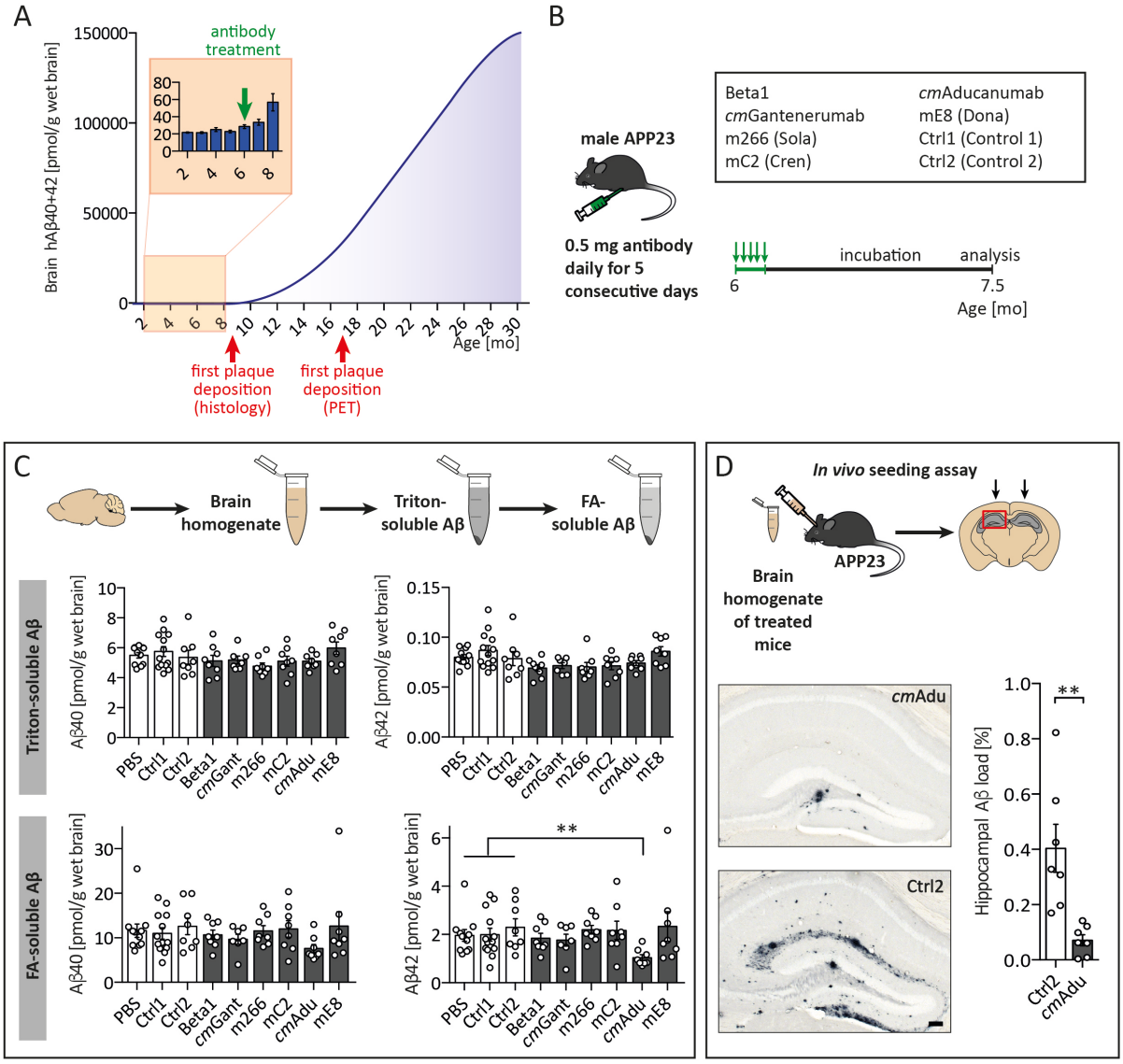

Figure 6. Targeting Aβ seeds at the pre-amyloid stage. (A) Brain Aβ in male APP23 mice as a function of age. The polynomial (4th degree) curve for Aβ concentration (Aβx-40 and Aβx-42 combined) at 10-30 months of age was calculated based on previous publications (Maia et al., 2013, 2015; Ye et al., 2017). In addition, Aβx-40 and Aβx-42 were measured in 2- to 8-month-old male APP23 mice (n=6-7/group) and revealed a first notable increase at 7-8 months of age. This is at least one month earlier than Aβ plaque deposition becomes apparent in male APP23 mice (Eisele et al., 2010; Langer et al., 2011; Ye et al., 2017) and nine months earlier than plaque deposition has been reported by PET imaging (Maier et al., 2014). **(B)** Schematic overview of antibody screening. Six-month-old male APP23 mice intraperitoneally received 0.5 mg of one of the six antibodies directed against Aβ or corresponding control (ctrl) antibodies on five consecutive days (n=11 [PBS], 13 [Ctrl1], 8 [Ctrl2], 8 [Beta1], 7 [*cm*Gant], 8 [m266], 8 [mC2], 8 [*cm*Adu], 8 [mE8]). All groups initially had n=8 mice. mE8 immunization and additional controls were performed in a separate experiment, explaining the higher number of mice receiving control antibody. One *cm*Gant animal died. Mice were sacrificed and analyzed at 7.5 months of age. **(C)** Brain homogenates were extracted by Triton and subsequently with FA. The Kruskal-Wallis-Test indicates group differences for the FA Aβx-42 measurements (PBS, Ctrl1, and Ctrl2 were pooled for this analysis; $H(6)=14.73$; P=0.0225) and *post hoc* Dunn's multiple comparison test demonstrated a significant reduction of FA-extracted Aβx-42 in *cm*Adu-injected mice compared to controls (P=0.0063). **(D)** Brain homogenates from *cm*Adu- and Ctrl2-treated (7.5-month-old) mice were inoculated into the hippocampus of 3-month-old male APP23 hosts. After an 8-month incubation time, the brain extract of *cm*Adu-treated mice induced markedly less Aβ deposition (n=7 for both *cm*Adu and Ctrl2, two-tailed unpaired *t*-test; $t(12)=3.726$; P=0.0029). All data are represented as group means ± SEM; **P<0.01; Scale bar in D: 100µm.

5.2 Characterization of pre-amyloid Aβ seeds

The finding that only *cm*Aducanumab removed Aβ seeds at pre-amyloid stages was surprising, especially in light of previous evidence that the Beta1 antibody recognizes and blocks Aβ seeds extracted from aged, amyloid-laden APP23 mouse brains (Meyer-Luehmann et al., 2006; Eisele et al., 2014). The characterization of native Aβ assemblies (and putative seeds) recognized by antibodies is inherently difficult. Thus, we used agarose-gel electrophoresis to separate brain-derived Aβ assemblies under semi-native conditions based on size, followed by enzymatic digestion of the agarose to liberate the Aβ assemblies. We then used antibody-immunoprecipitation to establish an Aβ-assembly recognition profile for a given antibody that we termed Antibody Recognition Profiling of Aβ assemblies (ARPA) (Figure 7A; supplementary Figure 1).

ARPA of PBS homogenates from amyloid-laden APP23 mouse brains revealed robust differences among the antibodies (Figure 7B). While *cm*Aducanumab and mE8 recognized almost exclusively larger Aβ assemblies, Beta1 and mC2 (and to some degree also *cm*Gantenerumab) recognized a variety of Aβ assemblies, including monomeric Aβ. In contrast, m266 mainly recognized monomeric Aβ. Similar results were found when AD brain samples were tested (supplementary Figure 2).

In 6-month-old APP23 mice, Beta1, mC2, *cm*Gantenerumab, and m266 again recognized monomeric Aβ, but they failed to bind larger Aβ assemblies due to the low abundance of Aβ assemblies (presumably Aβ seeds) at this stage (Figure 7C). Consistently, no signal was obtained with *cm*Aducanumab and mE8 in mice of this age. However, when direct immunoprecipitation from bulk brain homogenate was used, *cm*Aducanumab recognized an Aβ species even in the 6-month-old APP23 mouse brain, while no such signal was found for mE8 (Figure 7C). The latter finding is consistent with pyroglutamated Aβ occurring at later stages of cerebral Aβ-amyloidosis (Güntert et al., 2006; Frost et al., 2013; Rijal Upadhaya et al., 2014).

The inability of ARPA to reveal Aβ seeds at very early and pre-amyloid stages was not entirely unexpected given that pathogenic Aβ seeds can largely escape biochemical detection (Ye et al., 2015). However, when brain homogenates from the antibody-treated 7.5-month-old mice (see Figure 6) were examined with ARPA, faint bands of a higher molecular Aβ species were found in the control-treated mice, and these bands were absent in the *cm*Aducanumab-treated mice (supplementary Figure 3).

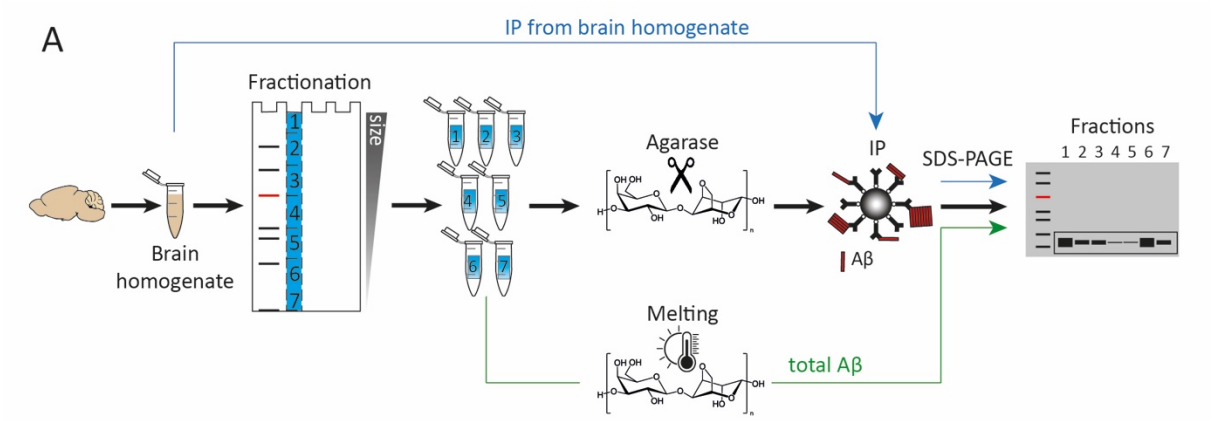
A
IP from brain homogenate
Fractionation
size
Brain homogenate
Agarase
IP
SDS-PAGE
Fractions
1 2 3 4 5 6 7
Aβ
Melting
total Aβ

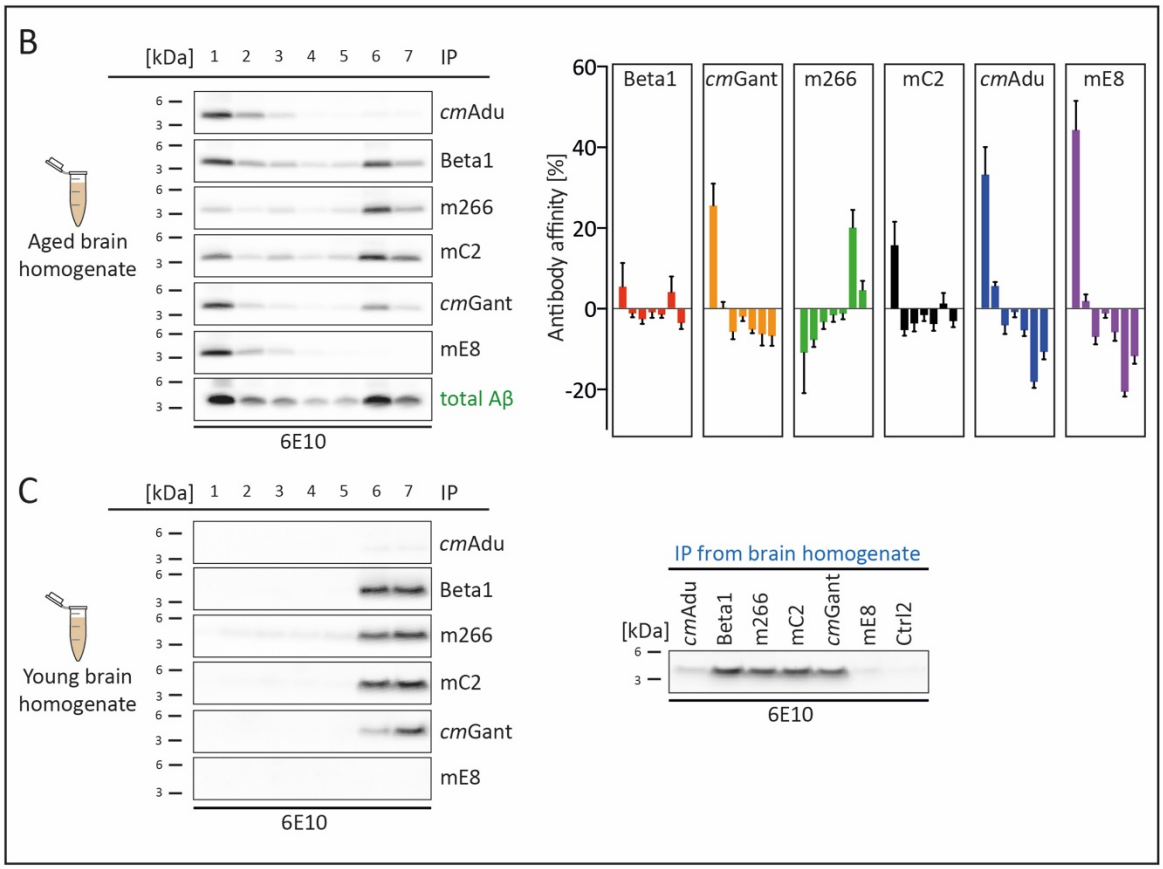
B
[kDa] 1 2 3 4 5 6 7 IP
cmAdu
Beta1
m266
mC2
cmGant
mE8
total Aβ
6E10
Aged brain homogenate
Antibody affinity [%]
60
40
20
0
-20
Beta1
cmGant
m266
mC2
cmAdu
mE8
C
[kDa] 1 2 3 4 5 6 7 IP
cmAdu
Beta1
m266
mC2
cmGant
mE8
6E10
Young brain homogenate
IP from brain homogenate
[kDa]
cmAdu
Beta1
m266
mC2
cmGant
mE8
Ctrl2
6E10

Figure 7. Brain Aβ assemblies recognized by the various antibodies. (A) Schematic overview of Antibody Recognition Profiling of Aβ assemblies (ARPA). In a first step, brain PBS homogenates are immunoprecipitated with the various antibodies followed by denaturing immunoblotting using 6E10 antibody. In a second step, brain PBS-homogenates are subjected to semi-native agarose gel electrophoresis. Liquefied agarose fractions containing Aβ assemblies of various sizes are then achieved by cutting the agarose gels into pieces and treating the pieces with Agarase. Within each individual fraction, Aβ is then immunoprecipitated with one of the various antibodies followed by denaturing immunoblotting. As a control for the total amount of Aβ in the individual fractions, agarose gel pieces are melted and subjected to denaturing immunoblotting. For a more detailed description of ARPA, see supplementary Figure 1 and Methods. **(B)** In fresh-frozen, amyloid-laden tissue samples from male 26-month-old APP23 mice (hemibrains from three mice were pooled), all Aβ antibodies recognized an Aβ-species using immunoprecipitation (left panel). ARPA revealed that *cm*Adu and mE8 recognized almost exclusively larger Aβ assemblies while Beta1 and mC2 (and to some degree also *cm*Gant) recognized larger but also low molecular weight (presumed monomeric) Aβ (bands 6 and 7). Antibody m266 mainly recognized monomeric Aβ. The Aβ band from a fraction was normalized to the total amount of Aβ detected in the sample and the difference in intensity compared to total Aβ in the melted fraction is shown (the experiment was repeated three times; mean and SEM are shown). Positive antibody affinity values indicate that the antibody recognizes Aβ species better than predicted from the total amount of Aβ, while a negative antibody affinity indicates that the antibody recognizes an Aβ species less than expected from the total amount of Aβ in this fraction (right panel). **(C)** In PBS homogenates of 6-month-old APP23 brains (male and female hemibrains from nine animals were pooled), ARPA revealed recognition of monomeric Aβ by Beta1, mC2, Gant, and m266, but these antibodies failed to detect larger Aβ assemblies. No signal was obtained with *cm*Adu and mE8. The experiment was repeated three times with similar results. However, using direct immunoprecipitation, *cm*Adu recognized Aβ species, while no such signal was found for mE8. Note that in amyloid-laden mouse (panel B) and human brain (supplementary Figure 2) monomeric Aβ largely runs in fraction 6 while in the young (pre-amyloid) brain it equally runs in 6 and 7 (panel C).

5.3 Pharmacokinetic of antibodies

It was possible that the successful targeting of pre-amyloid seeds in the brain by *cm*Aducanumab was based on a unique pharmacokinetic profile of *cm*Aducanumab rather than the recognition of seeding-active (pre-amyloid) Aβ species. To this end, we studied the pharmacokinetics of *cm*Aducanumab in comparison to m266 and Beta1 because of their markedly different Aβ assembly recognition profiles and different seed-removal capabilities. Six-month-old male APP23 mice and corresponding wt control mice were injected i.p. with the respective antibodies at 0.5 mg/mouse/day for five consecutive days (Figure 8), as in previous experiments. The concentrations of all three antibodies declined exponentially in the plasma within a similar range (Figure 8). For m266 and Beta1, the decline was faster in APP23 mice compared to wt mice, consistent with the binding of m266 and Beta1 to monomeric Aβ in the blood. In contrast, *cm*Aducanumab´s plasma half-life was similar in wt and APP23 mice, suggesting that this antibody does not recognize a specific target in blood. This observation is consistent with *cm*Aducanumab having a much higher affinity for Aβ assemblies than for monomeric forms of Aβ (Arndt et al., 2018).

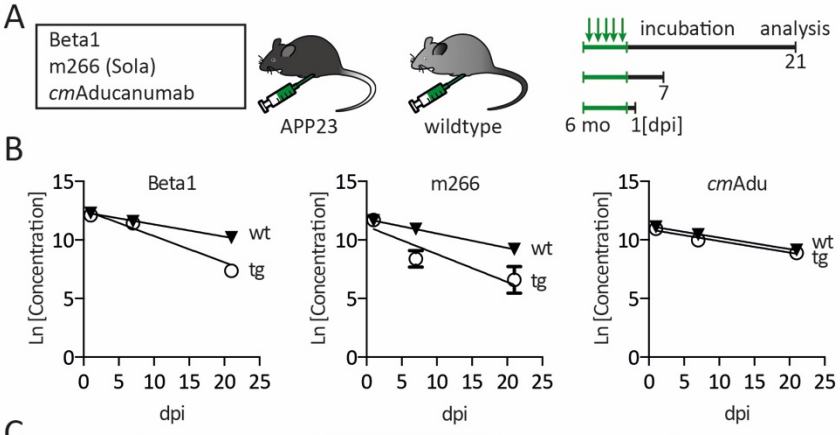

	Beta1		m266		*cm*Adu	
	wt	tg	wt	tg	wt	tg
k_{el} (days)	-0.098	-0.261	-0.125	-0.218	-0.1054	-0.0992
$t_{1/2}$ (days)	7.1	2.7	5.5	3.2	6.6	7.0

Figure 8. Pharmacokinetics and target engagement of antibodies at pre-amyloid stages. (A) Schematic overview of antibody titer measurements. Six-month-old male tg APP23 mice or 6-month-old male wt mice intraperitoneally received 0.5 mg of either Beta1, m266, or *cm*Aducanumab (*cm*Adu) on five consecutive days (n=5/group/antibody). Mice were analyzed 1, 7, or 21 days post immunization (dpi). **(B)** Plasma logarithmic changes (Ln) in antibody concentration over time (days) in APP23 and wt mice. For Beta1 in the tg group, there were 1 and 4 mice below detection at 7 and 21 dpi, respectively. **(C)** Calculated elimination rate (k_{el}) and half-life ($t_{1/2}$) of antibody elimination in plasma suggest binding of Beta1 and m266 to blood Aβ, thus accelerating removal from blood, whereas no such acceleration is seen for *cm*Adu. All data are represented as group means ± SEM.

5.4 Inactivation of pre-amyloid Aβ seeds leads to long-lasting prevention of Aβ deposition and downstream pathogenic changes

We then tested the hypothesis that acute targeting of Aβ seeds at a pre-amyloid stage (i.e., during the lag phase of amyloid aggregation) is effective for prevention of cerebral β-amyloidosis and associated pathologic changes. We again treated 6-month-old male APP23 mice with *cm*Aducanumab, m266 or Beta1 at 0.5 mg/mouse/day for five consecutive days. However, in this experiment, the animals were aged for another six months and analyzed at 12 months of age (Figure 9A, B).

Strikingly, while m266- and Beta1-treated animals did not differ in any measure relative to control antibody-treated mice, both FA-extracted Aβ and immunohistochemically-detected Aβ deposits were reduced (35% and 67%, respectively) in mice receiving a single, five-day regimen of *cm*Aducanumab six months earlier (Figure 9C, D). Further quantitative histopathological analyses indicated that the treatment mainly reduced the number of Aβ plaques (86%), whereas the average size of plaques only decreased by 17% (Figure 9D, E). The deposition of Aβ in the vasculature (cerebral β-amyloid angiopathy, CAA) was not lowered by antibody treatment, and in some mice even appeared to have increased (Figure 9D). However, no old or recent CAA-associated hemorrhages were detected in any of the groups using Perl´s stain for iron or hematoxylin and eosin, respectively.

The reduction of cerebral β-amyloidosis six months after a single, five-day treatment with *cm*Aducanumab also was accompanied by reductions in both microgliosis and p-tau-positive neuritic changes (Figure 9F, G). Measurement of NfL in CSF, a biomarker of neurodegeneration in APP transgenic mice (Bacioglu et al., 2016), revealed 603.7 $\pm$ 43.0 pg/ml for the *cm*Aducanumab-treated mice compared to 741.4 $\pm$ 98.8 pg/ml for the control antibody-treated mice (mean and SEM; n=9 and 8, respectively) but this comparison did not reach statistical significance.

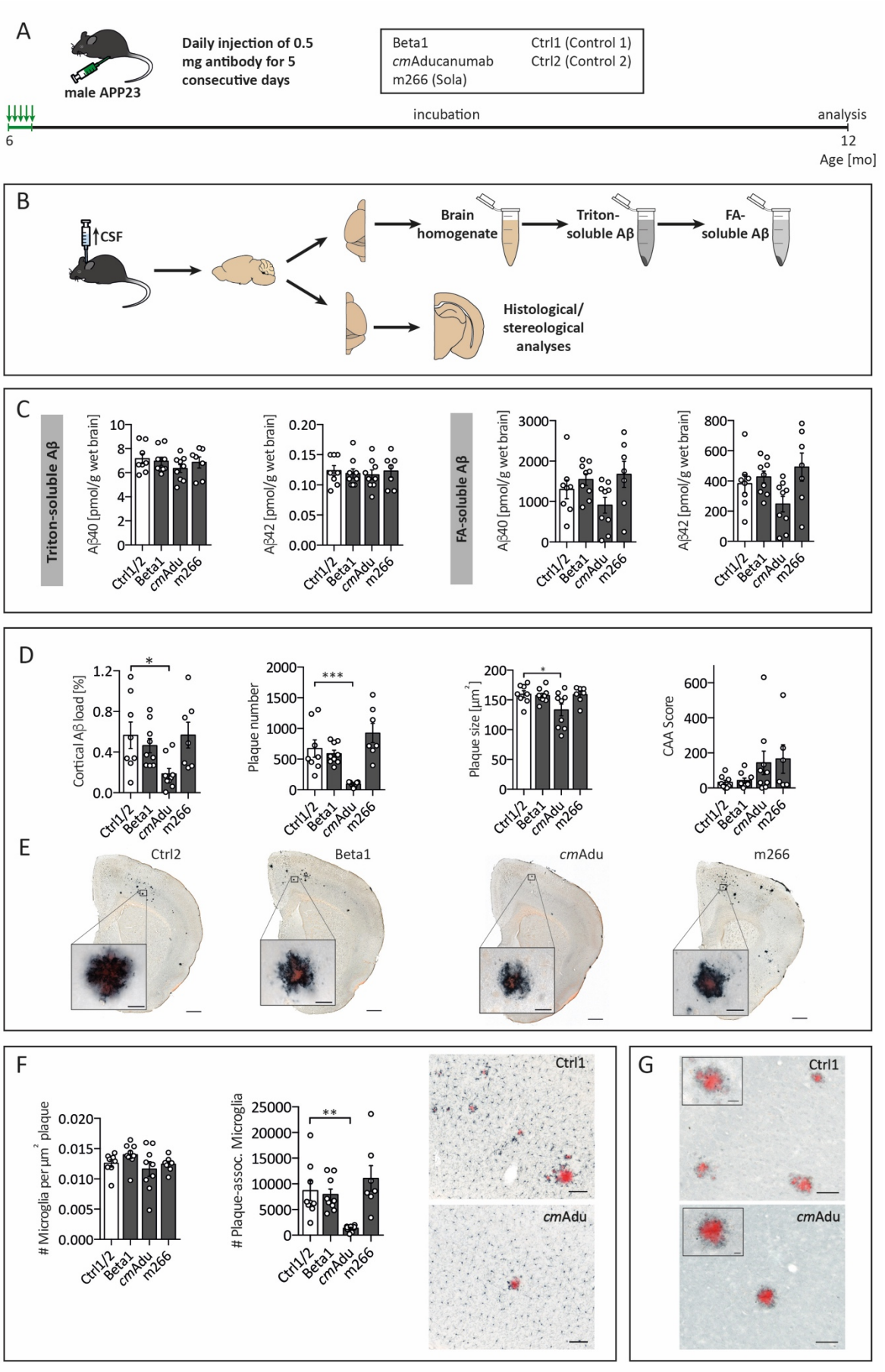
A
male APP23
Daily injection of 0.5 mg antibody for 5 consecutive days
Beta1
cmAducanumab
m266 (Sola)
Ctrl1 (Control 1)
Ctrl2 (Control 2)
incubation
analysis
6
12
Age [mo]
B
CSF
Brain homogenate
Triton-soluble Aβ
FA-soluble Aβ
Histological/ stereological analyses
C
Triton-soluble Aβ
FA-soluble Aβ
Aβ40 [pmol/g wet brain]
Aβ42 [pmol/g wet brain]
Ctrl1/2
Beta1
cmAdu
m266
D
Cortical Aβ load [%]
Plaque number
Plaque size [µm²]
CAA Score
E
Ctrl2
Beta1
cmAdu
m266
F
Microglia per µm² plaque
Plaque-assoc. Microglia
Ctrl1
cmAdu
G
Ctrl1
cmAdu

Figure 9. Targeting pre-amyloid Aβ seeds leads to long-lasting reduction of cerebral β-amyloidosis and associated pathologies. (A) Schematic overview of long-term incubation after acute early seed removal. Six-month-old male APP23 mice received i.p. injections of either 0.5 mg Beta1, *cm*Aducanumab (*cm*Adu) or m266 on five consecutive days. Mice were sacrificed and analyzed at 12 months of age. **(B)** Schematic overview of tissue processing. CSF was taken prior to perfusion and collection of tissue. The fresh-frozen left hemisphere was homogenized for biochemical analyses. Brain homogenates were extracted by Triton and subsequently with FA. The paraformaldehyde-fixed right hemisphere was used for immunohistochemical analyses. **(C)** Aβ measurement of the FA-soluble fractions showed reduced brain Aβ in *cm*Adu-treated mice although the reductions did not reach statistical significance (n=4 [Ctrl1], 4 [Ctrl2], 9 [Beta1], 9 [*cm*Adu], 7 [m266]; All groups initially had n=10 mice (each of the two controls n=5). During the six month-incubation period, one animal in each group died while in the m266 group three animals died. **(D)** Stereological quantification of Aβ-immunostaining (CN6 antibody) in the cortex revealed that Aβ load was significantly lower in mice receiving early *cm*Adu treatment compared to controls (one-way ANOVA: $F(3,29)=3.613$; $P=0.0248$ and *post hoc* Dunnett´s multiple comparisons test: $P=0.0223$). An even larger reduction was found for plaque number (one-way ANOVA: $F(3,29)=12.35$; $P<0.0001$ and *post hoc* Dunnett´s multiple comparisons test: $P=0.0007$). Plaque size was also reduced but smaller in magnitude (one-way ANOVA: $F(3,29)=3.6320$; $P=0.0247$ and *post hoc* Dunnett´s multiple comparisons test: $P=0.0268$). The amount of CAA was not significantly different in antibody-treated mice, although two mice treated with *cm*Adu and three treated with m266 had relatively high CAA counts. **(E)** Immunostaining with the Aβ-specific CN6 antibody along with Congo Red. One representative section from a 12-month-old APP23 mouse is shown for each experimental group. Scale bars = 500 µm (inserts = 20µm). **(F)** The number of Pu.1-positive microglia associated with individual plaques was not significantly changed, whereas the "total" number of plaque-associated (and thus activated) microglia after *cm*Adu-treatment was reduced (one-way ANOVA: $F(3,29)=7.516$; $P=0.0007$; *post hoc* Dunnett´s multiple comparisons test: $P=0.0049$). An overview of Iba1-immunostained microglia around congophilic plaques depicts the reduced number of activated microglia after *cm*Adu-treatment compared to Ctrl1-treated mice. Scale bar = 100 µm. **(G)** All plaques were surrounded by p-tau (AT8)-positive neuritic changes. Because of the significantly reduced plaque-load of the *cm*Adu-treated mice, the overall load of p-tau-positive neurites in the cortex also appeared reduced in *cm*Adu-treated compared to Ctrl1-treated mice. Scale bar = 100 µm (insert 50 µm). All data are represented as group means ± SEM; $*P < 0.05$; $**P<0.01$; $***P < 0.001$.

5.5 Discussion

The immunization study demonstrates the presence of therapeutically targetable Aβ seeds before Aβ aggregation and amyloid formation are detectable by current biochemical, histological, or imaging techniques. The finding that acutely targeting such early Aβ seeds for only five days leads to a significant reduction of Aβ deposition and associated pathologies six months later suggests that Aβ seeds are already present during the lag phase of cerebral β-amyloidosis. It also suggests that the formation and/or amplification of such early seeds is a slow process, even in APP transgenic mice that overproduce Aβ.

The structure and biochemical nature of pathogenic pre-amyloid seeds remain largely unknown because of their low concentration and the inherent difficulty in isolating them in their native state. A variety of seeding-active Aβ assemblies from brain have been characterized, but all of them have been isolated from end-stage AD or transgenic mouse brains (e.g. Langer et al., 2011; Katzmarski et al., 2019). Whether Aβ seeds differ in the early and late stages of disease is uncertain, but our findings suggest that they might. For example, Beta1 has been shown to greatly inactivate Aβ seeds derived from end-stage APP23 mouse brains (Meyer-Luehmann et al., 2006), while the same antibody in the present study was ineffective at inactivating early-stage seeds.

There is multiple evidence for differences in Aβ composition and conformation between Aβ deposits at early vs. late AD stages (Nyström et al., 2013; Rijal Upadhaya et al., 2014; Michno et al., 2019). Pyroglutamate-modified Aβ ($Aβ_{N3pE}$), which is recognized by antibody mE8, forms highly active seeds (Nussbaum et al., 2012), but it occurs predominantly at later stages of cerebral β-amyloidosis (Güntert et al., 2006; Frost et al., 2013; Rijal Upadhaya et al., 2014). This might explain why mE8 did not inhibit early seeds in the present study despite showing an ARPA profile almost identical to *cm*Aducanumab in end-stage AD and transgenic mouse brains.

Differences in the concentration of pathogenic Aβ seeds compared to Aβ species that are relatively benign might also have important implications for the efficacy of antibodies in a brain environment with high concentrations of monomeric (or possibly highly fibrillized) Aβ. ARPA and plasma pharmacokinetics revealed *cm*Aducanumab to be highly selective for Aβ aggregates over Aβ monomers even at pre-amyloid stages. Using synthetic Aβ, Aducanumab has been reported to have a >10,000-fold selectivity for Aβ aggregates over monomeric Aβ (Sevigny et al., 2016; Arndt et al., 2018). Whereas *cm*Aducanumab and mE8 recognize almost exclusively

larger Aβ assemblies, all other antibodies tested in the present study also recognize monomeric Aβ, which may explain why they failed to impede Aβ seeds in the present study (although we only tested the IgG1 version of *cm*Gantenerumab, whose effector function is reduced in mice; DeMattos et al., 2012; Fuller et al., 2015). The reasons that Beta1 inactivates exogenously applied seeds efficiently (e.g. Meyer-Luehmann et al., 2006), but was ineffective for endogenous seeds, could then also be explained by a much higher ratio of seeds to monomeric Aβ in the infusion paradigm. Another possibility is that the infused seeds end up in a brain compartment that is accessible to antibodies, whereas endogenous seeds may be intracellular, and thus are relatively inaccessible (Jucker and Walker, 2018). Thus, for future screening and identification of therapeutic agents targeting pre-amyloid seeds, ARPA appears to be a suitable method, with *cm*Aducanumab as the lead antibody identified thus far.

Of potential concern for the translation of the present results into clinical applications is the finding that *cm*Aducanumab did not reduce CAA. The same was reported when APP transgenic mice were passively immunized with *cm*Aducanumab (Sevigny et al., 2016). The failure to clear Aβ from the vasculature after immunization (or even the observation that immunization increases CAA) in amyloid-laden murine or human brains has been thought to be caused by a shift of antibody-bound Aβ from plaques in the parenchyma to the vessel wall (Pfeifer et al., 2002; Boche et al., 2008; Sperling et al., 2011c). The present results suggest that this translocation of Aβ might also remain active in mice acutely treated with antibodies at an early and pre-amyloid stage. It is also possible that the Aβ seeds that induce CAA are structurally different from parenchymal seeds (Kollmer et al., 2019), and therefore are not recognized by *cm*Aducanumab. The latter possibility will require a refinement of ARPA as a screening tool for reagents that inactivate early seeds.

While the efficacy of the early removal of Aβ seeds in humans has not been established, this study supports the concept that acute removal of seeds in the lag phase of cerebral β-amyloidogenesis delays the pathogenic cascade of amyloid formation and its toxic downstream effects (Karlnoski et al., 2009; Das et al., 2012). More work on the *in vivo* dynamics and turnover of pre-amyloid seeds is necessary (Arosio et al., 2015), in particular in the human brain where the first amyloid deposits are reported as manifesting as early as 30 to 50 years of age (Braak et al., 2011; Pletnikova et al., 2015). Thus, the preclinical phase of AD - defined as when Aβ deposition is present with no clinical symptoms (Sperling et al., 2014a) - may in fact be a later manifestation of a much earlier pathogenic process of seed propagation that currently escapes detection *in vivo*. By reducing the concentration of highly bioactive Aβ

seeds at critical early time points during this pre-amyloid phase, it might be possible to forestall the Aβ-cascade and the onset of AD indefinitely. Given growing evidence that seeding of specific proteins underlies several chronic neurodegenerative diseases and systemic diseases (Jucker and Walker, 2018; Westermark et al., 2018), it is likely that these disorders also can be delayed by the inactivation of proteopathic seeds in the lag-phase of protein deposition in brain.

6 Conclusions

In our studies, we used two different strategies, i.e. BACE1 inhibition and anti-Aβ immunization, to interfere with the amyloid cascade. We could show that both strategies are able to decelerate the process of Aβ deposition by reliable reduction of brain Aβ levels and alleviation of associated pathologies. Similar to current clinical secondary prevention approaches, the BACE1 inhibitor study revealed insight into the importance of early intervention to cause long-lasting outcomes since treatment becomes less effective as soon as pathology reached a more advanced stage. With this knowledge, we established a second therapeutical approach at an even earlier, pre-amyloid stage to cause primary prevention by passive immunization against early Aβ seeds. Inactivation of such seeds by an antibody that is highly specific for aggregated Aβ causes long-lasting reduction of brain Aβ and delayed the onset of deposition. While many anti-Aβ antibodies increase the clearance of both soluble and insoluble Aβ species, Aducanumab exclusively targets aggregated forms of Aβ thereby inducing a long-lasting shift of pathology.

Based on the complexity of AD, clinical outcome and long-term prevention of the disease might only be obtained by affecting multiple targets. More than one drug might be applied like it is the standard for many diseases, e.g. rheumatoid arthritis and the acquired immune deficiency syndrome. To maintain the impact of Aβ seed removal on pathology, a combination of acute Aducanumab immunization and additional chronic BACE1 inhibition to minimize Aβ production demonstrate a promising approach. In future, positive consequences of a combinatorial intervention may allow low dosing of the BACE1 inhibitor to narrow adverse effects based on long-term inhibition.

If applied at the timepoint of primary prevention, the highly specific immunization therapy using the anti-Aβ antibody Aducanumab together with an enhanced, safe and well tolerated BACE1 inhibitor could induce a long-lasting shift in pathology and paves the road for the preservation of brain function and hence, prevention of AD.

7 References

Abi-Saab, D., Andjelkovic, M., Delmar, P., Voyle, N., Esau, N., and Lasser, R. A. (2017). The effect of 6 months' dosing on the rate of amyloid-related imaging abnormalities (ARIA) in the Marguerite Road study. *Alzheimer's Dement.* 13, 252–253. doi:10.1016/j.jalz.2017.06.112.

Adolfsson, O., Pihlgren, M., Toni, N., Varisco, Y., Buccarello, A. L., Antoniello, K., et al. (2012). An effector-reduced anti-β-amyloid (Aβ) antibody with unique Aβ binding properties promotes neuroprotection and glial engulfment of Aβ. *J. Neurosci.* 32, 9677–9689. doi:10.1523/JNEUROSCI.4742-11.2012.

Al-Tel, T. H., Semreen, M. H., Al-Qawasmeh, R. A., Schmidt, M. F., El-Awadi, R., Ardah, M., et al. (2011). Design, synthesis, and qualitative structure-activity evaluations of novel β-secretase inhibitors as potential Alzheimer's drug leads. *J. Med. Chem.* 54, 8373–8385. doi:10.1021/jm201181f.

Albert, M. S., DeKosky, S. T., Dickson, D., Dubois, B., Feldman, H. H., Fox, N. C., et al. (2011). The diagnosis of mild cognitive impairment due to Alzheimer's disease: Recommendations from the National Institute on Aging-Alzheimer's Association workgroups on diagnostic guidelines for Alzheimer's disease. *Alzheimer's Dement.* 7, 270–279. doi:10.1016/J.JALZ.2011.03.008.

Alzforum Therapeutics: Donanemab. Available at: https://www.alzforum.org/therapeutics/donanemab [Accessed December 15, 2019].

Alzheimer Association (2019). 2019 Alzheimer's disease facts and figures. *Alzheimer's Dement.* 15, 321–387. doi:10.1016/j.jalz.2019.01.010.

Aoyagi, A., Condello, C., Stöhr, J., Yue, W., Rivera, B. M., Lee, J. C., et al. (2019). Aβ and tau prion-like activities decline with longevity in the Alzheimer's disease human brain. *Sci. Transl. Med.* 11, 1–14. doi:10.1126/scitranslmed.aat8462.

Arndt, J. W., Qian, F., Smith, B. A., Quan, C., Kilambi, K. P., Bush, M. W., et al. (2018). Structural and kinetic basis for the selectivity of aducanumab for aggregated forms of amyloid-β. *Sci. Rep.* 8, 1–16. doi:10.1038/s41598-018-24501-0.

Arosio, P., Knowles, T. P. J., and Linse, S. (2015). On the lag phase in amyloid fibril formation. *Phys. Chem. Chem. Phys.* 17, 7606–7618. doi:10.1039/C4CP05563B.

Bacioglu, M., Maia, L. F., Preische, O., Schelle, J., Apel, A., Kaeser, S. A., et al. (2016). Neurofilament light chain in blood and CSF as marker of disease progression in mouse models and in neurodegenerative diseases. *Neuron* 91, 56–66. doi:10.1016/j.neuron.2016.05.018.

Bagriantsev, S. N., Kushnirov, V. V., and Liebman, S. W. (2006). Analysis of amyloid aggregates using agarose gel electrophoresis. *Methods Enzymol.* 412, 33–48. doi:10.1016/S0076-6879(06)12003-0.

Ballard, C., Gauthier, S., Corbett, A., Brayne, C., Aarsland, D., and Jones, E. (2011). Alzheimer's disease. *Lancet* 377, 1019–1031. doi:10.1016/S0140-6736(10)61349-9.

Barão, S., Gärtner, A., Leyva-Díaz, E., Demyanenko, G., Munck, S., Vanhoutvin, T., et al. (2015). Antagonistic effects of BACE1 and APH1B-γ-secretase control axonal guidance by regulating growth cone collapse. *Cell Rep.* 12, 1367–1376. doi:10.1016/j.celrep.2015.07.059.

Barão, S., Moechars, D., Lichtenthaler, S. F., and De Strooper, B. (2016). BACE1 physiological functions may limit its use as therapeutic target for Alzheimer's disease. *Trends Neurosci.* 39, 158–169. doi:10.1016/j.tins.2016.01.003.

Bard, F., Cannon, C., Barbour, R., Burke, R. L., Games, D., Grajeda, H., et al. (2000). Peripherally administered antibodies against amyloid beta-peptide enter the central nervous system and reduce pathology in a mouse model of Alzheimer disease. *Nat. Med.* 6, 916–919. doi:10.1038/78682.

Bateman, R. J., Benzinger, T. L., Berry, S., Clifford, D. B., Duggan, C., Fagan, A. M., et al. (2017). The DIAN-TU Next Generation Alzheimer's prevention trial: adaptive design and disease progression model. *Alzheimer's Dement.* 13, 8–19. doi:10.1016/j.jalz.2016.07.005.

Bateman, R. J., Xiong, C., Benzinger, T. L. S., Fagan, A. M., Goate, A., Fox, N. C., et al. (2012). Clinical and biomarker changes in dominantly inherited Alzheimer's disease. *N. Engl. J. Med.* 367, 795–804. doi:10.1056/NEJMoa1202753.

Benedet, A. L., Ashton, N. J., Pascoal, T. A., Leuzy, A., Mathotaarachchi, S., Kang, M. S., et al. (2019). Plasma neurofilament light associates with Alzheimer's disease metabolic decline in amyloid-positive individuals. *Alzheimer's Dement. Diagnosis, Assess. Dis. Monit.* 11, 679–689. doi:10.1016/j.dadm.2019.08.002.

Benilova, I., Gallardo, R., Ungureanu, A. A., Cano, V. C., Snellinx, A., Ramakers, M., et al. (2014). The Alzheimer disease protective mutation A2T modulates kinetic and thermodynamic properties of amyloid-β (Aβ) aggregation. *J. Biol. Chem.* 289, 30977–30989. doi:10.1074/jbc.M114.599027.

Bennett, B. D., Babu-Khan, S., Loeloff, R., Louis, J. C., Curran, E., Citron, M., et al. (2000). Expression analysis of BACE2 in brain and peripheral tissues. *J. Biol. Chem.* 275, 20647–51. doi:10.1074/jbc.M002688200.

Biogen (2019). Third quarter 2019 Financial Results and Business Update.

Bischof, G. N., and Jacobs, H. I. L. (2019). Subthreshold amyloid and its biological and clinical meaning. *Neurology* 93, 72–79. doi:10.1212/WNL.0000000000007747.

Boche, D., Zotova, E., Weller, R. O., Love, S., Neal, J. W., Pickering, R. M., et al. (2008). Consequence of Aβ immunization on the vasculature of human Alzheimer's disease brain. *Brain* 131, 3299–3310. doi:10.1093/brain/awn261.

Bohrmann, B., Baumann, K., Benz, J., Gerber, F., Huber, W., Knoflach, F., et al. (2012). Gantenerumab: A novel human anti-Aβ antibody demonstrates sustained cerebral amyloid-β binding and elicits cell-mediated removal of human amyloid-β. *J. Alzheimer's Dis.* 28, 49–69. doi:10.3233/JAD-2011-110977.

Braak, H., Thal, D. R., Ghebremedhin, E., and Del Tredici, K. (2011). Stages of the pathologic process in Alzheimer disease: age categories from 1 to 100 years. *J. Neuropathol. Exp. Neurol.* 70, 960–969. doi:10.1097/NEN.0b013e318232a379.

Brookmeyer, R., Abdalla, N., Kawas, C. H., and Corrada, M. M. (2018). Forecasting the prevalence of preclinical and clinical Alzheimer's disease in the United States. *Alzheimers. Dement.* 14, 121–129. doi:10.1016/j.jalz.2017.10.009.

Bruen, P. D., McGeown, W. J., Shanks, M. F., and Venneri, A. (2008). Neuroanatomical correlates of neuropsychiatric symptoms in Alzheimer's disease. *Brain* 131, 2455–2463. doi:10.1093/brain/awn151.

Butovsky, O., and Weiner, H. L. (2018). Microglial signatures and their role in health and disease. *Nat. Rev. Neurosci.* 19, 622–635. doi:10.1038/s41583-018-0057-5.

Cai, H., Wang, Y., McCarthy, D., Wen, H., Borchelt, D. R., Price, D. L., et al. (2001). BACE1 is the major beta-secretase for generation of Aβ peptides by neurons. *Nat. Neurosci.* 4, 233–234. doi:10.1038/85064.

Cao, L., Rickenbacher, G. T., Rodriguez, S., Moulia, T. W., and Albers, M. W. (2012). The precision of axon targeting of mouse olfactory sensory neurons requires the BACE1 protease. *Sci. Rep.* 2, 231. doi:10.1038/srep00231.

Castellano, J. M., Kim, J., Stewart, F. R., Jiang, H., DeMattos, R. B., Patterson, B. W., et al. (2011). Human apoE isoforms differentially regulate brain amyloid-β peptide clearance. *Sci. Transl. Med.* 3, 89ra57. doi:10.1126/scitranslmed.3002156.

Cebers, G., Lejeune, T., Attalla, B., Soderberg, M., Alexander, R. C., Budd Haeberlein, S., et al. (2016). Reversible and species-specific depigmentation effects of AZD3293, a BACE inhibitor for the treatment of Alzheimer's disease, are related to BACE2 inhibition and confined to epidermis and hair. *J. Prev. Alzheimer's Dis.* 3, 202–218. doi:10.14283/jpad.2016.119.

Cerf, E., Sarroukh, R., Tamamizu-Kato, S., Breydo, L., Derclayes, S., Dufrênes, Y. F., et al. (2009). Antiparallel β-sheet: A signature structure of the oligomeric amyloid β-peptide. *Biochem. J.* 421, 415–423. doi:10.1042/BJ20090379.

Chatterjee, P., Goozee, K., Sohrabi, H. R., Shen, K., Shah, T., Asih, P. R., et al. (2018). Association of plasma neurofilament light chain with neocortical amyloid-β load and cognitive performance in cognitively normal elderly participants. *J. Alzheimer's Dis.* 63, 479–487. doi:10.3233/JAD-180025.

Cichorek, M., Wachulska, M., Stasiewicz, A., and Tymińska, A. (2013). Skin melanocytes: biology and development. *Adv. Dermatology Allergol.* 30, 30–41. doi:10.5114/pdia.2013.33376.

Cleveland, D. W., Hwo, S. Y., and Kirschner, M. W. (1977). Purification of tau, a microtubule-associated protein that induces assembly of microtubules from purified tubulin. *J. Mol. Biol.* 116, 207–225. doi:10.1016/0022-2836(77)90213-3.

Coimbra, J. R. M., Marques, D. F. F., Baptista, S. J., Pereira, C. M. F., Moreira, P. I., Dinis, T. C. P., et al. (2018). Highlights in BACE1 inhibitors for Alzheimer's disease treatment. *Front. Chem.* 6, 178. doi:10.3389/fchem.2018.00178.

Collins, S. J., Lawson, V. A., and Masters, C. L. (2004). Transmissible spongiform encephalopathies. *Lancet* 363, 51–61. doi:10.1016/S0140-6736(03)15171-9.

Corder, E. H., Saunders, A. M., Strittmatter, W. J., Schmechel, D. E., Gaskell, P. C., Small, G. W., et al. (1993). Gene dose of apolipoprotein E type 4 allele and the risk of Alzheimer's disease in late onset families. *Science* 261, 921–923. doi:10.1126/science.8346443.

Coric, V., Van Dyck, C. H., Salloway, S., Andreasen, N., Brody, M., Richter, R. W., et al. (2012). Safety and tolerability of the γ-secretase inhibitor avagacestat in a phase 2 study of mild to moderate Alzheimer disease. *Arch. Neurol.* 69, 1430–1440. doi:10.1001/archneurol.2012.2194.

Cummings, J. L., Cohen, S., Van Dyck, C. H., Brody, M., Curtis, C., Cho, W., et al. (2018). ABBY: A phase 2 randomized trial of crenezumab in mild to moderate Alzheimer disease. *Neurology* 90, 1889–1897. doi:10.1212/WNL.0b013e3182309fa5.

Cummings, J. L., Lee, G., Ritter, A., Sabbagh, M., and Zhong, K. (2019). Alzheimer's disease drug development pipeline: 2019. *Alzheimer's Dement. Transl. Res. Clin. Interv.* 5, 272–293. doi:10.1016/j.trci.2019.05.008.

Cummings, J. L., Morstorf, T., and Zhong, K. (2014). Alzheimer's disease drug-development pipeline: few candidates, frequent failures. *Alzheimers. Res. Ther.* 6, 37. doi:10.1186/alzrt269.

Das, P., Verbeeck, C., Minter, L., Chakrabarty, P., Felsenstein, K., Kukar, T., et al. (2012). Transient pharmacologic lowering of Aβ production prior to deposition results in sustained reduction of amyloid plaque pathology. *Mol. Neurodegener.* 7, 39. doi:10.1186/1750-1326-7-39.

De Strooper, B. (2014). Lessons from a failed γ-secretase Alzheimer trial. *Cell* 159, 721–726. doi:10.1016/j.cell.2014.10.016.

De Strooper, B., and Karran, E. (2016). The cellular phase of Alzheimer's disease. *Cell* 164, 603–615. doi:10.1016/j.cell.2015.12.056.

De Strooper, B., Saftig, P., Craessaerts, K., Vanderstichele, H., Guhde, G., Annaert, W., et al. (1998). Deficiency of presenilin-1 inhibits the normal cleavage of amyloid precursor protein. *Nature* 391, 387–390. doi:10.1038/34910.

DeMattos, R. B., Bales, K. R., Cummins, D. J., Dodart, J. C., Paul, S. M., and Holtzman, D. M. (2001). Peripheral anti-Aβ antibody alters CNS and plasma Aβ clearance and decreases brain Aβ burden in a mouse model of Alzheimer's disease. *Proc. Natl. Acad. Sci. U. S. A.* 98, 8850–8855. doi:10.1073/pnas.151261398.

DeMattos, R. B., Bales, K. R., Parsadanian, M., O'Dell, M. A., Foss, E. M., Paul, S. M., et al. (2002). Plaque-associated disruption of CSF and plasma amyloid-β (Aβ) equilibrium in a mouse model of Alzheimer's disease. *J. Neurochem.* 81, 229–236. doi:10.1046/j.1471-4159.2002.00889.x.

DeMattos, R. B., Lu, J., Tang, Y., Racke, M. M., DeLong, C. A., Tzaferis, J. A., et al. (2012). A plaque-specific antibody clears existing β-amyloid plaques in Alzheimer's disease mice. *Neuron* 76, 908–920. doi:10.1016/j.neuron.2012.10.029.

Deng, M., He, W., Tan, Y., Han, H., Hu, X., Xia, K., et al. (2013). Increased expression of reticulon 3 in neurons leads to reduced axonal transport of β site amyloid precursor protein-cleaving enzyme. *J. Biol. Chem.* 288, 30236–30245. doi:10.1074/jbc.M113.480079.

Dodart, J.-C., Bales, K. R., Gannon, K. S., Greene, S. J., DeMattos, R. B., Mathis, C., et al. (2002). Immunization reverses memory deficits without reducing brain Aβ burden in Alzheimer's disease model. *Nat. Neurosci.* 5, 452–457. doi:10.1038/nn842.

Dominguez, D., Tournoy, J., Hartmann, D., Huth, T., Cryns, K., Deforce, S., et al. (2005). Phenotypic and biochemical analyses of BACE1- and BACE2-deficient mice. *J. Biol. Chem.* 280, 30797–806. doi:10.1074/jbc.M505249200.

Doody, R. S., Raman, R., Farlow, M., Iwatsubo, T., Vellas, B., Joffe, S., et al. (2013). A phase 3 trial of Semagacestat for treatment of Alzheimer's disease. *N. Engl. J. Med.* 369, 341–350. doi:10.1056/NEJMoa1210951.

Doody, R. S., Thomas, R. G., Farlow, M., Iwatsubo, T., Vellas, B., Joffe, S., et al. (2014). Phase 3 trials of Solanezumab for mild-to-moderate Alzheimer's disease. *N. Engl. J. Med.* 370, 311–321. doi:10.1056/NEJMoa1312889.

Egan, M. F., Kost, J., Tariot, P. N., Aisen, P. S., Cummings, J. L., Vellas, B., et al. (2018). Randomized trial of Verubecestat for mild-to-moderate Alzheimer's disease. *N. Engl. J. Med.* 378, 1691–1703. doi:10.1056/NEJMoa1706441.

Egan, M. F., Kost, J., Voss, T., Mukai, Y., Aisen, P. S., Cummings, J. L., et al. (2019). Randomized trial of Verubecestat for prodromal Alzheimer's disease. *N. Engl. J. Med.* 380, 1408–1420. doi:10.1056/NEJMoa1812840.

Eisai and Biogen (2019). Discontinue phase III clinical studies of BACE inhibitor Elenbecestat in early Alzheimer's disease [Press Release]. Available at: http://eisai.mediaroom.com/2019-09-13-Eisai-And-Biogen-To-Discontinue-Phase-III-Clinical-Studies-Of-BACE-Inhibitor-Elenbecestat-In-Early-Alzheimers-Disease [Accessed December 14, 2019].

Eisele, Y. S., Fritschi, S. K., Hamaguchi, T., Obermüller, U., Fuger, P., Skodras, A., et al. (2014). Multiple factors contribute to the peripheral induction of cerebral-amyloidosis. *J. Neurosci.* 34, 10264–10273. doi:10.1523/jneurosci.1608-14.2014.

Eisele, Y. S., Obermüller, U., Heilbronner, G., Baumann, F., Kaeser, S. A., Wolburg, H., et al. (2010). Peripherally applied Aβ-containing inoculates induce cerebral β-amyloidosis. *Science* 330, 980–982. doi:10.1126/science.1194516.

Esparza, T. J., Zhao, H., Cirrito, J. R., Cairns, N. J., Bateman, R. J., Holtzman, D. M., et al. (2013). Amyloid-beta oligomerization in Alzheimer dementia versus high-pathology controls. *Ann. Neurol.* 73, 104–119. doi:10.1002/ana.23748.

Esterházy, D., Stützer, I., Wang, H., Rechsteiner, M. P., Beauchamp, J., Döbeli, H., et al. (2011). BACE2 is a β cell-enriched protease that regulates pancreatic β cell function and mass. *Cell Metab.* 14, 365–377. doi:10.1016/j.cmet.2011.06.018.

Evin, G., Lessene, G., and Wilkins, S. (2011). BACE inhibitors as potential drugs for the treatment of Alzheimer's disease: focus on bioactivity. *Recent Pat. CNS Drug Discov.* 6, 91–106. doi:10.2174/157488911795933938.

Farlow, M., Arnold, S. E., van Dyck, C. H., Aisen, P. S., Snider, B. J., Porsteinsson, A. P., et al. (2012). Safety and biomarker effects of Solanezumab in patients with Alzheimer's disease. *Alzheimer's Dement.* 8, 261–271. doi:10.1016/j.jalz.2011.09.224.

Farlow, M. R., Andreasen, N., Riviere, M.-E., Vostiar, I., Vitaliti, A., Sovago, J., et al. (2015). Long-term treatment with active Aβ immunotherapy with CAD106 in mild Alzheimer's disease. *Alzheimers. Res. Ther.* 7, 23. doi:10.1186/s13195-015-0108-3.

Farrer, L. A., Cupples, L. A., Haines, J. L., Hyman, B., Kukull, W. A., Mayeux, R., et al. (1997). Effects of age, sex, and ethnicity on the association between apolipoprotein E genotype and Alzheimer disease: A meta-analysis. *J. Am. Med. Assoc.* 278, 1349–1356. doi:10.1001/jama.278.16.1349.

Farzan, M., Schnitzler, C. E., Vasilieva, N., Leung, D., and Choe, H. (2000). BACE2, a β-secretase homolog, cleaves at the β site and within the amyloid-β region of the amyloid-β precursor protein. 97, 9712–9717. doi:10.1073/pnas.160115697.

Feuerbach, D., Schindler, P., Barske, C., Joller, S., Beng-Louka, E., Worringer, K. A., et al. (2017). ADAM17 is the main sheddase for the generation of human triggering receptor expressed in myeloid cells (hTREM2) ectodomain and cleaves TREM2 after Histidine 157. *Neurosci. Lett.* 660, 109–114. doi:10.1016/j.neulet.2017.09.034.

Fielden, M. R., Werner, J., Jamison, J. A., Coppi, A., Hickman, D., Dunn, R. T., et al. (2015). Retinal toxicity induced by a novel β-secretase inhibitor in the Sprague-Dawley rat. *Toxicol. Pathol.* 43, 581–592. doi:10.1177/0192623314553804.

Filser, S., Ovsepian, S. V., Masana, M., Blazquez-Llorca, L., Elvang, A. B., Volbracht, C., et al. (2015). Pharmacological inhibition of BACE1 impairs synaptic plasticity and cognitive functions. *Biol. Psychiatry* 77, 729–739. doi:10.1016/j.biopsych.2014.10.013.

Fleck, D., van Bebber, F., Colombo, A., Galante, C., Schwenk, B. M., Rabe, L., et al. (2013). Dual cleavage of neuregulin 1 type III by BACE1 and ADAM17 liberates its EGF-like domain and allows paracrine signaling. *J. Neurosci.* 33, 7856–7869. doi:10.1523/JNEUROSCI.3372-12.2013.

Francis, P. T., Palmer, A. M., Snape, M., and Wilcock, G. K. (1999). The cholinergic hypothesis of Alzheimer's disease: a review of progress. *J. Neurol. Neurosurg. Psychiatry* 66, 137–147. doi:10.1136/jnnp.66.2.137.

Fratiglioni, L., Ahlbom, A., Viitanen, M., and Winblad, B. (1993). Risk factors for late-onset Alzheimer's disease: A population-based, case-control study. *Ann. Neurol.* 33, 258–266. doi:10.1002/ana.410330306.

Frontzek, K., Lutz, M. I., Aguzzi, A., Kovacs, G. G., and Budka, H. (2016). Amyloid-β pathology and cerebral amyloid angiopathy are frequent in iatrogenic Creutzfeldt-Jakob disease after dural grafting. *Swiss Med. Wkly.* 146, w14287. doi:10.4414/smw.2016.14287.

Frost, J. L., Le, K. X., Cynis, H., Ekpo, E., Kleinschmidt, M., Palmour, R. M., et al. (2013). Pyroglutamate-3 amyloid-β deposition in the brains of humans, non-human primates, canines, and Alzheimer disease-like transgenic mouse models. *Am. J. Pathol.* 183, 369–381. doi:10.1016/j.ajpath.2013.05.005.

Fukumoto, H., Cheung, B. S., Hyman, B. T., and Irizarry, M. C. (2002). Beta-secretase protein and activity are increased in the neocortex in Alzheimer disease. *Arch. Neurol.* 59, 1381–9. doi:10.1001/archneur.59.9.1381.

Fuller, J. P., Stavenhagen, J. B., Christensen, S., Kartberg, F., Glennie, M. J., and Teeling, J. L. (2015). Comparing the efficacy and neuroinflammatory potential of three anti-Abeta antibodies. *Acta Neuropathol.* 130, 699–711. doi:10.1007/s00401-015-1484-2.

Fuller, J. P., Stavenhagen, J. B., and Teeling, J. L. (2014). New roles for Fc receptors in neurodegeneration-The impact on immunotherapy for Alzheimer's disease. *Front. Neurosci.* 8, 1–10. doi:10.3389/fnins.2014.00235.

Geisler, N., Kaufmann, E., Fischer, S., Plessmann, U., and Weber, K. (1983). Neurofilament architecture combines structural principles of intermediate filaments with carboxy-terminal extensions increasing in size between triplet proteins. *EMBO J.* 2, 1295–1302. doi:10.1002/j.1460-2075.1983.tb01584.x.

Gilman, S., Koller, M., Black, R. S., Jenkins, L., Griffith, S. G., Fox, N. C., et al. (2005). Clinical effects of Abeta immunization (AN1792) in patients with AD in an interrupted trial. *Neurology* 64, 1553–62. doi:10.1212/01.WNL.0000159740.16984.3C.

Gisslén, M., Price, R. W., Andreasson, U., Norgren, N., Nilsson, S., Hagberg, L., et al. (2016). Plasma concentration of the neurofilament light protein (NFL) is a biomarker of CNS injury in HIV infection: a cross-sectional study. *EBioMedicine* 3, 135–140. doi:10.1016/j.ebiom.2015.11.036.

Gordon, B. A., Blazey, T. M., Su, Y., Hari-Raj, A., Dincer, A., Flores, S., et al. (2018). Spatial patterns of neuroimaging biomarker change in individuals from families with autosomal dominant Alzheimer's disease: a longitudinal study. *Lancet Neurol.* 17, 241–250. doi:10.1016/S1474-4422(18)30028-0.

Graham, W. V., Bonito-Oliva, A., and Sakmar, T. P. (2017). Update on Alzheimer's disease therapy and prevention strategies. *Annu. Rev. Med.* 68, 413–430. doi:10.1146/annurev-med-042915-103753.

Green, R. C., Cupples, L. A., Go, R., Benke, K. S., Edeki, T., Griffith, P. A., et al. (2002). Risk of dementia among white and african american relatives of patients with Alzheimer disease. *J. Am. Med. Assoc.* 287, 329–336. doi:10.1001/jama.287.3.329.

Güntert, A., Döbeli, H., and Bohrmann, B. (2006). High sensitivity analysis of amyloid-beta peptide composition in amyloid deposits from human and PS2APP mouse brain. *Neuroscience* 143, 461–475. doi:10.1016/j.neuroscience.2006.08.027.

Gupta, P. P., Pandey, R. D., Jha, D., Shrivastav, V., and Kumar, S. (2015). Role of traditional nonsteroidal anti-inflammatory drugs in Alzheimer's disease: a meta-analysis of randomized clinical trials. *Am. J. Alzheimers. Dis. Other Demen.* 30, 178–182. doi:10.1177/1533317514542644.

Gupta, R. C. (2014). "Tacrine," in *Encyclopedia of Toxicology: Third Edition* (Elsevier), 466–467. doi:10.1016/B978-0-12-386454-3.00198-6.

Haass, C., Schlossmacher, M. G., Hung, A. Y., Vigo-Pelfrey, C., Mellon, A., Ostaszewski, B. L., et al. (1992). Amyloid β-peptide is produced by cultured cells during normal metabolism. *Nature* 359, 322–325. doi:10.1038/359322a0.

Hamaguchi, T., Taniguchi, Y., Sakai, K., Kitamoto, T., Takao, M., Murayama, S., et al. (2016). Significant association of cadaveric dura mater grafting with subpial Aβ deposition and meningeal amyloid angiopathy. *Acta Neuropathol.* 132, 313–315. doi:10.1007/s00401-016-1588-3.

Hansen, R. A., Gartlehner, G., Webb, A. P., Morgan, L. C., Moore, C. G., and Jonas, D. E. (2008). Efficacy and safety of Donepezil, Galantamine, and Rivastigmine for the treatment of Alzheimer's disease: a systematic review and meta-analysis. *Clin. Interv. Aging* 3, 211–225.

Hansen, D. V., Hanson, J. E., and Sheng, M. (2018). Microglia in Alzheimer's disease. *J. Cell Biol.* 217, 459–472. doi:10.1083/jcb.201709069.

Hansson, O., Janelidze, S., Hall, S., Magdalinou, N., Lees, A. J., Andreasson, U., et al. (2017). Blood-based NfL: a biomarker for differential diagnosis of parkinsonian disorder. *Neurology* 88, 930–937. doi:10.1212/WNL.0000000000003680.

Hardy, J. A., and Higgins, G. A. (1992). Alzheimer's disease: the amyloid cascade hypothesis. *Science* 256, 184–185. doi:10.1126/science.1566067.

Hardy, J., and Selkoe, D. J. (2002). The amyloid hypothesis of Alzheimer's disease: progress and problems on the road to therapeutics. *Science* 297, 353–356. doi:10.1126/science.1072994.

Hawkes, N. (2017). Merck ends trial of potential Alzheimer's drug Verubecestat. *BMJ* 356, j845. doi:10.1136/bmj.j845.

Hebert, L. E., Bienias, J. L., Aggarwal, N. T., Wilson, R. S., Bennett, D. A., Shah, R. C., et al. (2010). Change in risk of Alzheimer disease over time. *Neurology* 75, 786–791. doi:10.1212/WNL.0b013e3181f0754f.

Hebert, L. E., Weuve, J., Scherr, P. A., and Evans, D. A. (2013). Alzheimer disease in the United States (2010-2050) estimated using the 2010 census. *Neurology* 80, 1778–83. doi:10.1212/WNL.0b013e31828726f5.

Henley, D., Raghavan, N., Sperling, R., Aisen, P., Raman, R., and Romano, G. (2019). Preliminary results of a trial of Atabecestat in pre-clinical Alzheimer's disease. *N Engl J Med* 15, 1483–1485.

Heron, M. (2018). Deaths: leading causes for 2016. *Natl. Vital Stat. Reports* 67, 1–15.

Heslegrave, A., Heywood, W., Paterson, R., Magdalinou, N., Svensson, J., Johansson, P., et al. (2016). Increased cerebrospinal fluid soluble TREM2 concentration in Alzheimer's disease. *Mol. Neurodegener.* 11, 3. doi:10.1186/s13024-016-0071-x.

Hisanaga, S., Gonda, Y., Inagaki, M., Ikai, A., and Hirokawa, N. (1990). Effects of phosphorylation of the neurofilament L protein on filamentous structures. *Cell Regul.* 1, 237–248. doi:10.1091/mbc.1.2.237.

Hitt, B., Riordan, S. M., Kukreja, L., Eimer, W. A., Rajapaksha, T. W., and Vassar, R. (2012). β-site amyloid precursor protein (APP)-cleaving enzyme 1 (BACE1)-deficient mice exhibit a close homolog of L1 (CHL1) loss-of-function phenotype involving axon guidance defects. *J. Biol. Chem.* 287, 38408–38425. doi:10.1074/jbc.M112.415505.

Höglund, K., Fourier, A., Perret-Liaudet, A., Zetterberg, H., Blennow, K., and Portelius, E. (2015). Alzheimer's disease - recent biomarker developments in relation to updated diagnostic criteria. *Clin. Chim. Acta* 449, 3–8. doi:10.1016/j.cca.2015.01.041.

Hong, L., Turner, R. T., Koelsch, G., Shin, D., Ghosh, A. K., and Tang, J. (2002). Crystal structure of Memapsin 2 (β-secretase) in complex with an inhibitor OM00-3. *Biochemistry* 41, 10963–10967. doi:10.1021/bi026232n.

Honig, L. S., Vellas, B., Woodward, M., Boada, M., Bullock, R., Borrie, M., et al. (2018). Trial of Solanezumab for mild dementia due to Alzheimer's disease. *N. Engl. J. Med.* 378, 321–330. doi:10.1056/NEJMoa1705971.

Hsu, D., and Marshall, G. A. (2017). Primary and secondary prevention trials in Alzheimer disease: looking back, moving forward. *Curr. Alzheimer Res.* 14, 1–15. doi:10.2174/1567205013666160930.

Hu, X., Hicks, C. W., He, W., Wong, P., Macklin, W. B., Trapp, B. D., et al. (2006). BACE1 modulates myelination in the central and peripheral nervous system. *Nat. Neurosci.* 9, 1520–1525. doi:10.1038/nn1797.

Hu, X., Zhou, X., He, W., Yang, J., Xiong, W., Wong, P., et al. (2010). BACE1 deficiency causes altered neuronal activity and neurodegeneration. *J. Neurosci.* 30, 8819–8829. doi:10.1523/JNEUROSCI.1334-10.2010.

Hussain, I., Powell, D., Howlett, D. R., Tew, D. G., Meek, T. D., Chapman, C., et al. (1999). Identification of a novel aspartic protease (Asp 2) as β-secretase. *Mol. Cell. Neurosci.* 14, 419–427. doi:10.1006/mcne.1999.0811.

Ishikawa, H., Bischoff, R., and Holtzer, H. (1968). Mitosis and intermediate-sized filaments in developing skeletal muscle. *J. Cell Biol.* 38, 538–555. doi:10.1083/jcb.38.3.538.

Jack, C. R., Albert, M. S., Knopman, D. S., McKhann, G. M., Sperling, R. A., Carrillo, M. C., et al. (2011). Introduction to the recommendations from the National Institute on Aging-Alzheimer's Association workgroups on diagnostic guidelines for Alzheimer's disease. *Alzheimer's Dement.* 7, 257–262. doi:10.1016/J.JALZ.2011.03.004.

Jack, C. R., Bennett, D. A., Blennow, K., Carrillo, M. C., Dunn, B., Haeberlein, S. B., et al. (2018). NIA-AA Research Framework: Toward a biological definition of Alzheimer's disease. *Alzheimer's Dement.* 14, 535–562. doi:10.1016/j.jalz.2018.02.018.

Jack, C. R., Knopman, D. S., Jagust, W. J., Petersen, R. C., Weiner, M. W., Aisen, P. S., et al. (2013). Tracking pathophysiological processes in Alzheimer's disease: an updated hypothetical model of dynamic biomarkers. *Lancet. Neurol.* 12, 207–16. doi:10.1016/S1474-4422(12)70291-0.

Jack, C. R., Lowe, V. J., Weigand, S. D., Wiste, H. J., Senjem, M. L., Knopman, D. S., et al. (2009). Serial PIB and MRI in normal, mild cognitive impairment and Alzheimer's disease: implications for sequence of pathological events in Alzheimer's disease. *Brain* 132, 1355–1365. doi:10.1093/brain/awp062.

Jacobsen, H., Ozmen, L., Caruso, A., Narquizian, R., Hilpert, H., Jacobsen, B., et al. (2014). Combined treatment with a BACE inhibitor and anti-Aβ antibody Gantenerumab enhances amyloid reduction in APPLondon mice. *J. Neurosci.* 34, 11621–30. doi:10.1523/JNEUROSCI.1405-14.2014.

Janssen (2018). Update on Janssen's BACE Inhibitor Program [Press Release]. Available at: https://www.janssen.com/update-janssens-bace-inhibitor-program [Accessed December 14, 2019].

Jarrett, J. T., and Lansbury, P. T. (1993). Seeding "one-dimensional crystallization" of amyloid: a pathogenic mechanism in Alzheimer's disease and Scrapie? *Cell* 73, 1055–1058. doi:10.1016/0092-8674(93)90635-4.

Jaunmuktane, Z., Mead, S., Ellis, M., Wadsworth, J. D. F., Nicoll, A. J., Kenny, J., et al. (2015). Evidence for human transmission of amyloid-β pathology and cerebral amyloid angiopathy. *Nature* 525, 247–250. doi:10.1038/nature15369.

Jay, T. R., Von Saucken, V. E., and Landreth, G. E. (2017). TREM2 in neurodegenerative diseases. *Mol. Neurodegener.* 12, 56. doi:10.1186/s13024-017-0197-5.

Jin, M., Cao, L., and Dai, Y.-P. (2019). Role of neurofilament light chain as a potential biomarker for Alzheimer's disease: a correlative meta-analysis. *Front. Aging Neurosci.* 11, 1–10. doi:10.3389/fnagi.2019.00254.

Jonsson, T., Atwal, J. K., Steinberg, S., Snaedal, J., Jonsson, P. V., Bjornsson, S., et al. (2012). A mutation in APP protects against Alzheimer's disease and age-related cognitive decline. *Nature* 488, 96–99. doi:10.1038/nature11283.

Jonsson, T., Stefansson, H., Steinberg, S., Jonsdottir, I., Jonsson, P. V., Snaedal, J., et al. (2013). Variant of TREM2 associated with the risk of Alzheimer's disease. *N. Engl. J. Med.* 368, 107–116. doi:10.1056/NEJMoa1211103.

Jucker, M., and Walker, L. C. (2013). Self-propagation of pathogenic protein aggregates in neurodegenerative diseases. *Nature* 501, 45–51. doi:10.1038/nature12481.

Jucker, M., and Walker, L. C. (2018). Propagation and spread of pathogenic protein assemblies in neurodegenerative diseases. *Nat. Neurosci.* 21, 1341–1349. doi:10.1038/s41593-018-0238-6.

Kandalepas, P. C., Sadleir, K. R., Eimer, W. A., Zhao, J., Nicholson, D. A., and Vassar, R. (2013). The Alzheimer's β-secretase BACE1 localizes to normal presynaptic terminals and to dystrophic presynaptic terminals surrounding amyloid plaques. *Acta Neuropathol.* 126, 329–352. doi:10.1007/s00401-013-1152-3.

Kane, M. D., Lipinski, W. J., Callahan, M. J., Bian, F., Durham, R. A., Schwarz, R. D., et al. (2000). Evidence for seeding of β-amyloid by intracerebral infusion of Alzheimer brain extracts in β-amyloid precursor protein-transgenic mice. *J. Neurosci.* 20, 3606–3611. doi:10.1523/jneurosci.20-10-03606.2000.

Karlnoski, R. A., Rosenthal, A., Kobayashi, D., Pons, J., Alamed, J., Mercer, M., et al. (2009). Suppression of amyloid deposition leads to long-term reductions in Alzheimer's pathologies in Tg2576 mice. *J. Neurosci.* 29, 4964–4971. doi:10.1523/JNEUROSCI.4560-08.2009.

Karran, E., and Hardy, J. (2014). Antiamyloid therapy for Alzheimer's disease - are we on the right road? *N. Engl. J. Med.* 370, 377–378. doi:10.1056/NEJMe1313943.

Karran, E., Mercken, M., and De Strooper, B. (2011). The amyloid cascade hypothesis for Alzheimer's disease: An appraisal for the development of therapeutics. *Nat. Rev. Drug Discov.* 10, 698–712. doi:10.1038/nrd3505.

Kastanenka, K. V., Bussiere, T., Shakerdge, N., Qian, F., Weinreb, P. H., Rhodes, K., et al. (2016). Immunotherapy with Aducanumab restores calcium homeostasis in Tg2576 mice. *J. Neurosci.* 36, 12549–12558. doi:10.1523/JNEUROSCI.2080-16.2016.

Katzmarski, N., Ziegler-Waldkirch, S., Scheffler, N., Witt, C., Abou-Ajram, C., Nuscher, B., et al. (2019). Aβ oligomers trigger and accelerate Aβ seeding. *Brain Pathol.* 30, 36–45. doi:10.1111/bpa.12734.

Kawarabayashi, T., Younkin, L., Saido, T., Shoji, M., Ashe, K., and Younkin, S. (2001). Age-dependent changes in brain, CSF, and plasma amyloid β protein in the Tg2576 transgenic mouse model of Alzheimer's disease. *J. Neurosci.* 21, 372–381. doi:10.1523/JNEUROSCI.21-02-00372.2001.

Kemal, S., and Vassar, R. (2019). Death by microglia. *J. Exp. Med.* 216, 2451–2452. doi:10.1084/jem.20191536.

Kennedy, M. E., Stamford, A. W., Chen, X., Cox, K., Cumming, J. N., Dockendorf, M. F., et al. (2016). The BACE1 inhibitor Verubecestat (MK-8931) reduces CNS β-amyloid in animal models and in Alzheimer's disease patients. *Sci. Transl. Med.* 8, 363ra150. doi:10.1126/scitranslmed.aad9704.

Keren-Shaul, H., Spinrad, A., Weiner, A., Matcovitch-Natan, O., Dvir-Szternfeld, R., Ulland, T. K., et al. (2017). A unique microglia type associated with restricting development of Alzheimer's disease. *Cell* 169, 1276–1290. doi:10.1016/j.cell.2017.05.018.

Kleinberger, G., Yamanishi, Y., Suarez-Calvet, M., Czirr, E., Lohmann, E., Cuyvers, E., et al. (2014). TREM2 mutations implicated in neurodegeneration impair cell surface transport and phagocytosis. *Sci. Transl. Med.* 6, 243ra86. doi:10.1126/scitranslmed.3009093.

Knopman, D. S. (2019). Lowering of amyloid-beta by β-secretase inhibitors - some informative failures. *N. Engl. J. Med.* 380, 1476–1478. doi:10.1056/NEJMe1903193.

Kollmer, M., Close, W., Funk, L., Rasmussen, J., Bsoul, A., Schierhorn, A., et al. (2019). Cryo-EM structure and polymorphism of Aβ amyloid fibrils purified from Alzheimer's brain tissue. *Nat. Commun.* 10, 4760. doi:10.1038/s41467-019-12683-8.

Kopan, R., and Ilagan, M. X. G. (2004). γ-secretase: proteasome of the membrane? *Nat. Rev. Mol. Cell Biol.* 5, 499–504. doi:10.1038/nrm1406.

Kuhle, J., Gaiottino, J., Leppert, D., Petzold, A., Bestwick, J. P., Malaspina, A., et al. (2015). Serum neurofilament light chain is a biomarker of human spinal cord injury severity and outcome. *J. Neurol. Neurosurg. Psychiatry* 86, 273–279. doi:10.1136/jnnp-2013-307454.

Kuhn, P.-H., Wang, H., Dislich, B., Colombo, A., Zeitschel, U., Ellwart, J. W., et al. (2010). ADAM10 is the physiologically relevant, constitutive α-secretase of the amyloid precursor protein in primary neurons. *EMBO J.* 29, 3020–3032. doi:10.1038/emboj.2010.167.

La Joie, R., Ayakta, N., Seeley, W. W., Borys, E., Boxer, A. L., DeCarli, C., et al. (2019). Multisite study of the relationships between antemortem [11C]PIB-PET centiloid values and postmortem measures of Alzheimer's disease neuropathology. *Alzheimer's Dement.* 15, 205–216. doi:10.1016/j.jalz.2018.09.001.

Laird, F. M., Cai, H., Savonenko, A. V., Farah, M. H., He, K., Melnikova, T., et al. (2005). BACE1, a major determinant of selective vulnerability of the brain to amyloid-β amyloidogenesis, is essential for cognitive, emotional, and synaptic functions. *J. Neurosci.* 25, 11693–11709. doi:10.1523/JNEUROSCI.2766-05.2005.

Landau, S. M., Horng, A., and Jagust, W. J. (2018). Memory decline accompanies subthreshold amyloid accumulation. *Neurology* 90, 1452–1460. doi:10.1212/WNL.0000000000005354.

Lane, C. A., Hardy, J., and Schott, J. M. (2018). Alzheimer's disease. *Eur. J. Neurol.* 25, 59–70. doi:10.1111/ene.13439.

Langbaum, J. B., Hendrix, S., Ayutyanont, N., Bennett, D. A., Shah, R. C., Barnes, L. L., et al. (2015). Establishing composite cognitive endpoints for use in preclinical Alzheimer's disease trials. *J. Prev. Alzheimer's Dis.* 2, 2–3. doi:10.14283/jpad.2015.46.

Langer, F., Eisele, Y. S., Fritschi, S. K., Staufenbiel, M., Walker, L. C., and Jucker, M. (2011). Soluble Aβ seeds are potent inducers of cerebral β-amyloid deposition. *J. Neurosci.* 31, 14488–14495. doi:10.1523/JNEUROSCI.3088-11.2011.

Lautenschlager, N. T., Cupples, L. A., Rao, V. S., Auerbach, S. A., Becker, R., Burke, J., et al. (1996). Risk of dementia among relatives of Alzheimer's disease patients in the MIRAGE study: What is in store for the oldest old? *Neurology* 46, 641–650. doi:10.1212/WNL.46.3.641.

Lazic, D., Sagare, A. P., Nikolakopoulou, A. M., Griffin, J. H., Vassar, R., and Zlokovic, B. V. (2019). 3K3A-activated protein C blocks amyloidogenic BACE1 pathway and improves functional outcome in mice. *J. Exp. Med.* 216, 279–293. doi:10.1084/jem.20181035.

Lewis, J., Dickson, D. W., Lin, W. L., Chisholm, L., Corral, A., Jones, G., et al. (2001). Enhanced neurofibrillary degeneration in transgenic mice expressing mutant tau and APP. *Science* 293, 1487–1491. doi:10.1126/science.1058189.

Li, R., Lindholm, K., Yang, L. B., Yue, X., Citron, M., Yan, R., et al. (2004). Amyloid β peptide load is correlated with increased β-secretase activity in sporadic Alzheimer's disease patients. *Proc. Natl. Acad. Sci. U. S. A.* 101, 3632–3637. doi:10.1073/pnas.0205689101.

Lichtenthaler, S. F. (2011). Alpha-secretase in Alzheimer's disease: molecular identity, regulation and therapeutic potential. *J. Neurochem.* 116, 10–21. doi:10.1111/j.1471-4159.2010.07081.x.

Liebsch, F., Kulic, L., Teunissen, C., Shobo, A., Ulku, I., Engelschalt, V., et al. (2019). Aβ34 is a BACE1-derived degradation intermediate associated with amyloid clearance and Alzheimer's disease progression. *Nat. Commun.* 10, 2240. doi:10.1038/s41467-019-10152-w.

Lopez Lopez, C., Caputo, A., Liu, F., Riviere, M. E., Rouzade-Dominguez, M. L., Thomas, R. G., et al. (2017). The Alzheimer's Prevention Initiative generation program: evaluating CNP520 efficacy in the prevention of Alzheimer's disease. *J. Prev. Alzheimer's Dis.* 4, 242–246. doi:10.14283/jpad.2017.37.

Lopez Lopez, C., Tariot, P. N., Caputo, A., Langbaum, J. B., Liu, F., Riviere, M. E., et al. (2019). The Alzheimer's Prevention Initiative Generation Program: study design of two randomized controlled trials for individuals at risk for clinical onset of Alzheimer's disease. *Alzheimer's Dement. Transl. Res. Clin. Interv.* 5, 216–227. doi:10.1016/j.trci.2019.02.005.

Loy, C. T., Schofield, P. R., Turner, A. M., and Kwok, J. B. (2014). Genetics of dementia. *Lancet* 383, 828–840. doi:10.1016/S0140-6736(13)60630-3.

Lynch, S. Y., Kaplow, J., Zhao, J., Dhadda, S., Luthman, J., and Albala, B. (2018). Elenbecestat, E2609, a BACE inhibitor: results from a phase-2 study in subjects with mild cognitive impairment and mild-to-moderate dementia due to Alzheimer's disease. *Alzheimer's Dement.* 14, 1623. doi:10.1016/j.jalz.2018.07.213.

Maia, L. F., Kaeser, S. A., Reichwald, J., Hruscha, M., Martus, P., Staufenbiel, M., et al. (2013). Changes in amyloid- and tau in the cerebrospinal fluid of transgenic mice overexpressing amyloid precursor protein. *Sci. Transl. Med.* 5, 194re2. doi:10.1126/scitranslmed.3006446.

Maia, L. F., Kaeser, S. A., Reichwald, J., Lambert, M., Obermüller, U., Schelle, J., et al. (2015). Increased CSF Aβ during the very early phase of cerebral Aβ deposition in mouse models. *EMBO Mol. Med.* 7, 895–903. doi:10.15252/emmm.201505026.

Maier, F. C., Wehrl, H. F., Schmid, A. M., Mannheim, J. G., Wiehr, S., Lerdkrai, C., et al. (2014). Longitudinal PET-MRI reveals β-amyloid deposition and rCBF dynamics and connects vascular amyloidosis to quantitative loss of perfusion. *Nat. Med.* 20, 1485–1492. doi:10.1038/nm.3734.

Maruyama, M., Shimada, H., Suhara, T., Shinotoh, H., Ji, B., Maeda, J., et al. (2013). Imaging of tau pathology in a tauopathy mouse model and in Alzheimer patients compared to normal controls. *Neuron* 79, 1094–1108. doi:10.1016/j.neuron.2013.07.037.

Masters, C. L., and Selkoe, D. J. (2012). Biochemistry of amyloid β-protein and amyloid deposits in Alzheimer disease. *Cold Spring Harb. Perspect. Med.* 2, a006262. doi:10.1101/cshperspect.a006262.

Mattsson, N., Andreasson, U., Zetterberg, H., Blennow, K., Weiner, M. W., Aisen, P., et al. (2017). Association of plasma neurofilament light with neurodegeneration in patients with Alzheimer disease. *JAMA Neurol.* 74, 557–566. doi:10.1001/jamaneurol.2016.6117.

Mattsson, N., Palmqvist, S., Stomrud, E., Vogel, J., and Hansson, O. (2019). Staging β-amyloid pathology with amyloid positron emission tomography. *JAMA Neurol.* 76, 1319–1329. doi:10.1001/jamaneurol.2019.2214.

Mazaheri, F., Snaidero, N., Kleinberger, G., Madore, C., Daria, A., Werner, G., et al. (2017). TREM2 deficiency impairs chemotaxis and microglial responses to neuronal injury. *EMBO Rep.* 18, 1186–1198. doi:10.15252/embr.201743922.

McConlogue, L., Buttini, M., Anderson, J. P., Brigham, E. F., Chen, K. S., Freedman, S. B., et al. (2007). Partial reduction of BACE1 has dramatic effects on Alzheimer plaque and synaptic pathology in APP transgenic mice. *J. Biol. Chem.* 282, 26326–26334. doi:10.1074/jbc.M611687200.

McDade, E., and Bateman, R. J. (2017). Stop Alzheimer's before it starts. *Nature* 547, 153–155. doi:10.1038/547153a.

McDade, E., Wang, G., Gordon, B. A., Hassenstab, J., Benzinger, T. L. S., Buckles, V., et al. (2018). Longitudinal cognitive and biomarker changes in dominantly inherited Alzheimer disease. *Neurology* 91, 1295–1306. doi:10.1212/WNL.0000000000006277.

McKhann, G. M., Knopman, D. S., Chertkow, H., Hyman, B. T., Jack, C. R., Kawas, C. H., et al. (2011). The diagnosis of dementia due to Alzheimer's disease: recommendations from the National Institute on Aging-Alzheimer's Association workgroups on diagnostic guidelines for Alzheimer's disease. *Alzheimer's Dement.* 7, 263–269. doi:10.1016/j.jalz.2011.03.005.

Meyer-Luehmann, M., Coomaraswamy, J., Bolmont, T., Kaeser, S., Schaefer, C., Kilger, E., et al. (2006). Exogenous induction of cerebral beta-amyloidogenesis is governed by agent and host. *Science* 313, 1781–1784. doi:10.1126/science.1131864.

Michno, W., Nyström, S., Wehrli, P., Lashley, T., Brinkmalm, G., Guerard, L., et al. (2019). Pyroglutamation of amyloid-βx-42 (Aβx-42) followed by Aβ1-40 deposition underlies plaque polymorphism in progressing Alzheimer's disease pathology. *J. Biol. Chem.* 294, 6719–6732. doi:10.1074/jbc.RA118.006604.

Migliaccio, R., Agosta, F., Possin, K. L., Rabinovici, G. D., Miller, B. L., and Gorno-Tempini, M. L. (2012). White matter atrophy in Alzheimer's disease variants. *Alzheimer's Dement.* 8, S78-S87.e2. doi:10.1016/j.jalz.2012.04.010.

Montag-Sallaz, M., Schachner, M., and Montag, D. (2002). Misguided axonal projections, neural cell adhesion molecule 180 mRNA upregulation, and altered behavior in mice deficient for the close homolog of L1. *Mol. Cell. Biol.* 22, 7967–7981. doi:10.1128/mcb.22.22.7967-7981.2002.

Morris, J. C., Aisen, P. S., Bateman, R. J., Benzinger, T. L., Cairns, N. J., Fagan, A. M., et al. (2012). Developing an international network for Alzheimer's research: the Dominantly Inherited Alzheimer Network. *Clin. Investig. (Lond).* 2, 975–984. doi:10.4155/cli.12.93.

Mullane, K., and Williams, M. (2018). Alzheimer's disease (AD) therapeutics – 2: beyond amyloid – re-defining AD and its causality to discover effective therapeutics. *Biochem. Pharmacol.* 158, 376–401. doi:10.1016/j.bcp.2018.09.027.

Mullard, A. (2017). BACE inhibitor bust in Alzheimer trial. *Nat. Rev. Drug Discov.* 16, 155. doi:10.1038/nrd.2017.43.

Nakamura, Y., Takeda, M., Angelides, K. J., Tanaka, T., Tada, K., and Nishimura, T. (1990). Effect of phosphorylation on 68 KDa neurofilament subunit protein assembly by the cyclic AMP dependent protein kinase in vitro. *Biochem. Biophys. Res. Commun.* 169, 744–750. doi:10.1016/0006-291X(90)90394-3.

Neselius, S., Brisby, H., Theodorsson, A., Blennow, K., Zetterberg, H., and Marcusson, J. (2012). CSF-biomarkers in olympic boxing: diagnosis and effects of repetitive head trauma. *PLoS One* 7, e33606. doi:10.1371/journal.pone.0033606.

Neumann, U., Rueeger, H., Machauer, R., Veenstra, S. J., Lueoend, R. M., Tintelnot-Blomley, M., et al. (2015). A novel BACE inhibitor NB-360 shows a superior pharmacological profile and robust reduction of amyloid-β and neuroinflammation in APP transgenic mice. *Mol. Neurodegener.* 10, 44. doi:10.1186/s13024-015-0033-8.

Neumann, U., Ufer, M., Jacobson, L. H., Rouzade-Dominguez, M., Huledal, G., Kolly, C., et al. (2018). The BACE-1 inhibitor CNP520 for prevention trials in Alzheimer's disease. *EMBO Mol. Med.* 10, 1–18. doi:10.15252/emmm.201809316.

Newcombe, E. A., Camats-Perna, J., Silva, M. L., Valmas, N., Huat, T. J., and Medeiros, R. (2018). Inflammation: the link between comorbidities, genetics, and Alzheimer's disease. *J. Neuroinflammation* 15, 276. doi:10.1186/s12974-018-1313-3.

Nilsson, L., Nordberg, A., Hardy, J., Wester, P., and Winblad, B. (1986). Physostigmine restores 3H-acetylcholine efflux from Alzheimer brain slices to normal level. *J. Neural Transm.* 67, 275–285. doi:10.1007/BF01243353.

Novakova, L., Zetterberg, H., Sundström, P., Axelsson, M., Khademi, M., Gunnarsson, M., et al. (2017). Monitoring disease activity in multiple sclerosis using serum neurofilament light protein. *Neurology* 89, 2230–2237. doi:10.1212/WNL.0000000000004683.

Novartis International AG (2019). Novartis, Amgen and Banner Alzheimer's Institute discontinue clinical program with BACE inhibitor CNP520 for Alzheimer's prevention [media release].

Nussbaum, J. M., Schilling, S., Cynis, H., Silva, A., Swanson, E., Wangsanut, T., et al. (2012). Prion-like behaviour and tau-dependent cytotoxicity of pyroglutamylated amyloid-β. *Nature* 485, 651–655. doi:10.1038/nature11060.

Nyström, S., Psonka-Antonczyk, K. M., Ellingsen, P. G., Johansson, L. B. G., Reitan, N., Handrick, S., et al. (2013). Evidence for age-dependent in vivo conformational rearrangement within Aβ amyloid deposits. *ACS Chem. Biol.* 8, 1128–1133. doi:10.1021/cb4000376.

Ohno, M., Chang, L., Tseng, W., Oakley, H., Citron, M., Klein, W. L., et al. (2006). Temporal memory deficits in Alzheimer's mouse models: rescue by genetic deletion of BACE1. *Eur. J. Neurosci.* 23, 251–260. doi:10.1111/j.1460-9568.2005.04551.x.

Olsson, B., Alberg, L., Cullen, N. C., Michael, E., Wahlgren, L., Kroksmark, A.-K., et al. (2019). NFL is a marker of treatment response in children with SMA treated with nusinersen. *J. Neurol.* 266, 2129–2136. doi:10.1007/s00415-019-09389-8.

Olsson, B., Lautner, R., Andreasson, U., Öhrfelt, A., Portelius, E., Bjerke, M., et al. (2016). CSF and blood biomarkers for the diagnosis of Alzheimer's disease: a systematic review and meta-analysis. *Lancet Neurol.* 15, 673–684. doi:10.1016/S1474-4422(16)00070-3.

Ortman, J. M., Velkoff, V. A., and Hogan, H. (2014). An aging nation: the older population in the United States. *Curr. Popul. Reports, U.S. Census Bur. Washingt.* P25, 1140. Available at: census.gov.

Osborn, K. E., Khan, O. A., Kresge, H. A., Bown, C. W., Liu, D., Moore, E. E., et al. (2019). Cerebrospinal fluid and plasma neurofilament light relate to abnormal cognition. *Alzheimer's Dement. Diagnosis, Assess. Dis. Monit.* 11, 700–709. doi:10.1016/j.dadm.2019.08.008.

Ostrowitzki, S., Deptula, D., Thurfjell, L., Barkhof, F., Bohrmann, B., Brooks, D. J., et al. (2012). Mechanism of amyloid removal in patients with Alzheimer disease treated with Gantenerumab. *Arch. Neurol.* 69, 198–207. doi:10.1001/archneurol.2011.1538.

Ostrowitzki, S., Lasser, R. A., Dorflinger, E., Scheltens, P., Barkhof, F., Nikolcheva, T., et al. (2017). A phase III randomized trial of Gantenerumab in prodromal Alzheimer's disease. *Alzheimers. Res. Ther.* 9, 95. doi:10.1186/s13195-017-0318-y.

Ou-Yang, M.-H., Kurz, J. E., Nomura, T., Popovic, J., Rajapaksha, T. W., Dong, H., et al. (2018). Axonal organization defects in the hippocampus of adult conditional BACE1 knockout mice. *Sci. Transl. Med.* 10, eaao5620. doi:10.1126/scitranslmed.aao5620.

Paganetti, P. A., Lis, M., Klafki, H.-W., and Staufenbiel, M. (1996). Amyloid precursor protein truncated at any of the y-secretase sites is not cleaved to β-amyloid. *J. Neurosci. Res.* 46, 283–293. doi:10.1002/(SICI)1097-4547(19961101)46:3<283::AID-JNR1>3.0.CO;2-G.

Palmqvist, S., Insel, P. S., Stomrud, E., Janelidze, S., Zetterberg, H., Brix, B., et al. (2019). Cerebrospinal fluid and plasma biomarker trajectories with increasing amyloid deposition in Alzheimer's disease. *EMBO Mol. Med.* 11, e11170. doi:10.15252/emmm.201911170.

Palmqvist, S., Mattsson, N., and Hansson, O. (2016). Cerebrospinal fluid analysis detects cerebral amyloid-β accumulation earlier than positron emission tomography. *Brain* 139, 1226–1236. doi:10.1093/brain/aww015.

Panza, F., Lozupone, M., Logroscino, G., and Imbimbo, B. P. (2019). A critical appraisal of amyloid-β-targeting therapies for Alzheimer disease. *Nat. Rev. Neurol.* 15, 73–88. doi:10.1038/s41582-018-0116-6.

Petzold, A. (2005). Neurofilament phosphoforms: surrogate markers for axonal injury, degeneration and loss. *J. Neurol. Sci.* 233, 183–198. doi:10.1016/j.jns.2005.03.015.

Pfeifer, M., Boncristiano, S., Bondolfi, L., Stalder, A., Deller, T., Staufenbiel, M., et al. (2002). Cerebral hemorrhage after passive anti-Aβ immunotherapy. *Science* 298, 1379. doi:10.1126/science.1078259.

Piccio, L., Deming, Y., Del-Águila, J. L., Ghezzi, L., Holtzman, D. M., Fagan, A. M., et al. (2016). Cerebrospinal fluid soluble TREM2 is higher in Alzheimer disease and associated with mutation status. *Acta Neuropathol.* 131, 925–933. doi:10.1007/s00401-016-1533-5.

Piton, M., Hirtz, C., Desmetz, C., Milhau, J., Lajoix, A. D., Bennys, K., et al. (2018). Alzheimer's disease: advances in drug development. *J. Alzheimer's Dis.* 65, 3–13. doi:10.3233/JAD-180145.

Pletnikova, O., Rudow, G. L., Hyde, T. M., Kleinman, J. E., Ali, S. Z., Bharadwaj, R., et al. (2015). Alzheimer lesions in the autopsied brains of people 30 to 50 years of age. *Cogn. Behav. Neurol.* 28, 144–152. doi:10.1097/WNN.0000000000000071.

Preische, O., Schultz, S. A., Apel, A., Kuhle, J., Kaeser, S. A., Barro, C., et al. (2019). Serum neurofilament dynamics predicts neurodegeneration and clinical progression in presymptomatic Alzheimer's disease. *Nat. Med.* 25, 277–283. doi:10.1038/s41591-018-0304-3.

Probst, G., and Xu, Y. (2012). Small-molecule BACE1 inhibitors: a patent literature review (2006 – 2011). *Expert Opin. Ther. Pat.* 22, 511–540. doi:10.1517/13543776.2012.681302.

Prusiner, S. B. (1982). Novel proteinaceous infectious particles cause scrapie. *Science* 216, 136–144. doi:10.1126/science.6801762.

Prusiner, S. B. (1998). Prions. *Proc. Natl. Acad. Sci. U. S. A.* 95, 13363–13383. doi:10.1073/pnas.95.23.13363.

Prusiner, S. B. (2013). Biology and genetics of prions causing neurodegeneration. *Annu. Rev. Genet.* 47, 601–623. doi:10.1146/annurev-genet-110711-155524.

Rabe, S., Reichwald, J., Ammaturo, D., De Strooper, B., Saftig, P., Neumann, U., et al. (2011). The swedish APP mutation alters the effect of genetically reduced BACE1 expression on the APP processing. *J. Neurochem.* 119, 231–239. doi:10.1111/j.1471-4159.2011.07412.x.

Radde, R., Bolmont, T., Kaeser, S. A., Coomaraswamy, J., Lindau, D., Stoltze, L., et al. (2006). Aβ42-driven cerebral amyloidosis in transgenic mice reveals early and robust pathology. *EMBO Rep.* 7, 940–946. doi:10.1038/sj.embor.7400784.

Rajapaksha, T. W., Eimer, W. A., Bozza, T. C., and Vassar, R. (2011). The Alzheimer's β-secretase enzyme BACE1 is required for accurate axon guidance of olfactory sensory neurons and normal glomerulus formation in the olfactory bulb. *Mol. Neurodegener.* 6, 88. doi:10.1186/1750-1326-6-88.

Reiman, E. M., Quiroz, Y. T., Fleisher, A. S., Chen, K., Velez-Pardo, C., Jimenez-Del-Rio, M., et al. (2012). Brain imaging and fluid biomarker analysis in young adults at genetic risk for autosomal dominant Alzheimer's disease in the presenilin 1 E280A kindred: a case-control study. *Lancet Neurol.* 11, 1048–1056. doi:10.1016/S1474-4422(12)70228-4.

Reisberg, B., Doody, R., Stöffler, A., Schmitt, F., Ferris, S., and Möbius, H. J. (2003). Memantine in moderate-to-severe Alzheimer's disease. *N. Engl. J. Med.* 348, 1333–1341. doi:10.1056/NEJMoa013128.

Rijal Upadhaya, A., Kosterin, I., Kumar, S., Von Arnim, C. A. F., Yamaguchi, H., Fändrich, M., et al. (2014). Biochemical stages of amyloid-β peptide aggregation and accumulation in the human brain and their association with symptomatic and pathologically preclinical Alzheimer's disease. *Brain* 137, 887–903. doi:10.1093/brain/awt362.

Roberds, S. L., Anderson, J., Basi, G., Bienkowski, M. J., Branstetter, D. G., Chen, K. S., et al. (2001). BACE knockout mice are healthy despite lacking the primary beta-secretase activity in brain: implications for Alzheimer's disease therapeutics. *Hum. Mol. Genet.* 10, 1317–1324. doi:10.1093/hmg/10.12.1317.

Roberts, R., and Knopman, D. S. (2013). Classification and Epidemiology of MCI. *Clin. Geriatr. Med.* 29, 753–772. doi:10.1016/J.CGER.2013.07.003.

Rochin, L., Hurbain, I., Serneels, L., Fort, C., Watt, B., Leblanc, P., et al. (2013). BACE2 processes PMEL to form the melanosome amyloid matrix in pigment cells. *Proc. Natl. Acad. Sci. U. S. A.* 110, 10658–10663. doi:10.1073/pnas.1220748110.

Rodda, J., Morgan, S., and Walker, Z. (2009). Are cholinesterase inhibitors effective in the management of the behavioral and psychological symptoms of dementia in Alzheimer's disease? a systematic review of randomized, placebo-controlled trials of Donepezil, Rivastigmine and Galantamine. *Int. Psychogeriatrics* 21, 813–824. doi:10.1017/S1041610209990354.

Rogers, S. L., Farlow, M. R., Doody, R. S., Mohs, R., and Friedhoff, L. T. (1998). A 24-week, double-blind, placebo-controlled trial of donepezil in patients with Alzheimer's disease. *Neurology* 50, 136–145. doi:10.1212/WNL.50.1.136.

Rohrer, J. D., Woollacott, I. O. C., Dick, K. M., Brotherhood, E., Gordon, E., Fellows, A., et al. (2016). Serum neurofilament light chain protein is a measure of disease intensity in frontotemporal dementia. *Neurology* 87, 1329–1336. doi:10.1212/WNL.0000000000003154.

Rovelet-Lecrux, A., Hannequin, D., Raux, G., Le Meur, N., Laquerrière, A., Vital, A., et al. (2006). APP locus duplication causes autosomal dominant early-onset Alzheimer disease with cerebral amyloid angiopathy. *Nat. Genet.* 38, 24–26. doi:10.1038/ng1718.

Rudge, P., Jaunmuktane, Z., Adlard, P., Bjurstrom, N., Caine, D., Lowe, J., et al. (2015). Iatrogenic CJD due to pituitary-derived growth hormone with genetically determined incubation times of up to 40 years. *Brain* 138, 3386–3399. doi:10.1093/brain/awv235.

Ryan, D. A., Narrow, W. C., Federoff, H. J., and Bowers, W. J. (2010). An improved method for generating consistent soluble amyloid-beta oligomer preparations for in vitro neurotoxicity studies. *J. Neurosci. Methods* 190, 171–179. doi:10.1016/j.jneumeth.2010.05.001.

Rylett, R. J., Ball, M. J., and Colhoun, E. H. (1983). Evidence for high affinity choline transport in synaptosomes prepared from hippocampus and neocortex of patients with Alzheimer's disease. *Brain Res.* 289, 169–175. doi:10.1016/0006-8993(83)90017-3.

Salloway, S., Honigberg, L. A., Cho, W., Ward, M., Friesenhahn, M., Brunstein, F., et al. (2018). Amyloid positron emission tomography and cerebrospinal fluid results from a Crenezumab anti-amyloid-beta antibody double-blind, placebo-controlled, randomized phase II study in mild-to-moderate Alzheimer's disease (BLAZE). *Alzheimer's Res. Ther.* 10, 96. doi:10.1186/s13195-018-0424-5.

Salzer, J. L. (2012). Axonal regulation of Schwann cell ensheathment and myelination. *J. Peripher. Nerv. Syst.* 17, 14–19. doi:10.1111/j.1529-8027.2012.00425.x.

Saunders, A. M., Strittmatter, W. J., Schmechel, D., George-Hyslop, S., Pericak-Vance, M. A., Joo, S. H., et al. (1993). Association of apolipoprotein E allele ε4 with late-onset sporadic Alzheimer's disease. *Neurology* 43, 1467–1472. doi:10.1002/ajmg.1320540319.

Schelle, J., Häsler, L. M., Göpfert, J. C., Joos, T. O., Vanderstichele, H., Stoops, E., et al. (2017). Prevention of tau increase in cerebrospinal fluid of APP transgenic mice suggests downstream effect of BACE1 inhibition. *Alzheimer's Dement.* 13, 701–709. doi:10.1016/j.jalz.2016.09.005.

Schelle, J., Wegenast-Braun, B. M., Fritschi, S. K., Kaeser, S. A., Jährling, N., Eicke, D., et al. (2019). Early Aβ reduction prevents progression of cerebral amyloid angiopathy. *Ann. Neurol.* 00, 1–11. doi:10.1002/ana.25562.

Schlepckow, K., Kleinberger, G., Fukumori, A., Feederle, R., Lichtenthaler, S. F., Steiner, H., et al. (2017). An Alzheimer-associated TREM2 variant occurs at the ADAM cleavage site and affects shedding and phagocytic function. *EMBO Mol. Med.* 9, 1356–1365. doi:10.15252/emmm.201707672.

Schmid, C. D., Sautkulis, L. N., Danielson, P. E., Cooper, J., Hasel, K. W., Hilbush, B. S., et al. (2002). Heterogeneous expression of the triggering receptor expressed on myeloid cells-2 on adult murine microglia. *J. Neurochem.* 83, 1309–1320. doi:10.1046/j.1471-4159.2002.01243.x.

Selkoe, D. J. (2012). Preventing Alzheimer's disease. *Science* 337, 1488–1492. doi:10.1126/science.1228541.

Selkoe, D. J. (2019). Alzheimer disease and Aducanumab: adjusting our approach. *Nat. Rev. Neurol.* 15, 365–366. doi:10.1038/s41582-019-0205-1.

Selkoe, D. J., and Hardy, J. (2016). The amyloid hypothesis of Alzheimer's disease at 25 years. *EMBO Mol. Med.* 8, 595–608. doi:10.15252/emmm.201606210.

Serrano-Pozo, A., William, C. M., Ferrer, I., Uro-Coste, E., Delisle, M.-B., Maurage, C.-A., et al. (2010). Beneficial effect of human anti-amyloid-β active immunization on neurite morphology and tau pathology. *Brain* 133, 1312–1327. doi:10.1093/brain/awq056.

Sevigny, J., Chiao, P., Bussière, T., Weinreb, P. H., Williams, L., Maier, M., et al. (2016). The antibody Aducanumab reduces Aβ plaques in Alzheimer's disease. *Nature* 537, 50–56. doi:10.1038/nature19323.

Shankar, G. M., Li, S., Mehta, T. H., Garcia-Munoz, A., Shepardson, N. E., Smith, I., et al. (2008). Amyloid-β protein dimers isolated directly from Alzheimer's brains impair synaptic plasticity and memory. *Nat. Med.* 14, 837–842. doi:10.1038/nm1782.

Shi, Y., Manis, M., Long, J., Wang, K., Sullivan, P. M., Serrano, J. R., et al. (2019). Microglia drive APOE-dependent neurodegeneration in a tauopathy mouse model. *J. Exp. Med.* 216, 2546–2561. doi:10.1084/jem.20190980.

Shimshek, D. R., Jacobson, L. H., Kolly, C., Zamurovic, N., Balavenkatraman, K. K., Morawiec, L., et al. (2016). Pharmacological BACE1 and BACE2 inhibition induces hair depigmentation by inhibiting PMEL17 processing in mice. *Sci. Rep.* 6, 21917. doi:10.1038/srep21917.

Siemers, E. R., Sundell, K. L., Carlson, C., Case, M., Sethuraman, G., Liu-Seifert, H., et al. (2016). Phase 3 Solanezumab trials: secondary outcomes in mild Alzheimer's disease patients. *Alzheimer's Dement.* 12, 110–120. doi:10.1016/j.jalz.2015.06.1893.

Sinha, S., Anderson, J. P., Barbour, R., Basi, G. S., Caccaveffo, R., Davis, D., et al. (1999). Purification and cloning of amyloid precursor protein β-secretase from human brain. *Nature* 402, 537–540. doi:10.1038/990114.

Sipe, J. D., Benson, M. D., Buxbaum, J. N., Ikeda, S.-I., Merlini, G., Saraiva, M. J. M., et al. (2010). Amyloid fibril protein nomenclature: 2010 recommendations from the nomenclature committee of the International Society of Amyloidosis. *Amyloid* 17, 101–104. doi:10.3109/13506129.2010.526812.

Sjögren, M., Blomberg, M., Jonsson, M., Wahlund, L.-O., Edman, Å., Lind, K., et al. (2001). Neurofilament protein in cerebrospinal fluid: a marker of white matter changes. *J. Neurosci. Res.* 66, 510–516. doi:10.1002/jnr.1242.

Sperling, R. A., Aisen, P. S., Beckett, L. A., Bennett, D. A., Craft, S., Fagan, A. M., et al. (2011a). Toward defining the preclinical stages of Alzheimer's disease: recommendations from the National Institute on Aging-Alzheimer's Association workgroups on diagnostic guidelines for Alzheimer's disease. *Alzheimer's Dement.* 7, 280–292. doi:10.1016/j.jalz.2011.03.003.

Sperling, R. A., Jack, C. R., and Aisen, P. S. (2011b). Testing the right target and right drug at the right stage. *Sci. Transl. Med.* 3, 111cm33. doi:10.1126/scitranslmed.3002609.

Sperling, R. A., Jack, C. R., Black, S. E., Frosch, M. P., Greenberg, S. M., Hyman, B. T., et al. (2011c). Amyloid-related imaging abnormalities in amyloid-modifying therapeutic trials: recommendations from the Alzheimer's Association Research Roundtable Workgroup. *Alzheimer's Dement.* 7, 367–385. doi:10.1016/j.jalz.2011.05.2351.

Sperling, R. A., Karlawish, J., and Johnson, K. A. (2013). Preclinical Alzheimer disease - the challenges ahead. *Nat. Rev. Neurol.* 9, 54–58. doi:10.1038/nrneurol.2012.241.

Sperling, R. A., Mormino, E., and Johnson, K. (2014a). The evolution of preclinical Alzheimer's disease: implications for prevention trials. *Neuron* 84, 608–622. doi:10.1016/j.neuron.2014.10.038.

Sperling, R. A., Rentz, D. M., Johnson, K. A., Karlawish, J., Donohue, M., Salmon, D. P., et al. (2014b). The A4 study: stopping AD before symptoms begin? *Sci. Transl. Med.* 6, 228fs13. doi:10.1126/scitranslmed.3007941.

Streffer, J., Börjesson-Hanson, A., Van Broeck, B., Smekens, P., Timmers, M., Tesseur, I., et al. (2016). Pharmacodynamics of the oral BACE inhibitor JNJ-54861911 in early

Alzheimer's disease. *Alzheimer's Dement.* 12, P199–P200. doi:10.1016/j.jalz.2016.06.350.

Stürchler-Pierrat, C., Abramowski, D., Duke, M., Wiederhold, K.-H., Mistl, C., Rothacher, S., et al. (1997). Two amyloid precursor protein transgenic mouse models with Alzheimer disease-like pathology. *Proc. Natl. Acad. Sci.* 94, 13287–13292. doi:10.1073/pnas.94.24.13287.

Suárez-Calvet, M., Caballero, M. Á. A., Kleinberger, G., Bateman, R. J., Fagan, A. M., Morris, J. C., et al. (2016a). Early changes in CSF sTREM2 in dominantly inherited Alzheimer's disease occur after amyloid deposition and neuronal injury. *Sci. Transl. Med.* 8, 369ra178. doi:10.1126/scitranslmed.aag1767.

Suárez-Calvet, M., Kleinberger, G., Araque Caballero, M. Á., Brendel, M., Rominger, A., Alcolea, D., et al. (2016b). sTREM 2 cerebrospinal fluid levels are a potential biomarker for microglia activity in early-stage Alzheimer's disease and associate with neuronal injury markers. *EMBO Mol. Med.* 8, 466–476. doi:10.15252/emmm.201506123.

Suh, J., Choi, S. H., Romano, D. M., Gannon, M. A., Lesinski, A. N., Kim, D. Y., et al. (2013). ADAM10 missense mutations potentiate β-amyloid accumulation by impairing prodomain chaperone function. *Neuron* 80, 385–401. doi:10.1016/j.neuron.2013.08.035.

Tejada-Vera, B. (2013). Mortality from Alzheimer's disease in the United States: data for 2000 and 2010. *NCHS Data Brief*, 1–8.

Thal, D. R., Beach, T. G., Zanette, M., Lilja, J., Heurling, K., Chakrabarty, A., et al. (2018). Estimation of amyloid distribution by [18F]flutemetamol PET predicts the neuropathological phase of amyloid β-protein deposition. *Acta Neuropathol.* 136, 557–567. doi:10.1007/s00401-018-1897-9.

Thornton, P., Sevalle, J., Deery, M. J., Fraser, G., Zhou, Y., Ståhl, S., et al. (2017). TREM 2 shedding by cleavage at the H157-S158 bond is accelerated for the Alzheimer's disease-associated H157Y variant. *EMBO Mol. Med.* 9, 1366–1378. doi:10.15252/emmm.201707673.

Tucker, S., Möller, C., Tegerstedt, K., Lord, A., Laudon, H., Sjödahl, J., et al. (2015). The murine version of BAN2401 (mAb158) selectively reduces amyloid-β protofibrils in brain and cerebrospinal fluid of tg-ArcSwe mice. *J. Alzheimer's Dis.* 43, 575–588. doi:10.3233/JAD-140741.

U.S. Department of Health and Human Services, Centers for Disease Control and Prevention, N. C. for H. S. About underlying cause of death, 1999-2017. *CDC WONDER online database*.

Uenaka, K., Nakano, M., Willis, B. A., Friedrich, S., Ferguson-Sells, L., Dean, R. A., et al. (2012). Comparison of pharmacokinetics, pharmacodynamics, safety, and tolerability of the amyloid β monoclonal antibody Solanezumab in japanese and white patients with mild to moderate Alzheimer disease. *Clin. Neuropharmacol.* 35, 25–29. doi:10.1097/WNF.0b013e31823a13d3.

Ulrich, J. D., Finn, M., Wang, Y., Shen, A., Mahan, T. E., Jiang, H., et al. (2014). Altered microglial response to Aβ plaques in APPPS1-21 mice heterozygous for TREM2. *Mol. Neurodegener.* 9, 20. doi:10.1186/1750-1326-9-20.

Ultsch, M., Li, B., Maurer, T., Mathieu, M., Adolfsson, O., Muhs, A., et al. (2016). Structure of Crenezumab complex with Aβ shows loss of β-hairpin. *Sci. Rep.* 6, 1–11. doi:10.1038/srep39374.

Vassar, R., Bennett, B. D., Babu-Khan, S., Kahn, S., Mendiaz, E. A., Denis, P., et al. (1999). β-secretase cleavage of Alzheimer's amyloid precursor protein by the transmembrane aspartic protease BACE. *Science* 286, 735–741. doi:10.1126/science.286.5440.735.

Verheijen, J., and Sleegers, K. (2018). Understanding Alzheimer disease at the interface between genetics and transcriptomics. *Trends Genet.* 34, 434–447. doi:10.1016/j.tig.2018.02.007.

Villemagne, V. L., Burnham, S., Bourgeat, P., Brown, B., Ellis, K. A., Salvado, O., et al. (2013). Amyloid β deposition, neurodegeneration, and cognitive decline in sporadic Alzheimer's disease: a prospective cohort study. *Lancet Neurol.* 12, 357–367. doi:10.1016/S1474-4422(13)70044-9.

Villemagne, V. L., Doré, V., Burnham, S. C., Masters, C. L., and Rowe, C. C. (2018). Imaging tau and amyloid-β proteinopathies in Alzheimer disease and other conditions. *Nat. Rev. Neurol.* 14, 225–236. doi:10.1038/nrneurol.2018.9.

Walker, L. C. (2018). "Prion-like mechanisms in Alzheimer disease," in *Handbook of Clinical Neurology*, 303–319. doi:10.1016/B978-0-444-63945-5.00016-7.

Ward, A., Tardiff, S., Dye, C., and Arrighi, H. M. (2013). Rate of conversion from prodromal Alzheimer's disease to Alzheimer's dementia: a systematic review of the literature. *Dement. Geriatr. Cogn. Dis. Extra* 3, 320–332. doi:10.1159/000354370.

Weingarten, M. D., Lockwood, A. H., Hwo, S. Y., and Kirschner, M. W. (1975). A protein factor essential for microtubule assembly. *Proc. Natl. Acad. Sci. U. S. A.* 72, 1858–1862. doi:10.1073/pnas.72.5.1858.

Wessels, A. M., Tariot, P. N., Zimmer, J. A., Selzler, K. J., Bragg, S. M., Andersen, S. W., et al. (2019). Efficacy and safety of Lanabecestat for treatment of early and mild Alzheimer disease: the AMARANTH and DAYBREAK-ALZ randomized clinical trials. *JAMA Neurol.* 46285. doi:10.1001/jamaneurol.2019.3988.

Westermark, G. T., Fändrich, M., Lundmark, K., and Westermark, P. (2018). Noncerebral amyloidoses: aspects on seeding, cross-seeding, and transmission. *Cold Spring Harb. Perspect. Med.* 8, a024323. doi:10.1101/cshperspect.a024323.

Weston, P. S. J., Poole, T., Ryan, N. S., Nair, A., Liang, Y., Macpherson, K., et al. (2017). Serum neurofilament light in familial Alzheimer disease: a marker of early neurodegeneration. *Neurology* 89, 2167–2175. doi:10.1212/WNL.0000000000004667.

Willem, M., Garratt, A. N., Novak, B., Citron, M., Kaufmann, S., Rittger, A., et al. (2006). Control of peripheral nerve myelination by the β-secretase BACE1. *Science* 314, 664–666. doi:10.1126/science.1132341.

Winblad, B., Andreasen, N., Minthon, L., Floesser, A., Imbert, G., Dumortier, T., et al. (2012). Safety, tolerability, and antibody response of active Aβ immunotherapy with CAD106 in patients with Alzheimer's disease: randomised, double-blind, placebo-controlled, first-in-human study. *Lancet Neurol.* 11, 597–604. doi:10.1016/S1474-4422(12)70140-0.

Winkler, D. T., Bondolfi, L., Herzig, M. C., Jann, L., Calhoun, M. E., Wiederhold, K. H., et al. (2001). Spontaneous hemorrhagic stroke in a mouse model of cerebral amyloid angiopathy. *J. Neurosci.* 21, 1619–1627. doi:10.1523/jneurosci.21-05-01619.2001.

Wirth, M., Madison, C. M., Rabinovici, G. D., Oh, H., Landau, S. M., and Jagust, W. J. (2013). Alzheimer's disease neurodegenerative biomarkers are associated with decreased cognitive function but not β-amyloid in cognitively normal older individuals. *J. Neurosci.* 33, 5553–5563. doi:10.1523/JNEUROSCI.4409-12.2013.

Witt, A., Macdonald, N., and Kirkpatrick, P. (2004). Memantine hydrochloride. *Nat. Rev. Drug Discov.* 3, 109–110. doi:10.1038/nrd1311.

Wolfe, M. S. (2014). Unlocking truths of γ-secretase in Alzheimer's disease: what is the translational potential? *Future Neurol.* 9, 419–429. doi:10.2217/fnl.14.35.

Yamada, K., Yabuki, C., Seubert, P., Schenk, D., Hori, Y., Ohtsuki, S., et al. (2009). Aβ immunotherapy: intracerebral sequestration of Aβ by an anti-Aβ monoclonal antibody 266 with high affinity to soluble Aβ. *J. Neurosci.* 29, 11393–11398. doi:10.1523/JNEUROSCI.2021-09.2009.

Yan, R., Blenkowski, M. J., Shuck, M. E., Miao, H., Tory, M. C., Pauley, A. M., et al. (1999). Membrane-anchored aspartyl protease with Alzheimer's disease β-secretase activity. *Nature* 402, 533–537. doi:10.1038/990107.

Yan, R., and Vassar, R. (2014). Targeting the β secretase BACE1 for Alzheimer's disease therapy. *Lancet Neurol.* 13, 319–329. doi:10.1016/S1474-4422(13)70276-X.

Yang, L.-B., Lindholm, K., Yan, R., Citron, M., Xia, W., Yang, X.-L., et al. (2003). Elevated β-secretase expression and enzymatic activity detected in sporadic Alzheimer disease. *Nat. Med.* 9, 3–4. doi:10.1038/nm0103-3.

Ye, L., Fritschi, S. K., Schelle, J., Obermüller, U., Degenhardt, K., Kaeser, S. A., et al. (2015). Persistence of Aβ seeds in APP null mouse brain. *Nat. Neurosci.* 18, 1559–1561. doi:10.1038/nn.4117.

Ye, L., Rasmussen, J., Kaeser, S. A., Marzesco, A., Obermüller, U., Mahler, J., et al. (2017). Aβ seeding potency peaks in the early stages of cerebral β-amyloidosis. *EMBO Rep.* 18, 1536–1544. doi:10.15252/embr.201744067.

Yoon, S. S., and Jo, S. A. (2012). Mechanisms of amyloid-β peptide clearance: potential therapeutic targets for Alzheimer's disease. *Biomol. Ther.* 20, 245–255. doi:10.4062/biomolther.2012.20.3.245.

Yuan, A., Sershen, H., Veeranna, Basavarajappa, B. S., Kumar, A., Hashim, A., et al. (2015). Neurofilament subunits are integral components of synapses and modulate neurotransmission and behavior in vivo. *Mol. Psychiatry* 20, 986–994. doi:10.1038/mp.2015.45.

Zetterberg, H. (2017). Applying fluid biomarkers to Alzheimer's disease. *Am. J. Physiol. Physiol.* 313, C3–C10. doi:10.1152/ajpcell.00007.2017.

Zetterberg, H., and Blennow, K. (2018). From cerebrospinal fluid to blood: the third wave of fluid biomarkers for Alzheimer's disease. *J. Alzheimer's Dis.* 64, S271–S279. doi:10.3233/JAD-179926.

Zetterberg, H., Skillbäck, T., Mattsson, N., Trojanowski, J. Q., Portelius, E., Shaw, L. M., et al. (2016). Association of cerebrospinal fluid neurofilament light concentration with Alzheimer disease progression. *JAMA Neurol.* 73, 60–67. doi:10.1001/jamaneurol.2015.3037.

Zetterberg, H., Wahlund, L.-O., and Blennow, K. (2003). Cerebrospinal fluid markers for prediction of Alzheimer's disease. *Neurosci. Lett.* 352, 67–69. doi:10.1016/j.neulet.2003.08.011.

Zhao, J., Nussinov, R., and Ma, B. (2017a). Mechanisms of recognition of amyloid-β (Aβ) monomer, oligomer, and fibril by homologous antibodies. *J. Biol. Chem.* 292, 18325–18343. doi:10.1074/jbc.M117.801514.

Zhao, Y., Sivaji, S., Chiang, M. C., Ali, H., Zukowski, M., Ali, S., et al. (2017b). Amyloid beta peptides block new synapse assembly by Nogo receptor-mediated inhibition of T-type calcium channels. *Neuron* 96, 355-372.e6. doi:10.1016/j.neuron.2017.09.041.

Zheng, X., Liu, D., Roychaudhuri, R., Teplow, D. B., and Bowers, M. T. (2015). Amyloid β-protein assembly: differential effects of the protective A2T mutation and recessive A2V familial Alzheimer's disease mutation. *ACS Chem. Neurosci.* 6, 1732–1740. doi:10.1021/acschemneuro.5b00171.

Zhong, L., Chen, X. F., Wang, T., Wang, Z., Liao, C., Wang, Z., et al. (2017). Soluble TREM2 induces inflammatory responses and enhances microglial survival. *J. Exp. Med.* 214, 597–607. doi:10.1084/jem.20160844.

Zhong, L., Xu, Y., Zhuo, R., Wang, T., Wang, K., Huang, R., et al. (2019). Soluble TREM2 ameliorates pathological phenotypes by modulating microglial functions in an Alzheimer's disease model. *Nat. Commun.* 10, 1365. doi:10.1038/s41467-019-09118-9.

Zhu, K., Xiang, X., Filser, S., Marinković, P., Dorostkar, M. M., Crux, S., et al. (2018). Beta-site amyloid precursor protein cleaving enzyme 1 inhibition impairs synaptic plasticity via seizure protein 6. *Biol. Psychiatry* 83, 428–437. doi:10.1016/j.biopsych.2016.12.023.

8 Statement of contributions

Aβ restriction by BACE1 inhibition is most effective at initial disease stages

Ruth E. Uhlmann, Stephan A. Kaeser, Angelos Skodras, Giulia Salvadori, Juliane Schelle, Christine Rother, Lisa M. Häsler, Ulrike Obermüller, Derya R. Shimshek, Ulf Neumann, Matthias Staufenbiel, Mathias Jucker

Personal contribution: Experimental design of the study (together with J.S., M.S. and M.J.); BACE1 inhibitor treatment; CSF collection and tissue harvesting (together with J.S.); stereological analysis (together with G.S.); immunohistochemistry (together with U.O. and G.S.), image acquisition and processing; data acquisition, analysis and collection (together with C.R., A.S. and S.A.K); statistical analysis and figure preparation.

Others: L.M.H. and S.A.K. performed MSD ELISA and Simoa measurements. U.N. performed sTREM2 measurements; D.R.S. and U.N. contributed the BACE1 inhibitor.

Targetable pathogenic Aβ seeds prior to amyloid deposition

Ruth E. Uhlmann, Christine Rother, Jay Rasmussen, Juliane Schelle, Carina Bergmann, Emily M. Ullrich Gavilanes, Sarah K. Fritschi, Anika Buehler, Frank Baumann, Angelos Skodras, Rawaa Al-Shaana, Lan Ye, Stephan A. Kaeser, Ulrike Obermüller, Søren Christensen, Fredrik Kartberg, Jeffrey B. Stavenhagen, Jens-Ulrich Rahfeld, Holger Cynis, Fang Qian, Paul H. Weinreb, Thierry Bussiere, Lary C. Walker, Matthias Staufenbiel, Mathias Jucker

Personal contribution: Experimental design and performance of passive immunization and seeding experiments (together with J.S., S.K.F, L.Y. U.O. M.S. and M.J.); CSF collection and tissue harvesting (together with J.S. and C.R.); stereological analysis; design and performance of pharmacokinetics work (together with E.M.U.-G., and M.S.); immunohistochemistry (together with U.O.), image acquisition and processing (with the help of A.S.); statistical analysis (with the help of S.A.K.) and figure preparation (together with M.J.).

Others: C.R., J.R., C.B., A.B., F.B., R.A., S.A.K., M.S. and M.J. designed and performed biochemical work. S.C., F.K., J.B.S., J-U.R., H.C., F.Q., P.H.W., and T.B. contributed antibodies and provided experimental input.

9 Acknowledgements

First, I would like to express my gratitude to Prof. Mathias Jucker for giving me the opportunity to be part of his department at the Hertie Institute for Clinical Brain Research. For me, he was a conscientious supervisor and profound mentor. He gave support and meaningful advice during the work on these very interesting and challenging projects.

Furthermore, I would like to gratefully thank my Advisory Board members, Prof. Peter Heutink and Prof. Philipp Kahle, for their insightful comments and solid encouragement.

I would like to thank my colleagues and friends from the department "Cellular Neurology" for their scientific guidance, technical assistance and additional contribution: Natalie Beschorner, Jessica Wagner, Melanie Barth, Marc Welzer, Lisa Steinbrecher, Desirée Brösamle, Ping Liu, Ann-Christin Wendeln, Karoline Degenhardt, Jay Rasmussen, Deborah Kronenberg-Versteeg, Alejandro Ruiz Rilquelme, Gaye Tanriöver, Bettina Wegenast-Braun, Marius Lambert, Katleen Wild, Bernadette Graus and Gisela Rose. In particular, I would like to thank Juliane Schelle for the good introduction to the topic, Christine Rother for her excellent support regarding the projects and also in everything else, Angelos Skodras for his help with troubleshooting, support in technical issues, computational data acquisition and methodology, and Anika Bühler, Ulrike Obermüller, Melisa Ullrich Gavilanes and Giulia Salvadori for their laboratory help. Moreover, I am very grateful to Rawaa Al-Shaana and Lisa Häsler for their time and effort which they spent on the measurements, Stephan Käser for his patience in helping with data analysis and statistics as well as for the great times at conferences. Last but not least, I would like to express my gratefulness to Carina Leibssle and Jörg Odenthal for the active assistance with mouse work.

I would like to gratefully thank Matthias Staufenbiel for his instructive and solution-oriented advice, and all partners from Germany, Europe and the United States for the excellent and successful collaboration.

Furthermore, I would like to thank the animal caretakers of the FORS, especially Mohammed Saidi, and the Veterinarians of the Uniklinikum Tübingen for the great cooperation.

Last, I would like to sincerely thank my family for their all-out encouragement and ubiquitous motivation and inspiration at this important stage of my life.

10 Appendix

10.1 Supplementary figures

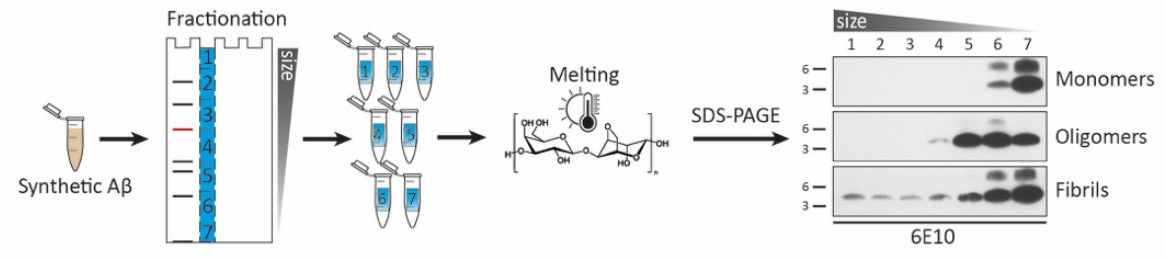

Supplementary Figure 1. Semi-native agarose gel electrophoresis on synthetic Aβ. Semi-native agarose gel electrophoresis was done using monomeric, oligomeric and fibrillary Aβ in the same fashion as the first steps of the ARPA method to determine Aβ distribution between fractions. Monomeric Aβ was prepared using Aβ1-40 (Bachem) in DMSO, oligomeric preparation followed a protocol for Aβ-derived diffusible ligands (Ryan et al., 2010) using Aβ1-42 and fibrils were prepared by incubating 100 µM Aβ1-42 at 37°C for 24 hours. Agarose lanes were cut as described in Figure 7a and the method section, and agarose gel pieces were melted followed by denaturing immunoblotting and probed for Aβ with antibody 6E10. Chemiluminescent signal was captured with Amersham Hyperfilm ECL (in contrast to the chemiluminescent imager used for quantitative analysis in Figure 7 and Supplementary Figure 2). See also Methods for detail. Note that (presumed) monomeric Aβ runs in fraction 6 and 7 while oligomeric Aβ species are additionally seen in 4 and 5 and Aβ fibrils in fraction 1 to 3.

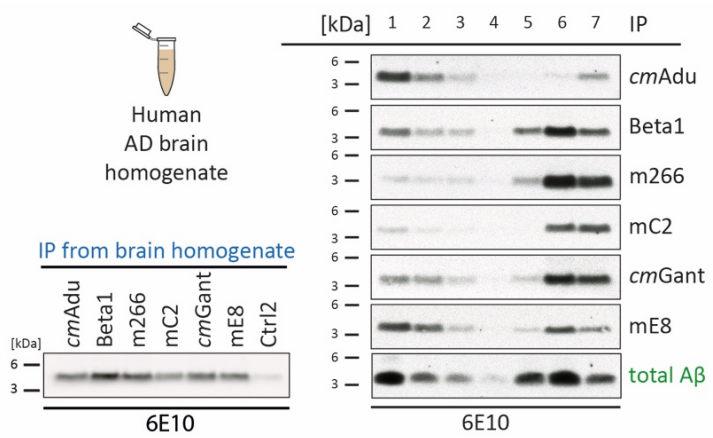

Supplementary Figure 2. Aβ assemblies from AD brain recognized by the various antibodies. See Figure 7 for a description of the ARPA methodology. PBS-homogenates from the frontal cortex of three AD subjects (Braak stage VI) were pooled. Direct immunoprecipitation (IP) or ARPA (right panel) are shown for the various antibodies. Immunoblots were probed for Aβ with antibody 6E10. The experiment was repeated three times obtaining similar results.

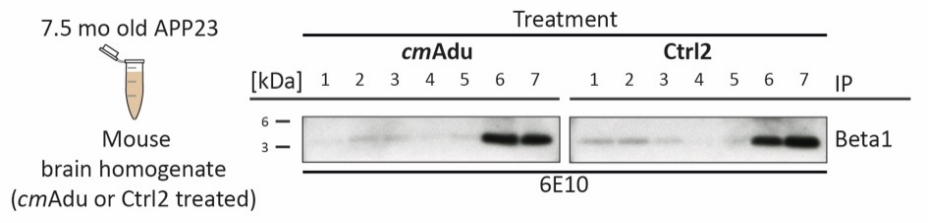

Supplemental Figure 3. Removal of higher molecular Aβ assemblies in *cm*Aducanumab-treated mice. Six month-old APP23 mice acutely treated with *cm*Aducanumab (*cm*Adu) and Control antibody (Ctrl2) were examined at 7.5-month of age (see Figure 6 for details). Brain PBS homogenates of all 8 *cm*Adu- and 8 Ctrl2-treated mice were pooled. Homogenates were examined with ARPA (see Figure 7 for a description of the ARPA methodology) using Beta1 antibody to pull down Aβ. Beta1 was used since it recognizes all Aβ species fairly equally in this assay (see Figure 7). Note the faint bands in fraction 1-3 in the Ctrl2-treated mice that are largely diminished in the *cm*Adu-treated mice. A reduction of faint bands in fraction 1-3 was also found in an additional experiment when antibody 4G8 (BioLegend, San Diego, CA) was used to pull down Aβ. The experiment was repeated three times obtaining similar results.

10.2 Abbreviations

A4	Anti-Amyloid Treatment in Asymptomatic Alzheimer's Disease trial
AD	Alzheimer's Disease
ADAD	Autosomal-Dominant AD
ADAM	A Disintegrin And Metalloprotease
ADRC	Emory University Alzheimer's Disease Research Center
AICD	APP Intracellular Domain
API	Alzheimer's Prevention Initiative
APICC	API Cognitive Composite
APOE	Apolipoprotein E
APP	β-Amyloid-Precursor-Protein
ARIA-H, -E	Amyloid-Related Imaging Abnormalities-Hemosiderin, -Edema
ARPA	Antibody Recognition Profiling of Aβ assemblies
Aβ	Amyloid-β peptide
BACE1/2	β-site APP Cleaving Enzyme 1/2
BBB	Blood-Brain-Barrier
BCA	Bicinchoninic Acid
BI	BACE inhibitor
CAA	Cerebral β-Amyloid Angiopathy
CatD	Cathepsin D
CDR-SB	Clinical Dementia Rating-Sum of Boxes
CHL1	Close Homolog of L1
cm	Chimeric Murinized
CSF	Cerebrospinal Fluid

Ctrl	Control
DIAN	Dominantly Inherited Alzheimer Network
DIAN-TU	DIAN-Trials Unit
DMSO	Dimethyl Sulfoxide
dpi	Days Post Immunization
DSM-V	Diagnostic and Statistical Manual of Mental Disorders, 5th edition
DTT	Dithiothreitol
ECL	Electrochemiluminescence
EDTA	Ethylenediaminetetraacetic Acid
ELISA	Enzyme-Linked Immunosorbent Assay
EYO	Estimated Years until symptom Onset
FA	Formic Acid
FDA	Food and Drug Administration
FDG	^{18}F-fluorodeoxyglucose
i.p.	Intraperitoneal
IP	Immunoprecipitation
IRB	Institutional Review Board
K_{el}	Elimination rate
MCI	Mild Cognitive Impairment
MMSE	Mini-Mental State Examination
MRI	Magnetic Resonance Imaging
NfL	Neurofilament Light chain
NIA-AA	National Institute on Aging – Alzheimer's Association
NINCDS-ADRDA	National Institute of Neurological and Communicative Disorders and Stroke – Alzheimer's Disease and Related Disorders Association

NMDA	N-Methyl-D-Aspartate
p-tau	Phosphorylated tau
PBS	Phosphate-Buffered Saline
PET	Positron Emission Tomography
PMEL	Pigment cell specific Melanocyte protein
pNPP	4-Nitrophenyl Phosphate
Prion	Proteinaceous infectious particle
PrP	Prion Protein
PS	Presenilin
PSEN	Presenilin gene
SDS	Sodium Dodecyl Sulfate
SEM	Standard Error of the Mean
Simoa	Single Molecule Array
sTREM2	Soluble TREM2
t-tau	Total tau
$t_{1/2}$	Half-life
tg	Transgenic
Thy1	Thymocyte differentiation antigen 1
TREM2	Triggering Receptor Expressed on Myeloid cells 2
v/v	volume/volume
w/v	weight/volume
wt	Wildtype (C57BL/6)